THE UNIVERSITY
of EDINBURGH

Targeting nuclear size for therapeutic intervention in cancer

Andrea Rizzotto

Thesis presented for the degree of Doctor of Philosophy

Wellcome Trust Centre for Cell Biology

School of Biological Sciences

University of Edinburgh

August 2018

Declaration

I declare that this thesis has been composed by myself and the work presented herein is my own, except where stated otherwise. This research has not been submitted for any other degree except as specified.

Andrea Rizzotto

Edinburgh

August 2018

Acknowledgments

First and foremost, I would like to express my gratitude to Eric for accepting me as PhD student in his lab, for the constant guidance and help from experimental design to bench work. Beside my advisor, I would like to thank all the present and past members of the Schirmer lab for the stimulating discussion and all the laughs while working at the bench, making long and mentally draining experiments more bearable.

My sincere thanks goes also to all the collaborators that helped in the realisation of this study. Prof. Mike Tyers and Dr. Silvain Tollis from the Université de Montreal for their help with the screening procedures and the data analysis; Prof. Neil Carragher and Dr. Scott Warchal at the IGMM, University of Edinburgh for the wound healing assays; Prof. Val Brunton and Morwenna Muir at the IGMM, University of Edinburgh for the help with the xenograft models.

At a personal level, my gratitude goes to my family. Firstly, my parents for believing I could do this alone in a foreign country, and for the constant support and excitement during the research time and thesis writing. My sister and brother, Giulia and Francesco for being the ones always cheering for my brief visits home.

After four and something years in Scotland, I cannot thank enough all the wonderful people I met during my journey here. All the “Italian mafia” for the numerous dinners, nights out and the guide in how to survive your PhD in Edinburgh. In particular, I want to thank Andrea, for sharing with me not only the master thesis but also the pains of a doctorate (and for all those board game nights), Francis and Jovana for being in this long path together and the exciting trip to San Francisco.

Last but not least, I want to thank the PG community, that became almost a second family in the last year or so and all the mod team for fun work done together (and the HiveTillFive nights). In particular, a special thanks goes to Peter, for his playlist that kept me company through all the thesis writing process and numerous supportive pints, and Glen for becoming the best flatmate someone could ask for.

Lay Abstract

Since tumours were first viewed on the predecessors of modern microscopes in the late 1860s, scientists observed notable visual differences from healthy tissues. Most of these differences were in the nucleus of the cell, which is easy to see through the microscope due to its size and darker staining because this is where the genome is kept. Most nuclear changes were in size and shape and these changes are still used today for both diagnosis and grading of tumours because nuclear size changes become stronger in later stage higher grade tumours that are more aggressive. This thesis investigates which proteins at the nuclear surface could be the factors leading to these changes in nuclear size and tries to dissect if the nuclear size change are a side effect of tumourigenesis or are a driving feature making the tumour that if targeted might improve patient survival. One of the biggest problems faced by researchers is that these nuclear modifications are specific for each type of cancer. Most cancer research is focused on finding common factors involved in cancer progression, but this work starts with the hypothesis that it may be better to target these tissue-specific differences. It has been established in our lab that proteins resident at the membrane defining the nucleus, the nuclear envelope, are tissue-restricted, therefore each type of tissue and accdordingly each tumour derived from that tissue has a different subset of these Nuclear Envelope Transmembrane proteins (NETs). As these NETs are tissue specific and alteration of nuclear size and shape are different for each tumour tissue type, we postulate that they might contribute to altering nuclear size. Therefore, their loss or gain during cancer progression may explain the differences identified in each tumour type. Indeed, we found several such NETs influence nuclear size and are altered in different tumour types. Targeting these proteins with drugs on top of existing chemotherapy regimens might improve patient survival. We also thus searched for drugs that alter nuclear size, expecting that they might be able to restore

correct nuclear size in tumours. We searched for drugs affecting three different tumour types where nuclear size changes are linked to lower survival rates: prostate cancer, colon cancer, and lung cancer. We identified some drugs affecting nuclear size for each of the different types of cancer; however, interestingly, each cancer type had a unique set of drugs affecting nuclear size. These findings suggest it may improve patient survival if some of these drugs are added to chemotherapy regimens and by specifically targeting the tissue containing the cancer this might also reduce organismal toxicity, a side-effect of chemotherapy that greatly lowers quality of life for the patients. Further applying this principle to other cancers tissue types and testing for better drugs targeting the tissue-specific NETs found to direct nuclear size changes may also prove beneficial.

Abstract

Nuclear size normally scales with cell size and is maintained throughout the cell cycle, but in cancer this karyoplasmic ratio, the ratio between the cytoplasm and the nucleoplasm, is disrupted, particularly in certain types of more metastatic tumours from certain cancer types. As the direction and scale of nuclear size changes differs for particular tumour types — for example in breast cancer larger nuclear size correlates with increased metastasis while for lung cancer smaller nuclear size correlates with increased metastasis — there must be tissue-specific drivers of these changes. This study aimed to screen several tissue-specific nuclear envelope transmembrane proteins (NETs) and separately a small molecule compound library for effects on nuclear size in cell lines from different cancer types. The NET screen was engaged in cells from prostate cancer (PC3) and cervical carcinoma (HeLa) and different sets of NETs affected nuclear size in each tumour type. Interestingly, these NETs also exhibited altered gene copy numbers in patient samples from particular tissue cancer types where their effects on nuclear size correlated with the directionality of nuclear size changes in the tumours. The compound screen was performed on the PC3 cells and on colonic adenocarcinoma (HCT116) and small cell lung carcinoma (H1299) cells. Each cancer type screened was affected by different compounds, so that both screens suggest a tissue-specific regulation of nuclear size. Interestingly, these compounds also reduced cell migration in wound healing assays, suggesting they might reduce tumour metastatic spread. Finally, merging both screens, the NET DHRS7/NET50 and the compound estradiol proprionate that both affect nuclear size in the prostate cancer model seem to intersect in the same pathway and we anticipate that further study will elucidate a mechanism for the nuclear size defects in late-stage prostate cancer.

Abbreviation

°C degree Celsius
2D two dimensional
3D three dimensional

A alanine
aa amino acid
Amp ampicillin
AP affinity purified
AR androgen receptor
ATP adenosine-5'-triphosphate

bp base pairs
BSA bovine serum albumin

cDNA complementary DNA
CMV cytomegalovirus
CRPC Castration Recurrent Prostate Cancer
ctrl control

DAPI 4',6-diamidino-2-phenylindole
DNA deoxyribonucleic acid
DNase deoxyribonuclease
dNTP deoxyribonucleotide
DTT dithiothreitol

E glutamic acid
E.coli Escherichia coli

EDTA ethylenediaminetetraacetic acid
E-GFP enchanced green fluorescent protein
ER endoplasmic reticulum

FBS fetal bovine serum
FITC fluorescein isothiocyanate
FT flow-through

KASH Klarsicht, ANC-1, Syne Homology

HEPES 4-(2-hydroxyethyl)-1-piperazineethanesulfonic acid

IF immunofluorescence
Ig immunoglobulin
INM inner nuclear membrane

Kan kanamycin

LINC links the nucleoskeleton and cytoskeleton (complex)

MEM minimal essential medium

mRFP monomeric red fluorescent protein

NADP/NADPH Nicotinamide adenine dinucleotide phosphate

NCBI National Center for Biotechnology information

NE nuclear envelope

NET nuclear envelope transmembrane protein

NPC nuclear pore complex

NTD N-terminal domain

ONM outer nuclear membrane

PBS phosphate buffered saline

PC Prostate Cancer

PCR polymerase chain reaction

pH $-\log_{10}(a_{H^+})$

pRb protein of the retionoblastoma

qPCR RT reverse transcription

R Arginine

SDR short dehydrogenase-reductase

List of figures

Table of Contents

1. Introduction

1.1 Nuclear size regulation in cancer

Phenotypic and morphological alterations in cell nuclei during cancer progression were first discovered in the mid-1800s when the first microscopes capable of resolving structures down to 1 μm resolution were built. One of the earliest descriptions of these changes, published in 1860 by Lionel S. Beale (King's College London), reported alteration of nuclear size and shape in the sputum of a patient with cancer of the pharynx (Beale 1860). These morphological alterations of the nuclear structure and size have been used for diagnosis of cancer ever since. Eighty years after Beale's seminal work, George Papanicolaou developed a stain to visualize cytoplasmic and nuclear structural features for an accurate diagnosis/staging of cervical cancer, setting a standard tool still used today (Cibas and Ducatman 2014). Though subsequent advances added many other altered nuclear features to fine-tune diagnoses such as chromatin organization and numbers and sizes of nucleoli, the nuclear size and shape changes are the most evident characteristics that can be distinguished by light microscopy in tumour progression and are highly characteristic for a given tumour type. At least a dozen different tumour types exhibit changes in nuclear size independent of ploidy that correlate with a worse prognosis for the patients (Cibas and Ducatman 2014; de Las Heras et al. 2014) (Table 1); hence, size and shape are used prognostically for stage and progression of each different tumour type (Zink, Fischer, and Nickerson

2004). Determining the function and mechanisms underlying these nuclear size changes in cancer is complicated as they tend to be tissue-specific in degree and direction, with some cancers showing smaller nuclei correlating with increased metastatic potential like osteosarcoma and lung carcinoma (de Andrea et al. 2011; Ladekarl et al. 1995) while others present larger nuclei that correlate with increased metastatic potential as in breast and prostate cancers (Abdalla et al. 2012; Nandakumar et al. 2012; Rashid and Ul Haque 2011; Tan et al. 2001).

The karyoplasmic ratio, the ratio between the nucleoplasm and the cytoplasm volume, is maintained during the cell cycle (Cavalier-Smith 2005; Edens et al. 2013) throughout which the nucleus typically increases several-fold in volume. Moreover, a general mechanism for this size scaling is conserved from higher eukaryotes to yeast (Jorgensen et al. 2007; Neumann and Nurse 2007). However, this karyoplasmic ratio scaling is not maintained in more metastatic cancer cells. This raises the question of whether the scaling disruption is just an indirect side effect of other changes that drive the tumour or if the nuclear size change itself contributes an advantage to or even underlies tumour generation. With the many functions now known for the nuclear envelope (NE), advantages could range from changes in gene regulation/signaling to mechanical nuclear aspects enabling faster migration or the easier squeezing of cancer cells through cell junctions to invade different tissues.

Table 1 Alteration of nuclear size in different cancer types

Cancer type	Nuclear Size change	Reference
Breast cancer	+	(Abdalla et al. 2012; Nandakumar et al. 2012; Tan et al. 2001)
Male Breast cancer	+	(Veta et al. 2012)
Cervical cancer	+	(Saad et al. 2006; Slater et al. 2005)
Small-cell Cervical cancer	+	(Giorgadze et al. 2012)
Colorectal cancer	+	(Eynard et al. 2009)
Epidermal squamous cancer	+	(Malhotra et al. 2013)
Cutaneous soft tissue sarcoma	+	(Meachem et al. 2012)
Gastric carcinoma	+	(Ikeguchi et al. 1999)
Lung squamous cell carcinoma	-	(Ladekarl et al. 1995)
Liver cancer	+	(Yan et al. 2012)
Melanoma	+	(Mossbacher et al. 1996; Na et al. 2009)
Invasive meningioma	+	(Madsen and Schrøder 1996)
Oral squamous carcinoma	+	(Natarajan et al. 2010)
Osteosarcoma	-	(de Andrea et al. 2011)
Ovarian cancer	+	(Zeimet et al. 2011)
Pancreatic cancer	+	(Taira et al. 2012a)
Prostate adenocarcinoma	+	(Rashid and Ul Haque 2011)
Papillary thyroid carcinoma	+	(Shih et al. 2013)
Urinary bladder carcinoma	+	(Fukuzawa et al. 1995; Helander, Hofer, and Holmberg 1984; van Velthoven et al. 1995)

1.2 Nuclear envelope changes in cancer

The NE undergoes extreme alterations and disruptions during cancer progression generally, but the changes are often tissue specific, with the particular phenotype depending on the tissue in which the cancer starts its development. For each tissue cancer type there are characteristic changes in size and morphology that moreover correlate with stage and grade of that cancer and so are used both diagnostically and prognostically (Fig 1A). As the NE forms the "walls" of the nucleus, nuclear size changes require growth at the NE and shape changes likewise involve deformation of the NE. Thus, it is reasonable to postulate that the physically observed changes under the microscope are driven at least in part by changes in proteins at the NE. The NE is not just the primary barrier between cytoplasm and the genetic material, but recent studies show that it has important signalling functions, contributes to cell migration through its cytoskeletal connections at the ONM, and through its many connections to chromatin at the INM adds additional layers of gene regulation as well as contributing to DNA-damage repair. Accordingly, more interest is being raised to understand the role of this compartment in the development of cancer and the possibility that the NE changes may contribute to as well as reflect disease progression.

A general categorization for nuclear envelope changes undergone in cancer progression has been proposed by Fisher that breaks down these alterations into three main general groups:

- NE changes associated with chromosomal instability
- Conserved NE structural features within a genetically unstable population
- NE changes in the absence of chromosomal instability

The first group is the most common phenotype identified in solid tumours as around 90% of them present chromosomal instability (Holland and Cleveland 2012). Chromosomal instability phenotypes across cancers are quite heterogeneous and can yield a variety of different morphological changes even within the same tumour mass such as alteration of the nuclear size and shape,

with the presence of polylobulation and deep infoldings. In addition to these alterations, this type of cancer is characterised by the presence of micronuclei, a characteristic phenotype of chromosomal instability formed when mis-segregated chromosomes acquire an independent NE from the nucleus containing the bulk of the chromosomes (Fig 1B) (Holland and Cleveland 2012). Nuclei of this group when in interphase can be visualized by a different cell-to-cell hematoxylin staining, due to a different DNA content resulting from the failure to equally distribute the genetic material to the daughter cells. For these types of cancer the shape of the NE is altered in aneuploid cells, but this change is maintained through cancer progression and therefore does not provide a basis for grading later stages of the cancer. As these cells lose the ability to retain a spherical or ovoid nuclear shape, they offer a simple typical phenotype that can be used by cytopathologists as a distinctive mark for the original cancer diagnosis (Samanta and Dey 2012).

The second group, in which NE features are conserved in the presence of chromosome instability, shows an increased nuclear lamina surface area or nuclear volume compared to cytoplasmic volume (N/C ratio). Moreover, these cancers show fragile nuclear lamina, a typical trait in the “small-cell carcinomas” (Fig 1C). This type of tumour can arise from anywhere in the body and is highly genetically unstable (Wistuba, Gazdar, and Minna 2001). Despite the elevated chromosomal instability of this type of cancer it conserves a series of morphological alterations, with the NE lacking strength and nuclei molding, assuming the shape of nearby nuclei or objects (Fischer 2014).

Finally, cells included in the third group, where NE changes occur in the absence of chromosomal instability, present long longitudinal intranuclear cytoplasmic inclusions and a nuclear groove. These alterations are commonly found in papillary thyroid carcinoma, Langherhans cell histiocytosis and adult granulosa cell tumours, for which they are precise diagnostic features (Fig 1 D-E)(Fischer 2014). This group will be the focus of this thesis work because the changes are very characteristic for each tumour/tissue type and occur with the change to more severe grading for later cancer stages with increased metastasis. Of particulate note, because changes in ploidy do not occur in this

group the changes in nuclear size and morphology are more likely to involve particular NE functions.

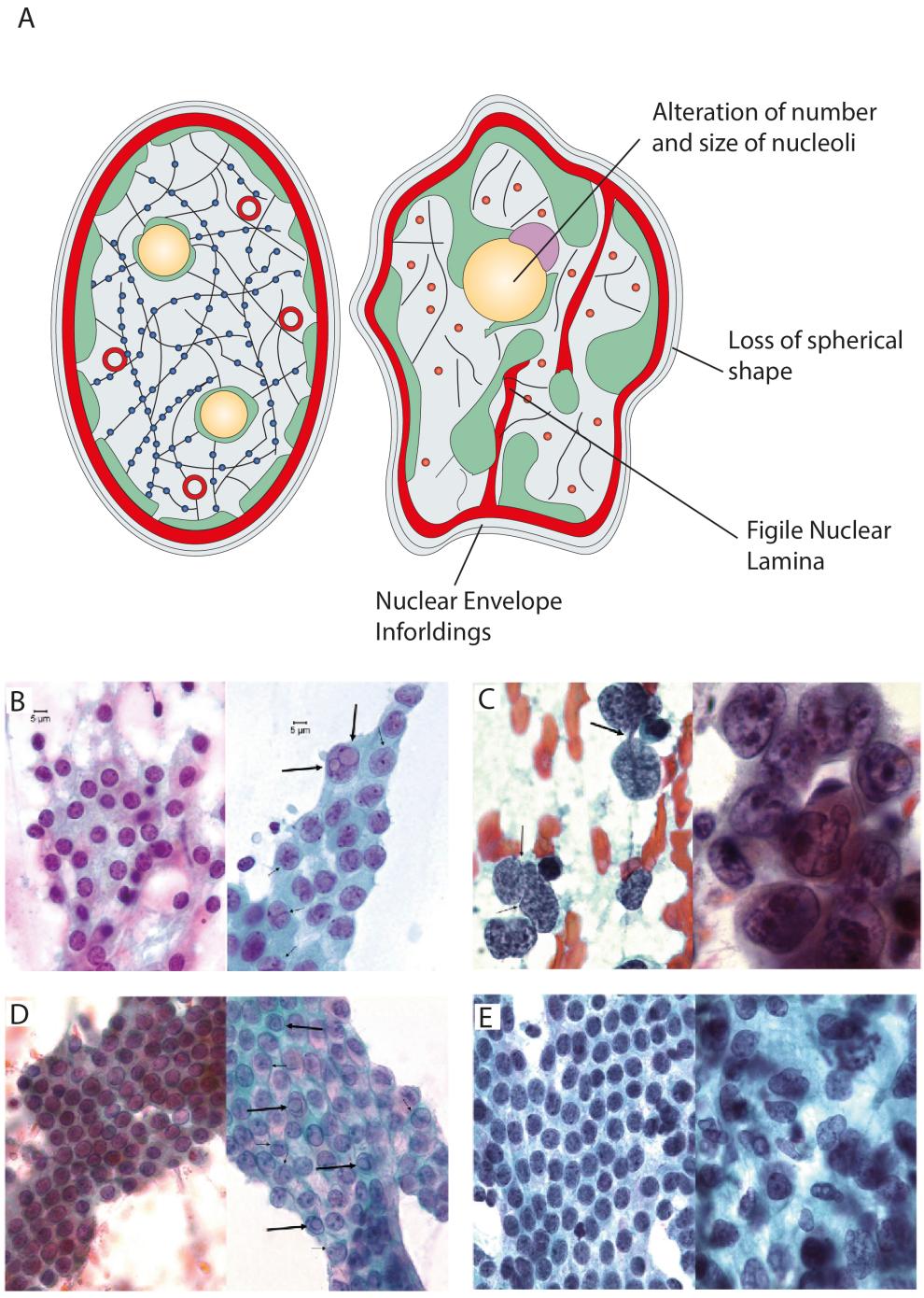

Figure 1 ***NE structural changes are key diagnostic traits of some cancers.*** *A.Schematic of alteration occulting in cancer (right) shape and size compared to normal nuclei (left), adapted from* Zink et al. 2004). *B. On the left is an alcohol- fixed, Papanicolaou-stained fine-needle aspirate of normal thyroid epithelial cells. On the right is a fine-needle aspiration biopsy with diagnostic features of papillary thyroid carcinoma (PTC), fixed and stained in the*

same manner as normal thyroid epithelium. Diagnostic features for the first group include the long linear infoldings of the NE (short thin arrows). Also very important diagnostically are the spherical invaginations of cytoplasm into the nucleus termed "intranuclear cytoplasmic inclusions" (long thick arrows) C. Fine-needle aspirations of small-cell lung cancer (left) and non- small-cell lung cancer (right, at slightly higher magnification). Cells of the second group usually show a fragile nuclear lamina (long thick arrow) and nuclear molding in which the shape of one nucleus conforms passively with the shape of an adjacent nucleus (short thin arrows). D. Fine-needle aspirations of normal pancreatic ductal cells (left), and the earliest known stage of a pancreatic adenocarcinoma (right). Note the typical characteristics of this group, the intranuclear cytoplasmic inclusions (long thick arrows) and nuclear grooves (short thin arrows). E. Fine-needle aspiration samples showing a comparison of normal ductal cells (left) with a "high-grade," chromosomally unstable, and aneuploid ductal carcinoma (right). Some nuclei are relatively spherical, while others show various lobulations and some longitudinal infoldings. (Adapted from (Fischer 2014))

1.3 Nuclear structure and organization

The NE is comprised of outer (ONM) and inner (INM) nuclear membranes and associated proteins (Fig 2) (Callan, Randall, and Tomlin 1949; Prunuske and Ullman 2006). The membranes are separated by a lumen and connected where nuclear pore complexes (NPCs), comprised of ~30 core proteins, are inserted (Grossman, Medalia, and Zwerger 2012; Suntharalingam and Wente 2003). NPCs contain multiple copies of only three transmembrane proteins, but there are hundreds of other Nuclear Envelope Transmembrane proteins (NETs) in both membranes (Korfali et al. 2010, 2012; Schirmer et al. 2003; Wilkie et al. 2011). Functions of ONM NETs are just beginning to be discovered, but many connect to cytoplasmic filaments (Buch et al. 2009; Crisp et al. 2006; Pfisterer, Jayo, and Parsons 2017; Wilhelmsen et al. 2005; Wilkie et al. 2011) while others function in cell cycle regulation (Johnson et al. 2004; Korfali et al. 2011; Srsen, Korfali, and Schirmer 2011). Thus far, many INM NETs characterized make connections important for genome organization, gene regulation, and signalling (Czapiewski, Robson, and Schirmer 2016; Holaska, Rais-Bahrami, and Wilson 2006; Kim et al. 2004; De Las Heras et al. 2017; Markiewicz et al. 2006; Parada, McQueen, and Misteli 2004; Robson et al. 2016, 2017). INM NETs also connect to a polymer of the type V intermediate filament nuclear lamins that confers structural stability to the nucleus (Crisp et al. 2006; Meinke and Schirmer 2015; Prunuske and Ullman 2006). These proteins such as Emerin, LAP1, LAP2β, LBR and

MAN1 not only have the ability to interact with lamins in different ways but are also able to recruit chromatin binding proteins such as HP1 and BAF, conferring them a central role in maintaining regions of the genome in a repressed state at the periphery of the nucleus (Solovei et al. 2013).

The NE is also connected to the cytoskeleton (Fig 2), helping the nucleus to maintain its position, shape and size and to transduce signalling stimuli deriving from the cytoplasm and the plasma membrane. The primary proteins involved in this connection are SUN-domain containing proteins of the INM and KASH-domain containing proteins, known as Nesprins, of the ONM. Together these form the Linker of Nucleoskeleton and Cytoskeleton (LINC) complex (Crisp et al. 2006) that also supports mechanosignal transduction to the nucleus (Ho et al. 2013; Swift et al. 2013). The LINC complex has been linked to nuclear size regulation and could contribute to cancer progression through the ability of controlling nuclear positioning and influencing migration (Gant Luxton et al. 2011; Lu et al. 2012; Luxton et al. 2010).

On the inner side the NE is in connection with the nuclear lamina, that offer support for the mechanical stability of the nucleus (Broers et al. 2004; Lammerding et al. 2004b; Lee et al. 2007) and therefore could be a major factor that can influence the nuclear size. When cells migrate and invasion cells have to navigate through tight spaces in the extracellular matrix and cell enjoinments that are smaller than the nucleus, this can happen through deformation of the nucleus (McGregor, Hsia, and Lammerding 2016) and remodeling of the nuclear stiffness manly dependent of altering the expression of the level of lamin A levels (Lammerding et al. 2004a, 2006). This results in cell lacking lamin A/C or with reduced expression levels to migrate faster on narrow constrictions (Davidson et al. 2014; Harada et al. 2014), suggesting that lamins could explain the alteration of nuclear size normally detected during cancer progression.

During mitosis of higher eukaryotes the NE disassembles to allow the sister chromatids to be separated and the reassembled daughter nuclei are much smaller compared to the mother cell. This is because at the end of S-phase the genome has doubled to 4N, the chromatin is decondensed and the

nucleus is filled with proteins and RNA whereas the reforming NE surrounds a 2N genome that is highly condensed. In general the nuclear volume increases around 2 fold through the cell cycle (Fidorra et al. 1981).

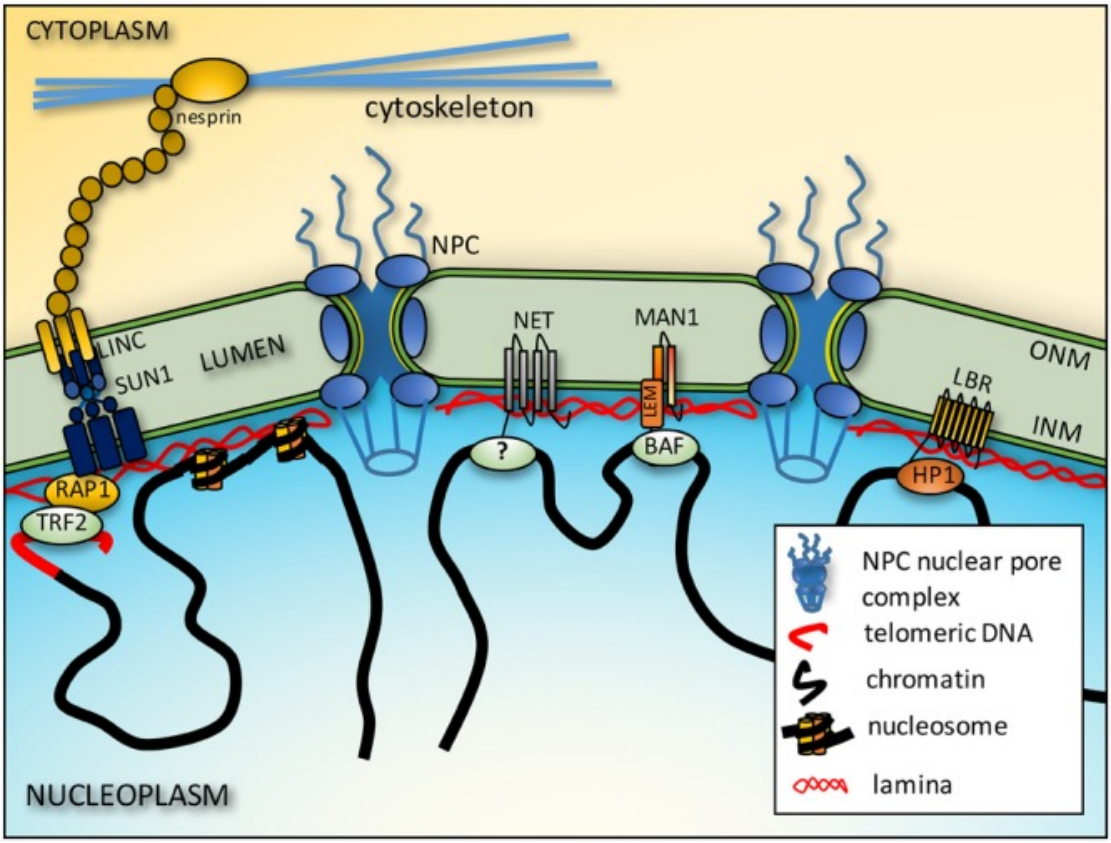

Figure 2. ***General schematic representation of nuclear envelope elements.*** *The nuclear envelope is a continuous with the ER and is formed by an inner and outer nuclear membrane separated by a lumen, interrupted by the nuclear pore complex. Different proteins insert in both the outer and inner nuclear envelope membranes called nuclear envelope transmembrane proteins (NETs) with different functions such as anchoring the genome, recruiting factors at the periphery and linking the nucleoskeleton to the cytoskeleton. (Czapiewski et al. 2016)*

1.4 Karyoplasmic ratio and factors that can regulate nuclear size

The ratio between the nucleoplasmic and the cytoplasmic volume, known as the karyoplasmic ratio or volume, has been proposed as one of the key mechanisms for a signalling feedback loop for scaling organelles, and to potentially trigger important checkpoints during the cell cycle (Cavalier-Smith 1978). The karyoplasmic ratio has been shown to be constant throughout the cell cycle and this feature is highly conserved in most unicellular and

multicellular organisms (Cavalier-Smith 2005), suggesting a key role for nuclear volume in determining cell size and vice versa. The mechanisms by which this process of scaling are regulated are still elusive and pose a challenge to researchers trying to elucidate the key players in how cells scale up or down the karyoplasmic ratio. One of the most accredited theories is that cytoplasmic volume and the amount of available NE components directly limit nuclear size (Fig 3). This is supported from experiments of heterokaryon formation between hen erythrocytes with HeLa cells, leading to expansion of the nucleus with changes in chromatin organization (Harris 1967).

Although how the karyoplasmic is maintained is still wildly debated, what has been clear for the last half century is that this ratio is altered in cancer cells (Cibas and Ducatman 2014; Frost 1986). This allowed the setup of standards to determine the presence and progression of cancer in standard haematoxylin and eosin stained biopsies. The nucleus and the nuclear envelope are two highly organized and specialized compartments of the cell, and dozens of different factors can influence directly or indirectly the maintenance of a normal nuclear size that will be explained in the following paragraphs of this chapter.

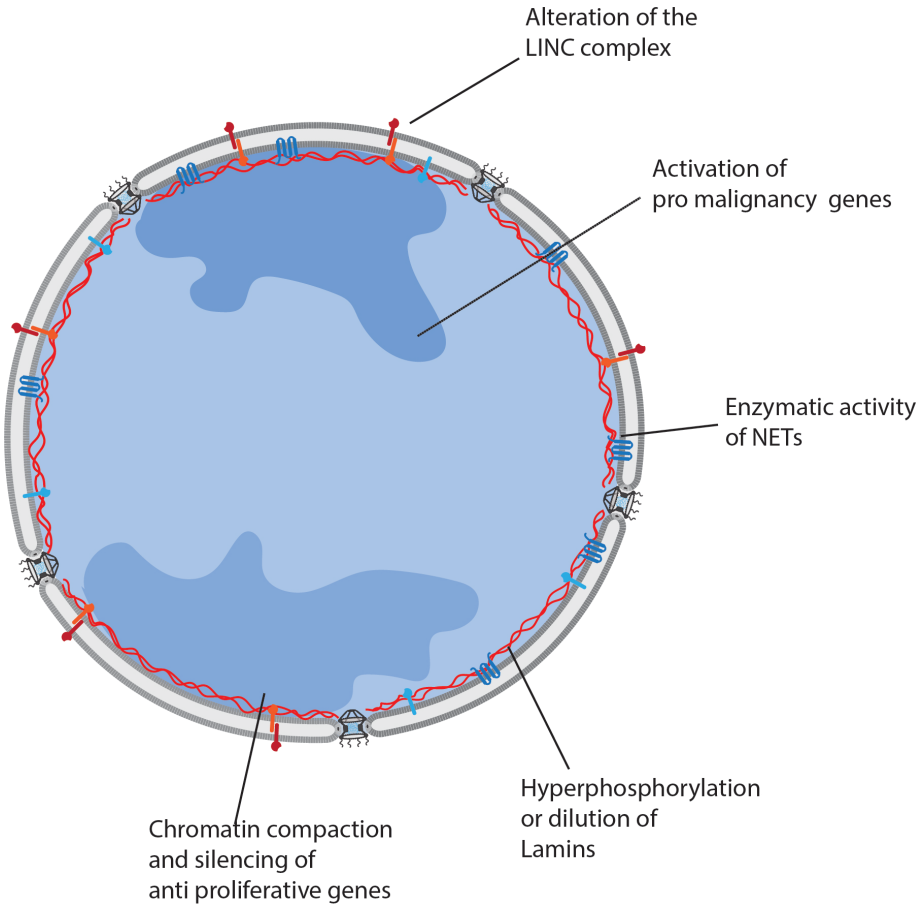

Figure 3 ***Schematic representation of possible factors influencing nuclear size.*** *Different factors can influence or alter nuclear size altering the karyoplasmic ratio, one of the morphological hellmarks of cancer. Enzymatic functions of NETs, for example lipid synthesis enzymes, lipid flippases or sterol-modifying enzymes, can directly influence the nuclear size by de-novo synthesis or degradation of lipids. Disassembly of lamins due to hyperphosphorylation, as the same principle of NE breakdown during mitosis, or dilution effects due to reduction or increment of expression may modulate nuclear size, increasing or decreasing the mechanical stability of the nuclear meshwork. Finally, recruitment and silencing of different genes at the periphery by NETs could affect key regulatory genes directly involved in the maintenance of the nuclear size.*

1.5 Components of the Nuclear Envelope that can regulate nuclear size

As is becoming more and more clear thanks to extensive research in the nucleus field, the NE is not just a mere barrier that separates the genetic information from the components of the cytoplasm, but is a dynamic organelle participating actively in different cell regulation processes. The NE comprises of several proteins with different functions that can also be responsible for regulation or maintenance of a correct nuclear size, and for which alteration during cancer progression may give cancer cells advantages resulting in more

aggressive tumours. Although there are several functional overlaps for proteins at the NE, as for example mechano-transduction of stimuli from the cytoplasm to the nucleoplasm, in general the INM has the functions to interact with chromatin and generate a transcriptionally repressed environment though it is more a regulatory environment than repressive as in cell types with less peripheral heterochromatin the NE can promote gene expression. This side of the NE comprises of the intermediate filament meshwork generated by lamins, proteins that interact with lamins and chromatin such as Emerin, LAP2 or MAN1 and the SUN proteins part of the LINC complex. On the other hand, the ONM has roles of connecting with the cytoskeleton, nuclear positioning and regulation of nucleoplasmic-cytoplasmic transport. This side of the NE comprises of Nesprin proteins that, connecting with the SUN proteins in the INM, form the cytoplasmic side of the LINC complex. Aside from these well-known proteins, there are other NETs that can localize either in the INM or the ONM and can interact with soluble factors and associated proteins, some of which may actively regulate nuclear size.

1.5.1 Lamins

Lamins are good candidates to limit/regulate nuclear size as they form an intermediate filament polymer, the nuclear lamina, that provides the main mechanical stability and architecture to the nucleus (Broers et al. 2004; Lammerding et al. 2004b; Lee et al. 2007). Moreover, lamins are also the most abundant NE proteins at ~9 million copies per mammalian cell nucleus (Busse et al. 2011). Thus their limitation due to down regulation or degradation might be predicted to restrict nuclear growth. Consistent with this view, lamins influence nuclear size in *Xenopus laevis* embryos in a manner that depends on import of lamin B3 which is reported to be required for NE growth during egg development (Jevtic and Levy 2015). Both *Xenopus* and mammalian studies have concluded that lamins are essential for nuclear scaling during interphase and their limitation leads to failure in proper nuclear scaling (Jenkins et al. 1993; Jevtić et al. 2015; Newport, Wilson, and Dunphy 1990).

Notably, from the standpoint of a limiting function, several NPC proteins have also been linked to cancer and nuclear size regulation (Simon and Rout 2014). Lamins could also contribute to nuclear shape changes in cancer cells as their loss or mutation in several heritable diseases yields defects in nuclear morphology (Brown et al. 2008; Schirmer, Guan, and Gerace 2001; Sullivan et al. 1999).

Despite these results, it is unlikely that, apart from being limiting for growth, lamins could actively regulate nuclear size on their own as both the total amount of lamin protein and the relative amounts of different lamin subtypes in the nuclear lamina change during development (Lehner et al. 1987; Röber, Weber, and Osborn 1989; Stick and Hausen 1985). A-type lamins, encoded by the *LMNA* gene, are present in the earliest embryonic stages from maternal protein, but are not expressed at these stages so that they quickly disappear and are not present through most embryonic stages until they are expressed and reappear later in tissue differentiation (Benavente, Krohne, and Franke 1985; Broers et al. 1997).

The changes in lamina constitution in development is interesting in light of changes observed in lamina constitution in some cancer types. The general tendency observed is that B-type lamins continue to be expressed in tumours while A-type lamins are down-regulated (Agrelo et al. 2005; Kaufmann et al. 1991; Venables et al. 2001). Because A-type lamins appear later in development, this led to the idea that their loss reflects retro-differentiation or de-differentiation and so might drive or at least reflect the return to a more proliferative and undifferentiated state (Kuzmina et al. 1984). However, research in this direction was dropped when it was observed that for some cancer types such as colorectal cancer the more metastatic tumours had increased A-type lamin levels (Willis et al. 2008). Though at the time this appeared to kill the retro-/de-differentiation theory, subsequent independent work outside the cancer field found that in epithelia such as the colonic crypts, the early progenitor cell lineages at the base of the crypts that are the most proliferative in fact express lamin A. Expression of lamin A then disappears along the sides of the crypt as the cells differentiate and it becomes expressed

again in the more differentiated cells at the top of the crypts (Willis et al. 2008). Much more recent work additionally revealed that lamin A functions inside the nucleus can influence the expression of genes encoding proteins that contribute to actin bundling and dynamics such as T-plastin (Willis et al. 2008). This could explain how a lamin A-expressing tumour could lead to metastasis and tumour spread as cell mobility would be increased and, indeed, other studies with lamin A knockout cells found that in the absence of lamin A, cells migrated into a scratch wound more slowly (Ho et al. 2013; Lee et al. 2007). Interestingly, while this beautifully explains how lamin A-expressing tumours can be more metastatic, it leaves us even more in the dark with regard to understanding the contribution of loss of lamin A in most cancer types to tumorigenesis. Moreover, as lamins are widely expressed in all the tissues, this is not consistent with the nuclear size tissue specificity shown in different types of cancer, suggesting the involvement of more tissue specific proteins contributing to specific cancer phenotypes.

1.5.2 Nuclear pore complex (NPC)

Another key perinuclear structure that can affect nuclear size and shape by mechanical support or by its function is the NPC. As the NPC in vertebrates is a >60 MDa macromolecular structure that facilitates nuclear-cytoplasmic transport and interacts with different NETs it is easy to speculate an important role for this structure in the regulation of nuclear size and shape. Nuclear size could be influenced by the amount of transported constituents into the nucleoplasm, and in fact defective assembly of NCPs in mammalian cells results in a reduction in nuclear growth (Franz et al. 2007; Walther et al. 2003). At the same time an increase in the number of NPCs is unlikely to account for nuclear growth, as shown when inhibition of de novo synthesis did not influence the nuclear growth rate (Maeshima et al. 2010). This could be due to the high capacity of transport of this structure, and there may be a threshold level and it does not take many NPCs to achieve that threshold. Therefore, the number of NPCs would need to be extremely altered to sufficiently block the transport of molecules into the nucleus. As most of proteic components of the

nucleoplasm are synthetized in the cytoplasm and rely on the association with their nuclear transport receptors and interaction with nucleoporins to be translocated, the NPC can be considered an indirect regulator of nuclear size, which if defective could limit the amount of molecules or proteins necessary for the maintenance of normal nuclear size and shape such as lamins. In fact, alterations of nuclear transport are frequently detected in cancer cells (Kau, Way, and Silver 2004), but they influence a vast range of mechanisms, such as alteration of expression levels, transport of tumour suppressor proteins, or posttranslational modifications of the nuclear transport receptor and their partner proteins.

Moreover, other than limiting the resources necessary for nuclear growth, cytoplasmic to nucleoplasmic transport can influence the nuclear size with the import of specific factors resident in the cytoplasm. This has been demonstrated in *X. laevis* and *X. tropicalis* where modulating the levels of importin α and Ntf2 was sufficient to alter nuclear size in both of the egg extracts, with importin α positively modulating bulk import rates and Ntf2 negatively regulating nuclear size by slowing down large cargo translocation through the NPC (Riddick and Macara 2005). Alteration of the transport of different factors is commonly seen in different cancers, Moreover importin α expression has been suggested as a good biomarker for aggressive cancers, as it is upregulated in metastatic breast (Dahl et al. 2006; Gluz et al. 2008) and non-small-cell lung cancer (Wang et al. 2011).

1.5.3 Linkers of the nucleoskeleton to the cytoskeleton (LINC) complex

Connections between the nucleus and the cytoskeleton contribute to both the overall mechanical stability of the cell and its migratory capacity (Broers et al. 2004; Lammerding et al. 2004b; Lee et al. 2007). Such connections could in theory enable all major cytoplasmic filament systems to contribute to nuclear size regulation as actin microfilaments, microtubules and intermediate filaments all connect to the NE (Roux et al. 2009; Wilhelmsen et al. 2005; Wilkie et al. 2011). As for lamins, nesprins also contribute to nuclear

size, so that mutations in nesprins have been linked to muscular dystrophies that also exhibit aberrant NE organization (Zhang et al. 2007) and two nesprins in particular, Nesprin-2 and Nesprin-3, have been proposed to form a cytoplasmic cage around the nucleus to contribute to its mechanical support (Lu et al. 2012). Moreover, NE blebbing and severely misshapen nuclei are the result of silencing the Nesprin-2 giant protein (Luke et al. 2008a), and removal of the nesprin proteins from the NE leads to an expansion of the NE lumen (Zhang et al. 2007).

The LINC complex is also involved in nuclear positioning and recent studies have shown the involvement of Transmembrane Actin-associated Nuclear (TAN) lines, composed of nesprin-2G and SUN2, in centrosome orientation (Gant Luxton et al. 2011; Luxton et al. 2010). As centrosome orientation has been directly implicated with cell migration (Gomes, Jani, and Gundersen 2005; Schmoranzer et al. 2009) it is easy to speculate that aberrant expression of these proteins in tumours can result in advantages in the migratory potential for cancer cells. Moreover, as these proteins link the nucleus with a complex meshwork of microtubules, actin and intermediate filaments, alteration of the amount of proteins can directly result in alteration of the nuclear size due to gain or loss of anchor points with the cytoplasmic connections. Furthermore, regarding the possible importance of the LINC complex in nuclear size regulation, it has been shown that siRNA knockdown of Nesprin-1α leads to enlarged cell size (Luke et al. 2008a), unbalancing the karyoplasmic ratio, and knockout mice for the giant isoform of Nesprin-2 present a thicker dermis attributed to enlarged nuclear size (Zhang et al. 2007).

1.5.4 Inner nuclear membrane NETs

In the same way that SUN and Nesprin family proteins segregate between the ONM and INM, so do other NETs. There are now many hundreds of NETs that have been identified by proteomics of isolated nuclear envelopes, most of which are tissue-restricted in expression or NE targeting (Fig 4) (Korfali

et al. 2010, 2012; Robson et al. 2016; Wilkie et al. 2011), suggesting that they might contribute to the tumour tissue-type specificity of nuclear size effects in cancer. Over 50 NETs have been characterized by super resolution microscopy for their accumulation in the ONM or INM, with a strong majority favouring the INM (Korfali et al. 2010; Malik, Korfali, et al. 2010; Wilkie et al. 2011).

Many INM NETs interact with lamins and chromatin and play important roles in gene/chromosome positioning, chromatin organization and epigenetics, and genome regulation (Mattout-Drubezki and Gruenbaum 2003; Robson et al. 2016; Schirmer and Foisner 2007; Solovei et al. 2013; Srsen et al. 2011). Though most of the general radial chromosome positioning is based on gene density (Croft et al. 1999), each tissue also has a subset of genes and chromosomes that reposition during differentiation in a tissue-specific manner (Kim et al. 2004; Morey et al. 2008; Parada et al. 2004; Szczerbal, Foster, and Bridger 2009). The general positioning trends appear to be driven by heterochromatin interactions with lamins and the NET, lamin B receptor (LBR), that binds directly to heterochromatin protein 1 (HP1) (Solovei et al. 2013). In general, the periphery tends to be a more silencing environment based on expression profiles and epigenetic marks of genome-wide identified genes that reside there (Akhtar et al. 2013). The more tissue-specific gene and chromosome positioning patterns are directed by tissue-specific NETs. For example, liver NETs NET45/Dak and NET47/TM7SF2 are important for positioning to the NE of chromosome 5 in liver cells (Zuleger et al. 2013) and muscle NETs NET39/PPAPDC3, Tmem38A, and WFS1 are important for positioning to the NE of several genes that need to be tightly shut down in a temporal fashion later in muscle differentiation though they are needed in earlier stages (Robson et al. 2016). Interestingly, there are also many genes involved in cell proliferation that reposition to the more repressive environment of the NE in tissue differentiation because they must be tightly shut down when the cells exit the cell cycle to differentiate (De Las Heras et al. 2017; Robson et al. 2016, 2017). Thus, alteration of the normal expression patterns for such

NETs in cancer could support metastasis by increasing expression of proliferative genes.

Other important proteins at the INM that may contribute to nuclear size regulation through contacts with the chromatin are LAP2, Emerin and MAN1. These proteins share the so called LEM domain, a bi-helical structural domain that can interact with several chromatin binding proteins (Cai et al. 2001). An important interaction, for both LAP2 and Emerin, is the Barrier-to-Autointeration Factor (BAF) involved in binding chromatin and repressing it at the NE (Cai et al. 2007; Shumaker et al. 2001). Moreover, both NETs are able to directly bind the histone deacetylase HDAC3 to further silence chromatin (Demmerle, Koch, and Holaska 2012) allowing promotion of chromatin compaction at the NE. It is clear that loss of these proteins during cancer progression can influence nuclear size regulation, both through loss of connections between the NE and chromatin and by release and activation of silenced genome regions containing pro-oncogenic genes.

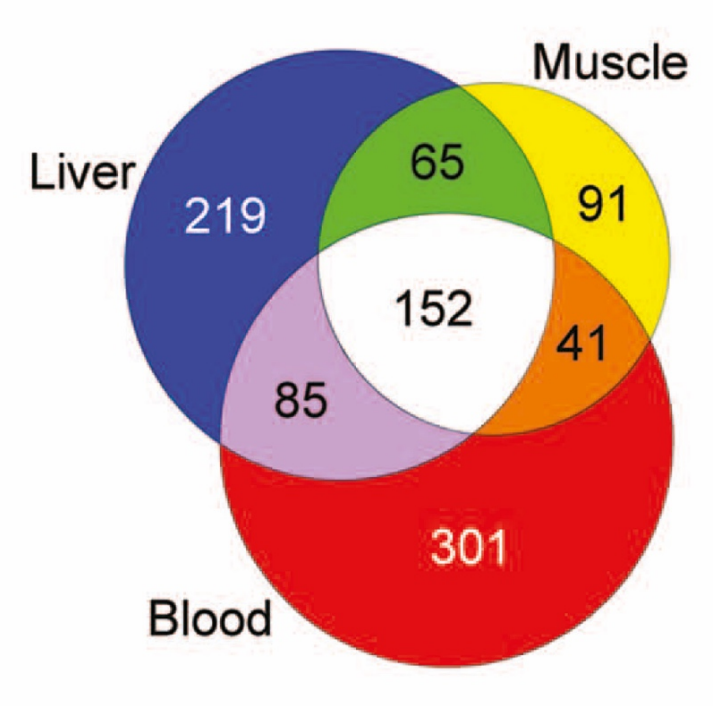

Figure 4 ***Tissue specificity of NETs.*** *NETs identified in Korfali et al. 2012 show a tissue restricted profile, with every tissue presenting a distinct and specific NE proteome.*

1.5.5 Outer nuclear membrane NETs

Some ONM NETs, like nesprins, mediate interactions with cytoplasmic filaments. For example, NET5/Samp1 is important for associations between the nucleus and the centrosome that organizes microtubules (Buch et al. 2009). Others are involved in cell cycle regulation, for example NET4/Tmem53 activates a seemingly stress-induced p38 kinase pathway that results in cell cycle withdrawal when its levels are perturbed (Korfali et al. 2011). Another ONM NET affecting the cell cycle, NET31/Tmem209, is able to alter cancer cell growth when overexpressed in lung cancer cells and interestingly is upregulated in lung cancer cells and normal testis that contain highly proliferative cells (Fujitomo et al. 2012). As loss of proliferation control is a hallmark of cancer cells, these NETs could also be highly relevant to metastatic tumours, though they have thus far not been linked to nuclear size regulation. Very little is known about most other ONM NETs.

1.5.6 Cytoskeleton

Due to the close interactions between the nucleus, NETs, LINC complex and the cytoskeleton, alterations of the main filament network of the cell can influence and alter the nuclear morphology. Throughout cell movement, the nucleus undergo shape and size alteration with the cytoskeleton rearranging actin filaments and microtubules to allow the process of migration. The nucleus is positioned away from the leading edge creating a leading edge/centrosome/nucleus axis in the direction of the migration. This nuclear rearward movement is driven by an actin retrograde flow mediated by myosin and Cdc42 (Barnhart et al. 2010; Gomes et al. 2005; Tsai and Gleeson 2005). The nucleus is also drastically pushed, pulled and deformed during migration through the ECM and endothelial cells possible by the activation of the ESRCT-III machinery and formation of perinuclear actin network that protect the nucleus while transitioning through confined spaces (Denais et al. 2016; Raab et al. 2016). It results clear that alterations of the expression or inhibition of the assembly of the cytoskeletal elements could result in the severe

alteration of the nuclear size and shape. This has been elegantly demonstrated with inhibition of the cytoskeletal filaments assembly preventing alteration of the nuclear shape and position when the cell is mechanically stressed with a micropipette (Ghosh et al. 2008; Maniotis, Chen, and Ingber 1997).

1.5.7 Non-resident factors

Different cytoplasmic factors have been shown to influence nuclear scaling. As the karyoplasmic ratio has been established to be maintained throughout the cell cycle, one of the first factors that has been investigated for the ability to alter nuclear size is the cytoplasmic volume. To test the dependency of nuclear size on the cytoplasmic volume a study generated a cytokine *S.pombe* mutant, allowing the formation of multinucleated cells. Nuclei surrounded by a greater cytoplasmic volume were bigger that the ones surrounded by a smaller cytoplasmic volume. If these cells are subjected to ultracentrifugation and then allowed to divide, cells with a larger amount of cytoplasm adjusted the nuclear volume rapidly to re-establish a normal karyoplasmic ratio, where cells in which the nuclei were too big for the surrounding cytoplasmic volume, nuclear growth was arrested until the cytoplasm reached an optimal volume (Neumann and Nurse 2007).

As well as soluble factors that can shuttle between cytoplasm and nucleoplasm also activation of oncogenes could potentially have an impact in nuclear size alteration. Throughout cancer progression several genes are repressed and activated due to the genomic instability of the cell, these genes could influence up or downregulation of proteins that can impact the stability of the nuclear architecture. A direct link between oncogenes and nuclear size regulation is not evident yet but the nuclear envelope interacts with several pathways, especially through lamin A/C interactions, that result altered during cancer progression. Lamin A/C for example interact directly with LAP2β, and both proteins can regulate pRB resulting in accumulation of hyperphosphorylated pRB, leading to delay in cell cycle (Johnson et al. 2004). Furthermore, downregulation of lamin A/C results in mislocalization and

proteasome degradation targeting of pRB, suggesting increase proliferation through the loss of the pRB checkpoint (Bell and Lammerding 2016).

The nuclear envelope can interact also with β-catenin, modulating the Wnt/β-catenin signalling. Recent studies have proven direct interaction of Emerin with β-catenin, repressing its activity through negative regulation of nuclear accumulation (Markiewicz et al. 2006). Furthermore, also Nesprin 2 is able to interact with both α-catenin and β-catenin and depletion of this protein lead to reduction of nuclear accumulation of β-catenin (Neumann et al. 2010), pointing to how the nuclear envelope is tightly interconnected in the regulation of different oncogenes pathways that could result in advantages for cancer cells.

It is quite clear then that different cytoplasmic factors can influence nuclear volume by different mechanisms and abundance of particular proteins. It remains to be elucidated what all of these factors are and if they can be modulated to reduce aberrant alteration of the nuclear size in order to treat patients more effectively.

1.6 Link between the NE and cancer

Although little is known about the majority of NETs, to determine their likelihood of contributing to cancer progression or metastasis, analysis of NETs identified in NE proteomic studies for changes in different tumour types using the TCGA cancer database (https://cancergenome.nih.gov) revealed that many tend to be lost or inappropriately expressed in a variety of tissue-specific tumour types (Fig 5B). The TCGA is a project funded by the NIH for the sequencing and identification of genetic mutations causing cancer. The project sequenced and determined gene copy number and SNPs alterations, among many other variations, in patients samples of around 20-25 types of different cancers. One example of tissue specific proteins altered in cancer is the NET, LPCAT3, a protein expressed relatively widely, but not in ovaries. Its expression profile changes drastically in certain cancer types, with it being strongly upregulated in ovarian cancer but down-regulated in lung cancer (Fig

5C) (de Las Heras, Batrakou, and Schirmer 2013; de Las Heras and Schirmer 2014). The tissue-specific differences characteristic of each tumour type may be at least partly explained by such changes in these tissue specific NETs during cancer progression.

Another interesting example is that analysis of patient sequences in the TCGA cancer database revealed relatively high mutation frequencies with mutations in *SYNE1* (encoding nesprin 1) reaching 26% in Stomach Adenocarcinoma, 24% in Skin Cutaneous Melanoma and 21% in Colon Adenocarcinoma. Other nesprins were also highly mutated in specific tumour types with *SYNE2* (encoding nesprin 2) mutated in 20% of Liver Hepatocellular Carcinoma patients and more than 10% in at least four different cancer types. Interestingly, *SYNE3* (encoding nesprin 3) was only highly mutated in Pancreatic Adenocarcinoma, at 24% of patients, with the next highest mutation frequency being at just 3% in Lung Adenocarcinoma, indicating considerable tissue-specificity even just amongst this protein family in its potential relationship to cancer. Notably, several different cancers had much lower levels of mutations in SYNE/nesprin proteins, often as much as 100-fold lower (Fig 5A).

Given the alteration of different genes and expression of proteins at the NE, screening for nuclear size alterations caused by lost or gain of these proteins might bring more clarity to tissue specific phenotypes detected in different type of cancers.

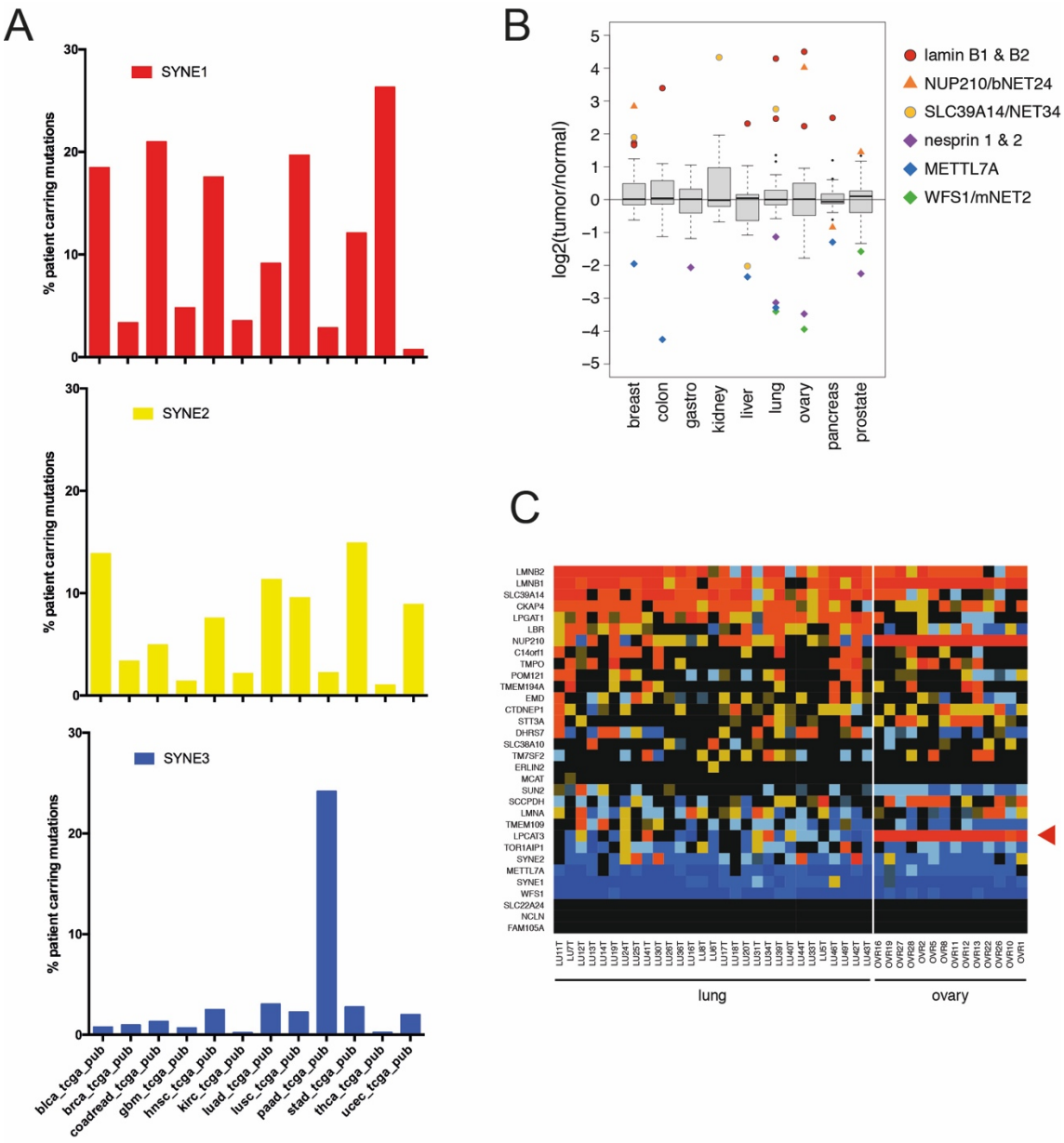

Figure 5 ***NET tissue specificity and alteration in cancer.*** *A Alteration of SYNE genes encoding nesprins in different cancer types. Accumulation of mutations in SYNE genes differs for each gene and for each tumour type. For example, SYNE3 is only highly mutated in Pancreatic Adenocarcinoma while SYNE1 and SYNE2 are highly mutated in a larger, but partly distinct, set of cancers. Blca: Bladder Urothelial Carcinoma; Brca: Breast Invasive Carcinoma; Coadread: Colon Adenocarcinoma; Gmb: Glioblastoma Multiforme; Hnsc: Head and Neck Squamous Cell Carcinoma; Kich: Kidney Chromophobe; Kirc: Kidney Renal Clear Cell Carcinoma; Luad: Lung Adenocarcinoma; Lusc: Lung Squamous Cell Carcinoma; Ov: Ovarian Serous Cystadenocarcinoma; Paad: Pancreatic Adenocarcinoma; Stad: Stomach Adenocarcinoma; Thca: Thyroid Carcinoma. B. Boxplot of log2(tumour/normal) microarrays signals form different nuclear genes in tumour different tissues. Some genes show upregulation (e.g. lamin B1 and B2) or downregulation (e.g. WFS1) in specific tissue tumours but not on others. C. Heatmap of 29 nuclear envelope genes up or downregulation in different lung and ovary tumour tissues. The nuclear envelope gene LPCAT3 (red arrow) is not normally expressed in healthy ovary tissues, but strongly upregulated in ovary cancer, where there is not significant alteration in lung tumour tissues. (de Las Heras and Schirmer 2014)*

1.7 Potential mechanism of nuclear size regulation

As the NE is the outer shell that delimits the nucleus, many NE proteins might be limiting or influencing nuclear size alterations. These range from NPC transport functions to the lamin scaffolding to the connections to cytoplasmic filaments or proteins involved in lipid synthesis. Such proteins could be under a feedback regulatory mechanism for amounts synthesized or a timed mechanism that links nuclear size increases during the cell cycle to the length of a particular stage. Thus changes to gene expression and cell proliferation in cancer cells might underlie nuclear size changes. Notably, such changes in gene expression could themselves be influenced by nuclear size changes if this alters the relative amount of peripheral heterochromatin and gene silencing (Fig 6A). Some of the NETs have been shown to be able to reposition entire chromosome from an active state to the NE periphery where the genes get repressed (De Las Heras et al. 2017; Zuleger et al. 2013). Examples of these NETs are NET39, WFS1 and TAPBPL. These proteins are able to reposition chromosome 5 from the interior to the periphery of the nucleus, leading to inactivation of important genes for muscle development (Robson et al. 2016). It results clear that loss of proteins with this ability to anchor genes to a heterochromatin environment during cancer progression can lead to alteration of genes that regulate nuclear size and can therefore drastically influence the nuclear architecture. At the same time an abnormal alteration of the nuclear size without a feedback mechanism that can re-supply the physiological amount of protein at the NE can lead to less anchor points at the membrane and therefore to the release of a gene that would be normally repressed.

It is also possible that a completely independent sensor mechanism maintains the karyoplasmic ratio, for example sensing a change in tension between chromatin contacts and the NE on one side and connections with cytoplasmic filaments on the other. If this were the case then changes in cancer cells to NE-chromatin or NE-cytoplasmic filament interactions might underlie nuclear size changes. For example alteration of key proteins in the

LINC complex using a dominant-negative nesprin mutant led to nuclear size defects (Lu et al. 2012) and knockout mice lacking the Nesprin-2 giant isoform resulted in thickening of the dermis due to increased nuclear size (Luke et al. 2008a). Such changes could also explain nuclear shape changes and NE blebbing that often accompanies the size changes in cancer cells (Fig 6B).

Thus, in theory, alteration of the expression of nesprins in cancer could lead to changes in cytoskeleton and nuclear stiffness and elasticity, nuclear shape, and nuclear size and accordingly enable extravasation of tumour cells during metastatic spread

A third mechanism might involve post-translational modifications, particularly phosphorylation cascades that often go awry in cancer cells. Such modifications are important for both the stability of the lamin polymer and for NE-chromatin interactions. Indeed, mitotic disassembly of the lamin polymer is coupled with hyperphosphorylation of both lamins and NETs to break the interactions between them and their interactions with chromatin (Fig 6C).

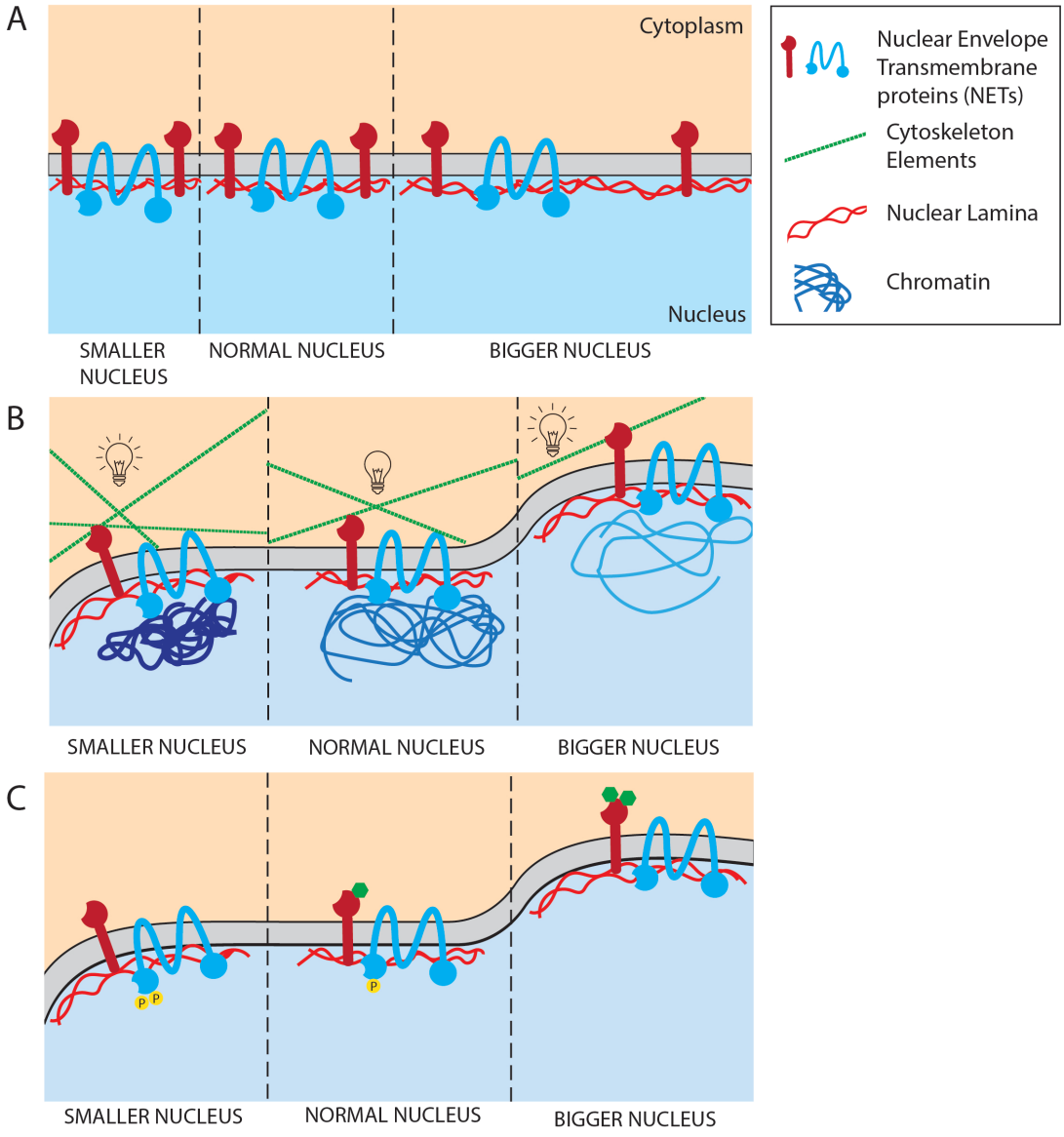

Figure 6 ***Potential mechanism of nuclear size regulation.*** *A. Control of expression levels for scaffolding proteins regulating nuclear size. Reduction of scaffolding proteins such as lamins through gene misregulation could be limiting for nuclear size increases (left). At the same time, up-regulation of such proteins could promote nuclear growth (right). B. Sensor mechanism regulating the nucleoplasmic-cytoplasmic ratio. The sensor might sense alterations of tension between the NE and chromatin and/or the cytoskeleton and alter nuclear size accordingly. C. Post-translational modifications occurring on NE proteins. Analogous to how hyperphosphorylation of lamins triggers their disassembly in mitosis, modifying proteins at the NE could alter nuclear size. (Rizzotto and Schirmer 2017)*

1.8 Advantages of nuclear size alteration in cancer

The central conundrum that faces us is how can both nuclear size increases and decreases promote increased metastasis in different tumour types? A smaller nuclear size could obviously convey the advantage of being able to squeeze through junctions between cells during invasion of other tissues, but one might expect that a larger nuclear size would hinder this. This apparent contradiction might be resolved when considering that the NE connects to both cytoplasmic filaments on one side and chromatin on the other side. The largest molecules in the cell are the chromosomes that reach gigadalton masses and dwarf even actin stress fibers in total size. Several studies have shown that chromatin connections to the NE are similarly important as the intermediate filament lamin polymer for nuclear shape and mechanical stability (Thorpe and Charpentier 2017; Thorpe and Lee 2017). If the increase in nuclear size reduces the strength of heterochromatin interactions with the NE then this could enable an even larger nucleus to distort and squeeze between cell-cell junctions for invasion (Fig. 7). At the same time, there might be an even simpler explanation if both nuclear size increases and decreases are associated with changes in cytoplasmic filament connections that facilitate cell migration. The findings that altering levels of both lamins and LINC components affects cell migration in wound healing assays (Lee et al. 2007) indicates the likelihood of this possibility. Furthermore, tissue-specific NETs that contribute to lamin-LINC-cytoplasmic filament connections could confer the tumour-type specificity for this nexus. Importantly, such disruption of the even larger chromatin-lamin-LINC-cytoplasmic filament nexus could additionally weaken the mechanical stability of the nucleus to explain the changes in nuclear shape including blebbing that often accompanies nuclear size changes (Fig. 7).

A larger nuclear size accompanied by a reduced heterochromatin interaction with the nuclear periphery might also enable faster proliferation for metastasis, not just through changes in gene expression or post-translational

modifications as mentioned above, but also by having less late-replicating peripheral heterochromatin and having to break fewer genome-NE contacts when replicating the genome. Changes in such contacts could also influence overall genome stability whether due to loss of lamin A or a tissue-specific NET. Notably, lamins also bind pRb and can affect proliferation by sequestering or releasing pRb (Van Berlo et al. 2005; Johnson et al. 2004). Similarly several NETs have been shown to bind transcriptional regulators and Smads for example are sequestered by the NET MAN1 away from target genes in the nucleoplasm such that altering MAN1 can yield bone disorders (Ishimura et al. 2006; Osada 2003; Pan et al. 2005). Thus both lamins and tissue-specific NETs can influence metastasis through effects on proliferation that could parallel nuclear size changes from the same proteins.

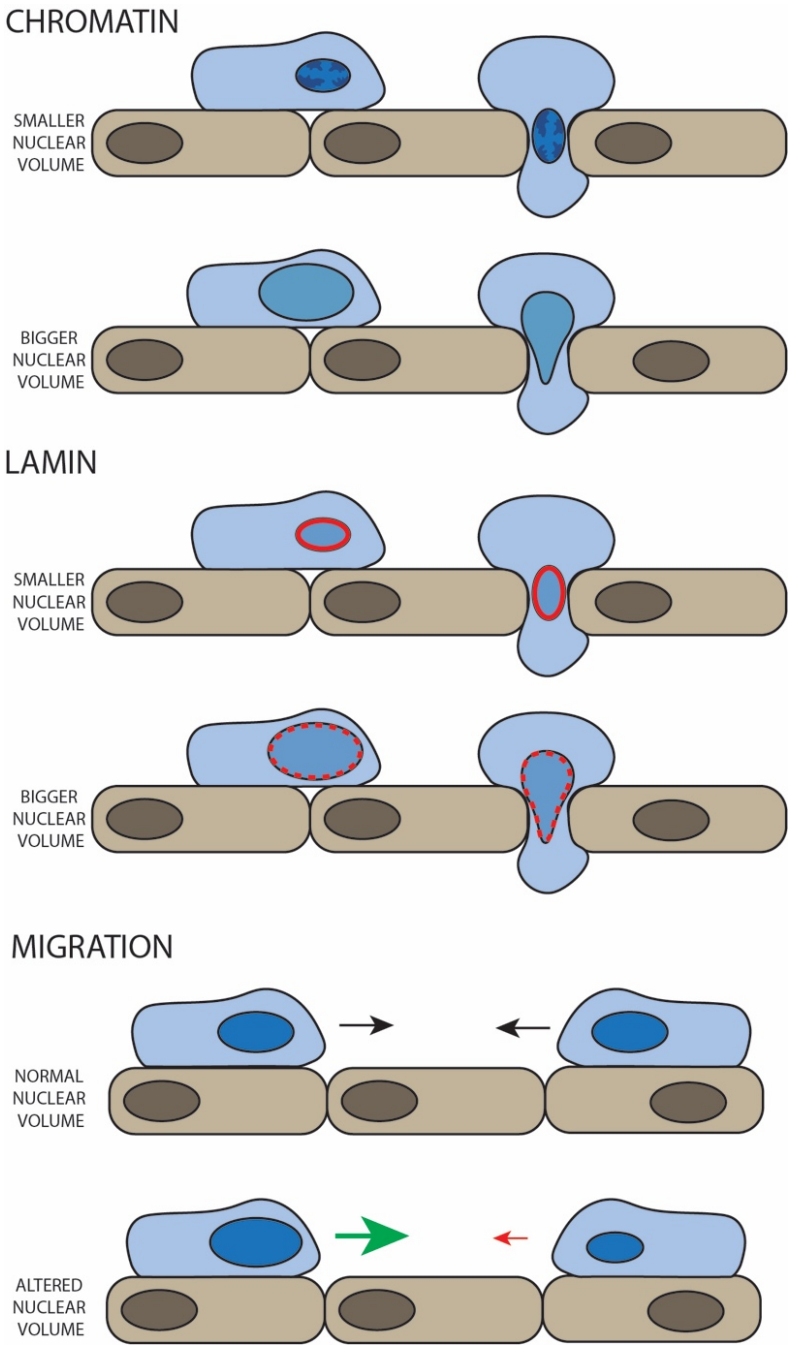

Figure 7 ***Advantages to cancer cells of nuclear size changes.*** *A. Smaller nuclei with more compact chromatin could more readily squeeze between tight cell–cell junctions to invade a tissue (top). If a bigger nucleus has fewer interactions with chromatin and/or more euchromatin, this might enable greater malleability for the nucleus to change shape to squeeze between cell–cell junctions (bottom). B. Alterations of lamin and LINC complex connections. Loss of lamins can weaken the mechanical properties of the nucleus, allowing easier deformability in squeezing through cell–cell junctions and so increasing metastasis (upper panels). The connections between the nucleoskeleton and cytoplasmic filaments also affect cell migration in wound healing assays, and so, their disruption could result in an increased speed for migration of the cancer cell (bottom panels). Note that in this case both changes to larger and smaller nuclear size could alter nuclear migration properties.(Rizzotto and Schirmer 2017)*

1.9 Aims and hypothesis

Regulation of nuclear size and shape is a complex mechanism that may be important in many aspect of cancer progression, from diagnosis to potential alteration to gene expression favouring more metastatic tumours. As these alterations are characteristic of different tumour types the efforts to identify the factors that direct the process of maintaining a normal nuclear size and shape have been focusing on communal structures such as lamins or the LINC complex, and not taking into consideration the tissue specificity of phenotypes. NETs have been shown to be tissue specific, or at least tissue restricted, and with effects in genome repositioning highly dependent of the tissue where they are expressed. Therefore, NETs can be one of the key players in conferring the tissue specific alterations found in different tumour types.

Targeting proteins involved in nuclear size regulation can result in better outcomes for patients, and provide valuable new targets for new drugs to be added to chemotherapy regimens. Importantly the tissue specificity should focus toxicity and thus reduce some of the side effects typical in chemotherapy regimens. For this reason, we are also interested in identifying potential small molecules that are able to alter nuclear size, in order to restore normal size, that can be used in conjunction with other drugs to reduce tumour size or slow down generation of metastasis.

1.9.1 Pervious work towards understanding nuclear size regulation

In line with this hypothesis, a previous MSc student and honours student have screened for NETs altering the nuclear size through transient transfection of some of the constructs used in this study. A 2D nuclear size screen of 10 different NETs was performed analysing the mid-cross sectional area of the nucleus in an asynchronous HT1080 population. This screen identified 4 proteins with potential nuclear size regulation, namely NKP9, NET50, NET26 and Emerin (Bernard Hörmann Master thesis) (Fig 8). To have more precise

and robust measurements and overcome the problem of different nuclear sizes across an asynchronous population, a more in depth 3D analysis was carried out in a double thymidine blocked population, focusing on the positive hits identified in the first screen. NETs were transiently expressed in the synchronised culture and volume reconstruction of the whole nucleus was extrapolated from deconvolved z-stack series. This analysis revealed that emerin, NKP9 and NET50 have effects on the nuclear size and may be active in the nuclear size regulation (Edward Jarman Honours project) (Fig 8). Based on this preliminary data we decided to screen for more NETs to potentially identify tissue specific nuclear size regulators that can be involved in or responsible for the phenotypes detected in different type of cancers and also screen for small molecules affecting nuclear size. This is the work that will be presented in the following chapters.

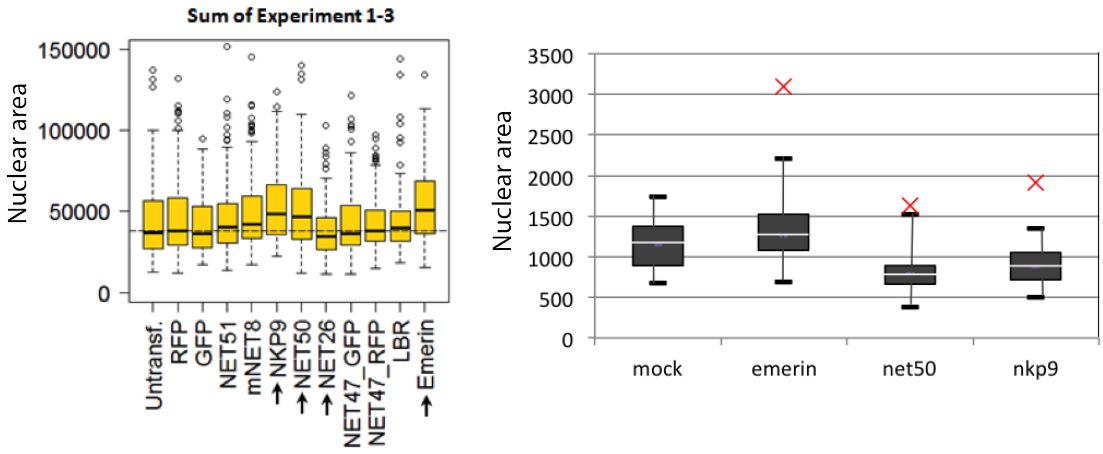

Figure 8 ***NETs affecting nuclear size.*** *Box plots showing the sum of preliminary experiments for the identification of NETs affecting the nuclear size. The screens identified three potential NETs (Emerin, NET50 and NKP9) able to alter the nuclear architecture when overexpressed in the HT1080 human fibroblast cell line. (Hörmann and Jarman Master thesis)*

2. Material and methods

2.1 Materials

2.1.1 Bacterial strains and genotypes

DH5alpha

F– endA1 glnV44 thi1 recA1 relA1 gyrA96 deoR nupG purB20 φ80dlacZΔM1 5 Δ(lacZYA-argF)U169, hsdR17(rK–mK+), λ–

Sure2

endA1 glnV44 thi-1 gyrA96 relA1 lac recB recJ sbcC umuC::Tn5 uvrC e14- Δ(mcrCB-hsdSMR-mrr)171 F'[proAB+ lacIq lacZΔM15 Tn10 Amy CmR]

PLys-S

F– ompT gal dcm lon hsdSB(rB–mB–) λ(DE3 [lacI lacUV5-
T7p07 ind1 sam7 nin5]) [malB+]K-12(λS) pLysS[T7p20 orip15A](CmR)

TOP10

F- mcrA Δ(mrr-hsdRMS-mcrBC) φ80lacZΔM15 ΔlacX74 nupG recA1 araD139 Δ(ara-leu)7697 galE15 galK16 rpsL(StrR) endA1 λ-

Rosetta (DE3)pLysS

E. coli str. B F– ompT gal dcm lon? hsdSB(rB–mB–) λ(DE3 [lacI lacUV5-
T7p07 ind1 sam7 nin5]) [malB+]K-12(λS)
pLysSRARE[T7p20 ileX argU thrU tyrU glyT thrT argW metT leuW proL orip1 5A](CmR)

2.1.2 Buffers and solutions

Table 2 ***Buffer used and relative composition***

Buffer/Solution name	Composition
Luria Bertani (LB) medium	1% Tryptone 0.5% yeast extract 200 mM NaCl
Super Optimal broth with Catabolite repression (SOC)	2% tryptone 0.5% Yeast extract 10mM NaCl 2.5mM KCl 20mM glucose
Phosphate saline buffer (PBS)	50 mM potassium phosphate 150 mM NaCl; pH 7.4
Alkaline Lysis Buffer 1	50 mM glucose 10 mM EDTA 25 mM Tris (pH 8.0)
Alkaline Lysis Buffer 2	0.2 N NaOH 1% SDS
Alkaline Lysis Buffer 3	3 M KOAc (pH 6.0)
Dulbecco's Modified Eagle Medium (DMEM)	High glucose (1 g/L), 100 mM Sodium piruvate Lonza, 12-604F
Roswell Park Memorial Institute medium (RPMI) 1640	High glucose (1 g/L), 100 mM Sodium piruvate Gibco, 11875-093

Opti-MEM	Reduced Serum Medium Gibco, 31985062
TAE	40 mM Tris-acetate 1 mM EDTA
Protein Running Buffer (SDS-Page)	25 mM Tris pH 8.3 35 mM SDS 150 mM NaCl 192 mM glycine

2.1.3 Primary antibodies

Epitope	Host	IF dilution	WB dilution	Band size	Source
NET50/DHRS7	Rabbit	1:50	1:1000	38 kDa	Abcam ab156021
Lamin A/C	Rabbit	1:50	1:1000	70 kDa	Schirmer, 2001
SUN1	Rabbit	1:50	N/A	N/A	Atlas antibodies HPA 008346
GFP	Rabbit	1:100	1:200	25 kDa	Generated by Dizmity Batrakou
RFP	Rabbit	1:100	1:200	25 kDa	Generated by Dizmity Batrakou
α Tubulin	Mouse	1:500	1:2000	50 kDa	Sigma T6074-200UL
γ Tubulin	Goat	1:500	N/A	N/A	Sigma T6557
Emerin	Rabbit	1:50	N/A	N/A	Glenn Morris
Phospho-Stat3	Rabbit	N/A	N/A	N/A	Merck RAB0447
Pan-Stat3	N/A	N/A	N/A	N/A	Merck RAB0447
GAPDH	N/A	N/A	N/A	37 kDa	Thermo Fisher InstaOne ELISA kit 85-86131-11

2.1.4 Secondary antibodies

Antigens targets, source and dilution of antibody used in this study are summarised in table 3. To reduce cross-reactivity in double staining all secondary antibodies were raised in donkey against mouse or rabbit IgG. To reduce signal:noise ratios conjugants to Alexa Fluor® dyes (Molecular Probes, Invitrogen) were used. For Western Blotting, fluorescence labelled IRDye® (Licor) anti-mouse or anti-rabbit were used.

Table 3 ***Secondary antibody used in this study***

Antibody	Host	Dye	Dilution	Source
Anti-mouse	Donkey	Alexa 488	1:500	Invitrogen (A21202)
Anti-rabbit	Donkey	Alexa 488	1:500	Invitrogen (A21206)
Anti-mouse	Donkey	Alexa 568	1:500	Invitrogen (A10037)
Anti-rabbit	Donkey	Alexa 568	1:500	Invitrogen (A10042)
Anti-rabbit	Donkey	Alexa 630	1:500	Invitrogen (A21202)
Anti-mouse	Donkey	IRDye® 800CW	1.1000	Licor (926-32212)
Anti-rabbit	Donkey	IRDye® 800CW	1:1000	Licor (926-32213)

Anti-mouse	Donkey	IRDye® 680CW	1:1000	Licor (926-68073)
Anti-rabbit	Donkey	IRDye® 680CW	1:1000	Licor (926-68073)

2.1.4 Mammalian cells

Human fibrosarcoma cell line HT1080, human cervix adenocarcinoma cell line HeLa, human prostate carcinoma cell line PC3, human colorectal carcinoma cell line HCT116 and human non-small cell lung cancer cell line H1299 were purchased from the American Type Culture Collection (ATCC) collection. Several of these lines were modified to express RFP or other markers as described in the table below.

Table 4 ***Cell lines used in this study***

Cell Line	Type of cancer	Source	Reporter
PC3	Human prostate carcinoma	ATCC® CRL-1435™	
PC3-H2B.mRFP	Human prostate carcinoma	Derived from PC3 cell line	Monomeric RFP
PC3-LUC	Human prostate carcinoma	Derived from PC3 cell line	Enhanced GFP and Luciferase
HCT116	Human colorectal carcinoma cell	ATCC® CCL-247™	
HCT116-H2B.mRFP	Human colorectal carcinoma cell	Derived from HCT116 cell line	Monomeric RFP

H1299	Human non-small cell lung cancer	ATCC® CRL-5803™	
H1299-H2B.RFP	Human non-small cell lung cancer	Derived from H1299 cell line	Monomeric RFP
LNCaP	Human prostate carcinoma	ATCC® CRL-1740™	
HeLa	Human cervix adenocarcinoma		
HeLa-H2B.mRFP	Human cervix adenocarcinoma		Monomeric RFP
HeLa-H2B.GFP	Human cervix adenocarcinoma		Enhanced GFP
HT1080	Human fibrosarcoma cell line		

2.1.5 Chemical compounds

Identified compounds in the screens were purchased in larger quantities from Sigma-Aldrich or CarboSynth (table 5) and were diluted to a 10 mM stock concentration in DMSO and used at the concentration reported in the figures.

Table 5 ***Chemical compinds used in this study.***

Compound name	Source	CAS number	Reference
Oxyphenbutazone	Sigma-Aldrich	129-20-4	SML0540
Paroxetine Hydrocloride	Sigma-Aldrich	110429-35-1	PHR1804

Parbendazole	Sigma-Aldrich	14255-87-9	32438
Piperlongumine	Sigma-Aldrich	20069-09-4	SML0221
Digitoxigenin	Sigma-Aldrich	143-62-4	D9404
Estradiol propionate	CarboSynth	3758-34-7	FE22825

2.2 DNA procedures

2.2.1 Plasmid DNA sequencing

All plasmids used in this study were verified by sequencing. The sequencing was performed by the GenePool facility (University of Edinburgh) using standard Sanger sequencing techniques. Sequence chromatograms were analysed and cross-referenced with the software Lasergene (DNA Star). A full list of plasmids used in this study is reported in the appendix.

2.2.2 Cloning and site direct mutagenesis

Cloning was performed using general restriction enzyme digest and ligation cloning protocols or with the Gibson methodology. All restriction endonucleases II were from the FastDigest system (Fermentas), Phusion DNA polymerase and DNA ligase from New England BioLabs.
The Gibson Assembly Mix was produced in house or via the commercial NEBuilder Assembly Kit (New England BioLabs) following the manufacturer's

recommendations. Briefly, between 50 and 100 ng of vector, depending on the number of inserts used in the reaction mix, were incubated with 0.2-0.5 pmol of inserts at 50°C for 1 h and transformed in DH5alpha cells after DpnI digestion.

Generation of the expression plasmids for mammalian protein expression in bacteria were performed with the BioBrick cloning systems. Inserts were amplified with the addition of overhangs (Forward: 5'-TACTTCCCAATCCAATGCA; Reverse: 5'- TTATTCACTTCCAATTTATTA). The backbone vector was linearized with Ssp I restriction endonuclease II enzyme (NEB) and processed with T4 polymerase (NEB) in presence of dGTP. The inserts were processed in the same reaction mix but in the presence of dCTP. Vector and inserts were annealed at RT for 10 min, transformed and plated in XL1Blue bacteria in the presence of selection antibiotics.

Site direct mutagenesis was performed according to the manufacturer's recommendations for the QuikChange II Site-Directed Mutagenesis Kit (Agilent) with primers designed with the Agilent on-line tool (https://www.genomics.agilent.com/). 4 µl of the PCR amplification product were transformed in TOP10 bacteria via heat shock, after DpnI digestion for 1 h, and spread on plates with the opportune antibiotic resistance.

Extraction and purification of plasmid DNA was performed either with standard alkaline extraction (Buffer 1, buffer 2 and buffer 3) or with QIAprep Spin Miniprep Kit (Qiagen).

2.3 Mammalian cell culture

2.3.1 Mammalian cell lines and maintenance

HT1080, HeLa, PC3, H1299, HCT116 and their derivatives (see Generation of stable cell lines) cell lines were maintained in Dulbecco's Modified Eagle Medium (Lonza) containing 4.5 g/L glucose and L-Glutamine

and supplemented with 10% FBS (HyClone). Human prostate carcinoma cell line LNCaP was maintained in Roswell Park Memorial Institute (RPMI) 1640 Medium containing 4.5 g/L glucose and L-Glutamine and supplemented with 10% FBS (HyClone). All cell lines were maintained at 37°C, 5% CO_2 in a humidified environment.

For experiments where estradiol or estradiol propionate was used cells were maintained in the same condition as above with the substitution of normal FBS with 10% charcoal stripped FBS to deplete hormones intrinsically present in normal FBS. This enables a more clean analysis in hormone experiments with NET50 such that the drug being analysed is not be masked by a mixture of unknown hormones from serum.

2.3.2 Generation of stable cell lines

PC3.H2B.mRFP, HCT116.H2B.mRFP and H1299.H2B.mRFP were generated with co-transfection of linearized H2B.mRFP.BL vector and pTol2 encoding for transposase with JetPrime (PolyPlus transfection) transfection reagent, following the manufacturer's directions. 24 h post transfection the medium was replaced with medium containing 8 µg/ml blasticidin (Thermo Fisher Scientific) to select stable integrated transfectants.

After stable selection and amplification cells were FACS sorted for the brighter mRFP population that retained normal morphology and further amplified before storage in liquid nitrogen.

For the generation of PC3.LUC reporter cells, the progenitor cells were seeded at a concentration of 10^5 cells/well in a standard tissue culture 6 well plate the night before virus transduction. Cells were incubated with 0.5ml lentiviruses carrying the plasmid pHIV-Luc-ZsGreen1, 0.5 ml of standard medium and 0.1 µl of polybrene (stock 10mg/ml,) and allowed to react overnight. Medium was changed the following morning and cells were grown for 48 h to allow expression of the construct and then FACS sorted for GFP expression (FACSAria, BD).

2.3.3 Transfection procedures

Transfections were performed with Fugene 6 (Promega) or Lipofectamine 2000 (Life technologies) following the manufacturer's recommendations. In short for standard transfections, ~10^6 cells were transfected in suspension with 1.6 mg of the desired plasmid. Transfection medium was replaced with full fresh medium after 16 h to avoid excessive cell death. Cells were allowed at least 48 h for expression of the construct before follow up procedures.

2.3.4 siRNA transfections

For siRNA transfection 1.5x10^6 cells were seeded the day before transfection and allowed to attach to 6 well plates. The following morning 25 pm or 100 pmol of siRNA was mixed with 4 µl of JetPrime (PolyPlus transfection) transfection reagent in 200 µl of JetPrime buffer and added to the cells. Cells were allowed 72 h before analysis of protein levels by Western blot or fixation for immunofluorescence processing.

Table 6 siRNA used in this study

Target	Ref	Sequence	Source	Code
DHRS7 Human		GAAUGGGAGCUGACUGAUA CAGCAUGGCCAAUGAUUUG GCUAAUAGAGCUUAACUAC GGAUGCAGACUCUUCUUAU	GE Darmacon Smart Pool	L-009573-00-0005

2.3.5 Cell viability and Apoptosis/Necrosis assays

For cell viability assays cells were seeded onto PE96 plates (PerkinElmer) at a concentration of 5,000 cells/well in a final volume of 100 µl before compound addition. Growing media was replaced with media containing six serial dilutions of each compound and cells were allowed to grow for either 6 or 36 h. 10 µl Alamar blue (Thermo Fisher) reagent was added on each single well and allowed to react for 3 hrs prior to taking an absorbance reading at 530 nm or a fluorescence reading with excitation at 560 nm and emission at 590 nm on a microplate reader (JASCO V-550).

For apoptosis and necrosis analysis cells were incubated with each compound at a concentration of 10µM in standard 6 well tissue culture plates. Around 10^6 cells were counted, washed with ice cold PBS and stained with 5 µl of the Annexin V apoptosis marker conjugate with the 647 Alexafluor chromophore (Thermo Fisher Scientific) and 5µl of 50µg/ml Propidium Iodide (Biotium) for cell death detection, in 10 mM HEPES, 140 mM NaCl, and 2.5 mM $CaCl_2$, pH 7.4 for 15 min before FACS analysis. The 647 nm signal was used for detection of early stages of apoptosis as cells are not permeable to propidium iodide at this stage. Late stage apoptosis was detected by presence of both of the markers and necrotic cells by the presence of propidium iodide signal only.

2.3.6 Wound Healing assays

For wound healing assays around 25,000 cells per well were seeded on a BioEssence 96 LockView well plate (BioEssence) the night prior to wound formation. The cell monolayer was scratched with the IncuCyte® WoundMaker, that simultaneously makes equivalently-sized scratch wounds in the monolayer in all wells, and medium replaced with compounds containing medium supplemented with 1% FBS to induce cell migration and reduce cell proliferation. Plates were placed in the IncuCyte® incubator and imaged in bright field every 3 h for 48 h. Analysis of the wound closure time were

performed with an automated script provided by BioEssence determining the percentage of wound closure. The script allows masking of the wound area due to a different light reflection determining the presence and absence of cells and therefore percentages of wound closure. As the images are taken within a short period of time, the script allows the possibility of tracking single cells to discriminate between migration and cell division that could alter the final read out. The experiments in this study were conducted in 1% FBS to avoid this erroneous measurements and therefore the tracking of cell movements was not analysed.

2.3 Protein procedures

2.3.1 SDS page and Western Blotting

Protein lysates were analysed on 12-15% SDS- polyacrylamide gels casted using the BioRad mini PROTEAN ® Handcast system (BioRad). The resolving gel at the required percentage (10 - 15 %) was prepared and poured in between 1 mm glass plates. Stacking gel with 10 or 15 well combs was layered on top of the resolving gel once set. Protein samples were mixed with SDS loading dye, boiled for 1 min at 95°C before loading, along with 5 µl of protein molecular weight marker (Pierce). SDS-PAGE was run for 10 min at 100 Volts to pack proteins in one band and allow them to migrate through the separating gel at the same time, obtaining the optimal resolution of different size proteins. The gel was run continuously at 150 volts until the dye front reached the bottom of the SDS-PAGE.

The visualisation of proteins in the gel was achieved by staining with Coomassie stain using a Thermo Scientific™ Pierce™ Power Stainer (Thermo Scientific, 2011). According to the manufacturer guidelines, gels were boiled in water and then sandwiched in between 4 pieces of Whatman paper, soaked in either destain and Coomassie staining solution. For subsequent destaining procedures, the gel was places in water with a piece of tissue, to absorb the residual staining solution.

For Western blotting the proteins were transferred without prior Coomassie staining onto PVDF membranes with a pore size 0.45 µm (Millipore, IPFL00010) using a Thermo Scientific™ Pierce™ Power Stainer (Thermo Scientific, 2011). The membrane was blocked with 4% non fat milk in PBS with 1% Tween 20 for 1 h to saturate potential reactive epitopes, and subsequently incubated with primary antibodies against the target for 1h. Signals were detected with InfraRed Dye (LiCor) conjugated secondary antibody after incubation for 20 min. InfraRed Dye bands were scanned on a LiCor scanner and analysed using Odyssey software.

2.4 Fluorescence procedures

2.4.1 Immunofluorescence microscopy

For general antibody staining, after 48 h post transfection cells were directly fixed either for 7 min in 4% formaldehyde or for 10 min in ice cold 100% methanol at -20°C. Formaldehyde-fixed cells were permeabilised for 7 min in 0.2% Triton X-100 (Sigma) and blocked with 4% BSA (PAA laboratories, GmbH) in PBS and incubated for 1 h at RT with relevant antibodies. DNA was visualized with DAPI (Biotium) at a final concentration of 4 µg/ml and coverslips mounted in Vectashield (VectorLabs).

For protein topology analysis, transfected cells were seeded onto Ø 13 mm coverslips 48 h prior to fixation with 4% formaldehyde for 7 min. Coverslips were placed on an ice-cold metal block and treated with 150 µg/ml Digitonin (Sigma) in PBS was added for 7 min. This digitonin concentration was chosen as it allowed permeabilization of the plasma membrane but not of the nuclear membrane for the cell line used for this experiment in a previous titration of the frozen and aliquoted digitonin prep. Control coverslips were permeabilized with 0.2% Triton X-100 for 7 min. All coverslips were washed in ice-cold PBS and blocked with 4% BSA for at least 20min. Primary antibodies against either GFP or RFP were incubated for 40min and appropriate fluorophore-conjugated secondary antibodies were incubated for 20min at RT with DAPI.

Images were obtained using a Nikon TE-2000 microscope equipped with a 1.45 NA 100x objective, Sedat quad filter set and CoolSnapHQ High Speed Monochrome charge-coupled device camera (Photometrics) connected to a PC running Metamorph software. Images were deconvolved with the AutoQuant X3 software (Media Cybernetics) and 3D iso-surface volume reconstructions were generated with 3D image Pro (Media Cybernetics).

2.5 Screening procedures

2.5.1 Opera High content screening platform

The Opera® high content screen platform (Perkin Elmer) is an automated spinning disk fluorescence confocal microscope for plate imaging. The characteristics (lasers, objectives and main optical configuration) of this platform are listed below (Table 7-8, Figure 9). The platform works in the native Acapella software that allows the set-up of the laser lines to use, number of fields of view per well, focus point, power and exposure parameters for each laser. Images can be analysed during imaging or after the imaging process with the pre-set or adapted scripts. The Opera can be couple with a robotic arm allowing full automation of entire screens. The robotic arm moves plates form a physical stack into the imaging unit allowing unique identification of each single plate via a barcode labelling system.

Table 7 ***Laser characteristics on the OPERA High content platform.***

Laser	Wavelength	Laser type
Blue	488nm	Solid state laser
Green/Yellow	561nm	Laser diode
Red	640nm	Laser diode
Violet	445nm	Laser diode
UV/Vis	350-680nm	Xe-lamp with monochromator

Table 8 ***Objective lens specification on the OPERA High content platform.***

Objective feature	20x air	20x water immersion	40x water immersion	60x water immersion
Numerical aperture	0.45	0.7	0.9	1.2
Working distance	6.9mm	0.6mm	0.16mm	0.28mm
Field of view	430 x 345 μm^2	430 x 345 μm^2	215 x 173 μm^2	215 x 173 μm^2
Depth of focal plane	6 µm	2 µm	1.2 µm	0.7 µm

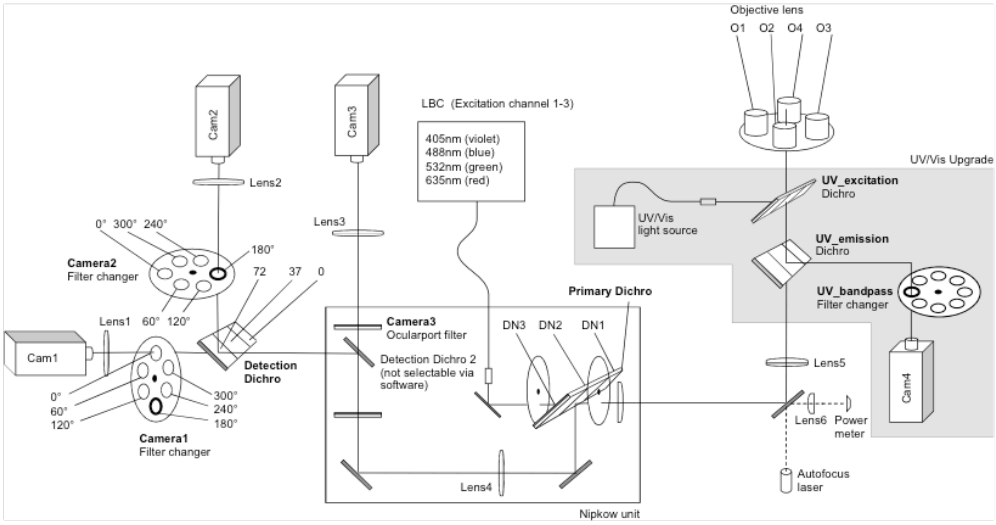

Figure 9 ***Optical configuration of the OPERA High Content Screen platform.*** *The main core of the system is the spinning disk Nipkow confocal unit, that allow the imaging of parallel points on the specimen for faster image acquisition compared to a standard confocal microscope.*

2.5.2 Compound screening

For compound screening PC3 H2B.RFP, HCT116 H2B.RFP and H1299 H2B.RFP cells were seeded onto PE96 plates (PerkinElmer) at a concentration of 5,000 cells/well in a final volume of 99 µl at 14 h before compound addition. 1 µl of each library compound was added from 96 well stock plates using the Biomek automated liquid handler (Beckman) robotics platform or manually. Cells were incubated 6 h or 36 h before fixation with a final concentration of 4% PFA for 15 min. 50µl HCS CellMask Deep Red 0.5X (Molecular Probes) was added to the fixed cells for 15min to stain for the plasma membrane and determine cell area. Wells were then washed with PBS 3 times for 5 min. Plates were loaded onto the robotic unit in groups of 15 after being marked with specific barcodes used for identification of unique runs and imaged overnight. Each well was imaged with 20 random fields of view with a 20X air objective, avoiding the edge of the well where cells accumulate for capillarity. The adapted Acapella script was run at the same time of imaging, generating masks in both channels (cytoplasm and nucleus area) and exported in a .txt file for subsequent analysis in MathLab (The Mathwork).

2.3.2 NETs screening

For the NETs screen HeLa H2B.RFP, HeLa H2B.GFP and PC3 H2B.RFP were seeded in PE96 well plates (Perkin Elmer) at a concentration of 2,500 cells/well in final volume of 100 µl the day before transfection. Cells were incubated with 5 µl of a mixture of 400 ng and 0.75 µl of Fugene (Promega) (200 ng/well final DNA) for each plasmid the day of transfection and incubated 48h to allow at least one cell division after induction of expression of the exogenous NETs. Plates were fixed with 4% PFA for 15 min, washed 3 times in PBS and maintained in 100 µl/well PBS at 4°C until analysis on the Opera. Plates were allowed to warm up at RT for at least 30 min before imaging to allow condensation to dry and imaged with 2 different laser exposition (488 nm and 561 nm laser lines) for each of the 20 fields of view per well with a 20X water immersion objective. An adapted Acapella script, wrote by Jan Wildenhain and Silvain Tollis, was subsequently run to identify transfected cells and determine nuclear area of transfected and untransfected cells.

2.3.3 Compound Libraries

The main library used in this work is the Prestwick Chemicals Library (PCL) that comprises 1280 compounds approved by different drug agencies (FDA, EMEA and other) exploring different therapeutic chemical spaces. A scheme of the EMA classification of the library is reported in figure 10. All compounds are diluted from a Master plate concentration of 1mM and used at 10µM in each screen, with controls being DMSO.

For the setup of the compound screening a single plate from the MicroSource Spectrum library (Discovery systems, Inc.) was used, with the same dilution applied for the Prestwick library.

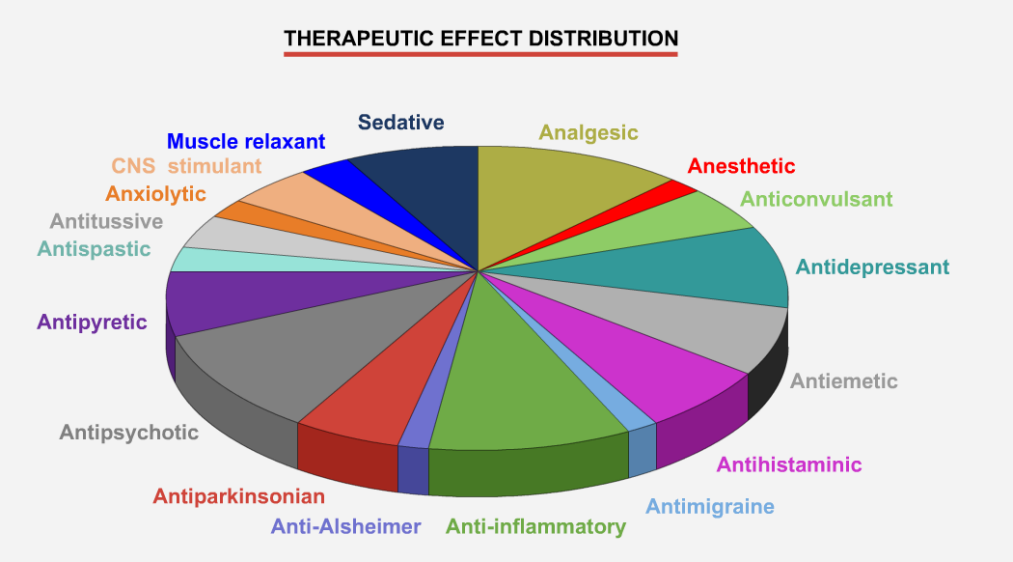

*Figure **10 European Medical Association (EMA) drug classification of the Prestwick Pre Approved library.** (http://www.prestwickchemical.com)*

2.4 In vivo models

2 million PC3-LUC cells for each tumour injection were mixed in a 1:1 ratio with Matrigel (Corning) and subcutaneously inoculated into both flanks of 6-week-old male nude mice (5 mice per group, Charles River). After 1 week, mice were randomized (average tumour size ~30mm^3 per group) and received 15 mg/kg in 50 µl piperlongumine or 10% DMSO in physiological solution intraperitoneally 5 days per week, excluding the weekends, for 3 weeks. Tumour sizes were measured twice weekly with a calliper. Tumour volume is effected by a physiological reduction after 7-10 days after the injection due to Matrigel slowly dissolving while the tumour mass grows and replace the Matrigel volume.

Tumours were collected and halved 2 h from the last injection and either snap frozen in liquid nitrogen for storage before ELISA assays or processed for standard haematoxylin and eosin staining.

2.4.1 ELISA assays

ELISA assays for pSTAT3 and tSTAT3 (Sigma-Aldrich) and GAPDH (ThermoFisher) were preformed according with recommended manufacture procedures. Briefly, tumours were frozen in liquid nitrogen and reduced to powder. Tumours were lysated with the provided lysis buffer for 10 min at RT in an orbital shaker. Derbies were removed by centrifugation in a micro-centrifuge at 13000 RPM for 15 min and surnatant was transferred in a clear tube. Total amount of proteins was detected by NanoDrop and diluted to reach a concentration of 0.05 mg/ml of protein. For GAPDH measurements 50 µl of each sample were incubated, in the provided 96 well-plate, with a 50:50 mixture of capture and detection antibody and incubated, in agitation, for 1 h at RT. Wells were washed 3 times with 100 µl of washing buffer and 100 µl of detection reagent was add. Absorbance was read through a microplate reader at 450 nm after 15 min of incubation of the detection reagent.

For tSTAT3 and pSTAT3 cell lysates were incubated in a pre-coated 96 well plate for 2.5 h. Primary antibody against tSTAT3 and biotinylated antibody against pSTAT3 were incubated for 1 h at RT in agitation; and secondary anti rabbit IgG coupled with HRP and HRP-streptavidin for 45 min at RT. TMB substrate solution was allowed to develop for 30 min at RT in agitation and reaction stopped prior absorbance reading at 450 nm.

2.5 Statistics and Analysis

2.5.1 High throughput analysis

Individual cells and nuclei within each field of view were masked using the automated threshold-based detection algorithm built into the Opera device (aCapella scripting environment, Perkin Elmer). Specifically, intensity threshold filters, size filters, and morphological filters were used to filter out detection artefacts, multiple detection of single cell/nuclei or unique detection

of cell clusters. Individual cell output data, comprising nuclear size generated by masking the RFP channel, the cytoplasm size generated by subtracting the nucleus mask from the mask detected for the plasma membrane channel, and average signal intensities was saved as text files that were loaded in Matlab (The Mathworks) for further analysis. Of note, identical detection and filtering parameters were used in aCapella to identify cells and nuclei under all conditions to normalise different runs to the same baseline data analysis and prevent post-acquisition processing biases. Specifically, for each condition separately, the entire cell size distribution was analysed, the median size (M) was calculated along with the first and third size quartiles Q1 and Q3 respectively. Following standard outlier removal procedures, detections with a size larger than the outlier threshold M+6*(Q3-M), considered most likely cell clusters, and the detections smaller than M-6*(M-Q1), considered cell derbies o artefacts, were filtered out. All DMSO control wells of a single plate were treated together in this step.

2.5.2 Statistics

Statistics for NET50 nuclear volume reconstruction, wound healing, viability assays and xenograft tumour analysis were generated in Prism 6 (Graphpad) using the appropriate statistical test for each set of experiments reported in each figure legend.

3. Screening for compounds and NETs affecting nuclear size

3.1 Introduction

Nuclear size and shape is altered in most types of cancer and commonly used as a diagnostic tool for staging and grading cancer. Although it is not yet tested whether these changes are a consequence of other factors that drive increased metastasis or if they themselves are the drivers, in the latter case they would make promising therapeutic targets. Thus, we sought to identify proteins that can regulate or affect these features in cancer as potential future targets. We focused on NETs because they are perfectly placed physically to mediate nuclear size changes. Moreover, many of these proteins are tissue specific and so if they are involved it could explain differences in nuclear size and shape changes that are characteristic for different tissue cancer types.

Along with identification of key proteins for nuclear size regulation, we are interested in identifying small molecules that can correct defects of the nuclei and that can be potentially added to chemotherapy regimens to improve survival rates by reducing metastatic spread or other characteristics associated with nuclear size changes that could give tumour cells an advantage. This chapter will focus on the set up of high throughput screening for the identification of NETs or compounds that affect nuclear size.

3.2 Optimization of screening parameters

The idea for setting up a high throughput screening is the possibility to have several conditions that can be tested at the same time in a relative short time. The Opera confocal system allows to set up fully automated screens generating high resolution images in 96 or 384 well plate formats with up to 5 different laser exposures. This greatly reduces times for screening a large number of conditions: our screens involve 50 different NET transfections and entire drug libraries and the screening for each individual replicate can be performed within weeks once assays are optimised. The idea of this project is to screen for NETs that can influence nuclear size, and separately for compounds that can alter or restore aberrant nuclear size and restore karyoplasmic ratio in different cancer types. Even though the OPERA screening and analysis are similar for the two screens, each of required setting up specific parameters due to the differences in cell treatments before the imaging process.

3.3 Cell confluency and plating procedures

There are several variables to be considered while setting up an automated phenotypic high-throughput screen. The first consideration is the number of cells plated on an optical 96 well plate. If the number of cells is too low, cells might suffer from lack of contacts with neighbouring cells. Another factor that can alter normal survival of cells is the surface substratum which can affect the growth rate of the culture in addition to the more important effects on the strength of cell-substratum contacts which affects cell spreading and so can make the visualization of the nuclear and cytoplasmic area much easier or harder to quantify. More importantly for this screen where the read out is nuclear size, too confluent cultures might underestimate the real nuclear size due to squeezing by adjacent cells so that cells cannot spread properly. Moreover, as the analyses are carried out by an automated script that relies on a clear distinction between background and cells, overly confluent cells can

be interpreted as a large single cell rather than a cluster, generating artefacts in the final output. To avoid these erroneous readings several cell plating concentrations were tested to identify the correct concentration to reproducibly achieve an optimal density for visualization after 48 hours post transfection, and two different types of plates were tested for optimal cell attachment, spreading, and growth. Perkin Elmer plates were chosen due to the more robust attachment of cells and less cell cytotoxicity, with cells being seeded at a concentration of 2,500 cells per well to reach optimal density for imaging at 48 h post-transfection for the NETs screen and 5,000 cells per well for the compound screen.

Power calculations were used to determine the minimum number of cells required to detect at least a nuclear size alteration of 20% (Eq. 1). Power calculations allow determination of the sample size with a specific power for the test knowing the mean value (μ) of the population and its standard deviation (σ^2). The power of a test is defined as 1-β where β is a type II error, occurring when the hypothesis H0 is accepted when false. For both screens the minimum sample size is 400 cells with a power of β=0.80 and α=0.5. According to this power calculation, number of cells plated and parameters decided were sufficient to achieve the minimal number of analysed cells.

3.4 Optimization of microscope objectives

To optimise screening parameters for both screens we tested what type of objective could best balance speed of screening against resolution. The two objectives tested were air 20X and water 40X. Each of these objectives have their own pro and cons as the 20X allows for a faster screening as the field of view is greater, therefore less fields are required for a satisfactory number of cells to achieve statistical differences, considering that the cells are not synchronized for the screen so the total distributions will already be at least 2-3 fold. The 40X allows a better resolution and definition of the nuclei imaged, but at the same time requires at least twice as many fields to be imaged, compared with a 20X objective. To perform the setup of the screen a single

plate from the Spectrum library was used to compare the two objectives. Analysis revealed that both the 20X air and 40X water objectives identify cells with significant changes to the N/C ratio, with no statistical significance between the two objectives. The effects of identified compounds are consistent in the replicates and between the 20X and the 40X objectives (Fig 11). Using a 20X air objective and imaging 20 fields of view gave the best balance between time for imaging, with around 1h for each plate, and number of cells imaged (around 1,000 cells per condition).

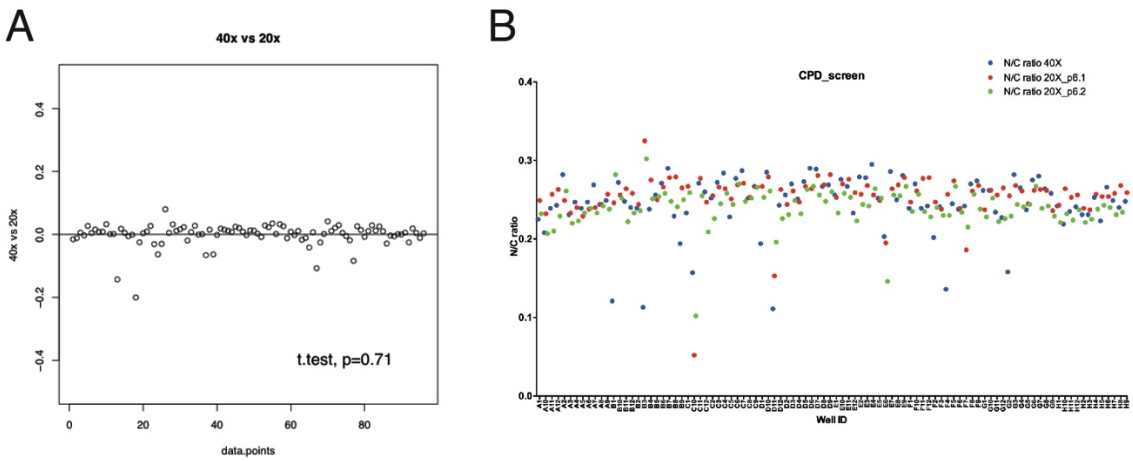

*Figure **11 Objectives set up experiments for 20X and 40X objectives.** A. T-test for 40X versus 20X objectives. T-test was performed with a script in R, to identify if there are any statistical differences between using the a 40X or a 20X objective. The p-value of the test illustrate no difference in the hit identified with the 40X and 20X, allowing to use the 2oX objective for faster screening. B. Hits identification for 20X and 40X objectives. Data for the karyoplasmic ratio identified with the set up runs, showing the same hits identified between the 40X and the 20X objective performed in replicate (p6.1 and p6.2) for the same plate.*

3.5 Transfection procedures optimization

Another variable that may have a great impact in the NETs screen is the transfection procedure, as the aim is to find an optimal balance between transfection efficiency and cell death. Different liposome-based transfection reagents were tested, each with different ratios between plasmid DNA and cationic liposomes to identify the best compromise. One finding was that too much DNA in the medium generates cell death. Lipofectamine 2000 and 3000 resulted in a too high cell toxicity to leave a sufficient number of cells for analysis to support robust statistics plus the high number of apoptotic cells

yielded a high percentage of misreads with the Acapella software which could not be effectively programmed to discount apoptotic cells. Effectine (Roche) and JetPrime (PolyPlus transfections) transfections resulted in less cell toxicity, but lower and comparable transfection efficiency between each other. Fugene6 in contrast had a higher transfection efficiency and less cell toxicity with a final concentration of 100 ng of plasmid DNA per well and so it was chosen to use for the screen.

3.6 Screening for NETs altering nuclear size

Once all the parameters had been optimised the NET screen was performed in duplicate with 2 technical replicate wells on each plate. 52 different GFP expressing NETs were screened and for each plate a NLS-GFP control, carrying the SV40 large T-antigen sequence (PKKKRKV) was added so that the control both underwent the same transfection procedure and expressed a protein that gets into the nucleus but doesn't affect the NE. An adapted Acapella script, reported in the appendix section, for detection of transfected cells was implemented. The script identifies transfected cells based on the GFP channel from NET-GFP transfected and measures nuclear size on the RFP channel based on the cell line stably expressing H2B-RFP and thus allowing the determination of nuclear size of both the transfected and untransfected cells within a population as an additional internal control for population drift across the experiment. The ratio between transfected and untransfected cells for all conditions was normalized against the NLS-GFP control, and a threshold set for NETs with alteration of nuclear size greater than 20%. This identified a pool of NETs that might have regulatory effects on nuclear size (Fig 12).

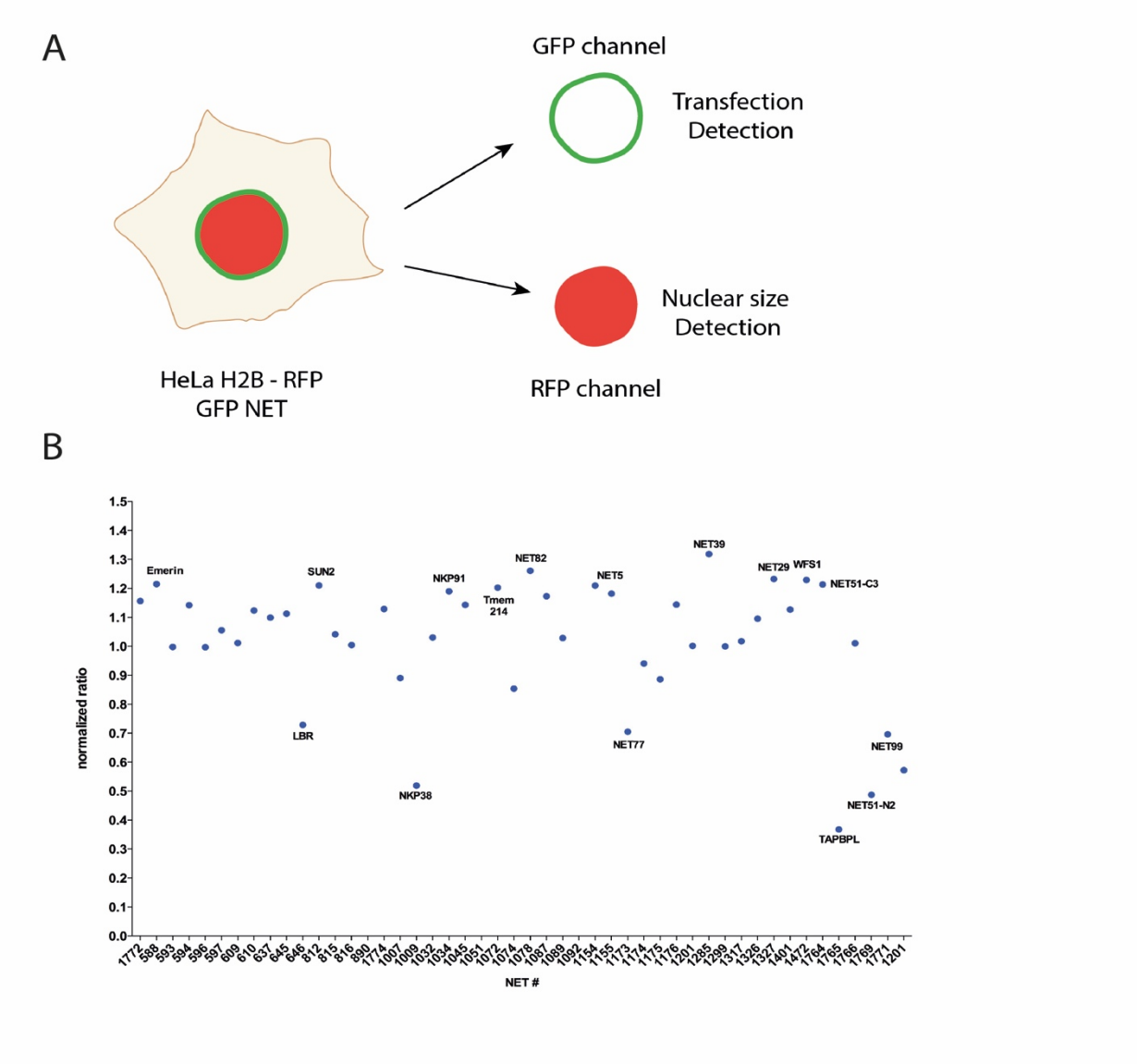

Figure 12 ***Screening for nuclear envelope proteins affecting nuclear size.*** *A. Schematic of the screen. H2B.RFP cells are transfected with GFP-NET vectors in a 96 well plate format. Transfection is detected on the GFP channel and nuclear size in the RFP channel by an adapted screen that calculates nuclear size for the untransfected and transfected pool of each well. B. Normalized ratio results for HeLa cell line. The ratio between untransfected and transfected cells is normalized against the internal control NLS-GFP, carrying the SV40 Large T-antigen sequence, to detect alteration of nuclear size. A threshold of at least 20% of nuclear size change has been applied, highlighting the NETs having effects on nuclear size when overexpressed, namely Emerin, SUN2, LBR, NKP38, NKP91, Tmem214, NET82, NET5, NET77, NET39, NET29, WFS1, NET51 TAPBPL and NET99.*

Among the positive NETs from this screen, there were some of particular interest based on their known or predicted functions and known partners at the nuclear envelope. Emerin had already been identified prior to the high throughput screen by an Honours student in the Schirmer lab as a protein that increases nuclear size when overexpressed. This had been tested

both in 2D and using 3D reconstructions from deconvolved z-stacks (Hormann MSc Thesis and Jarman Honours Thesis). Interestingly it has been reported that nuclear size is altered in patients with Emery-Dreifuss muscular dystrophy caused by mutations in emerin (Shimojima et al. 2017). SUN2, a core protein of the LINC complex is of particular interest as SUN partner Nesprins have been previously liked to nuclear size regulation (Luke et al. 2008a). Finally, NET51 shows an interesting nuclear size alteration pattern as, depending on the part of the protein (N or C-terminus) tagged, the directionality of the change is the opposite. This could indicate the tag interfering with the activity of the protein, though which reflects the functional state is unclear.

To verify that protein overexpression is not too high, as most of the NETs are driven from the strong CMV promoter, fluorescence levels were plotted against the nuclear sizes calculated. As shown in figure 13 most of the identified NETs with effects on nuclear size do not have high fluorescence levels, therefore reducing the possibility of artefacts deriving from a too strong expression. It is also an important control that fluorescence does not correlate with the nuclear size alteration, suggesting that some NETs may have a more fundamental role in regulating nuclear size than others and a lesser amount of protein is required to detect a significant change.

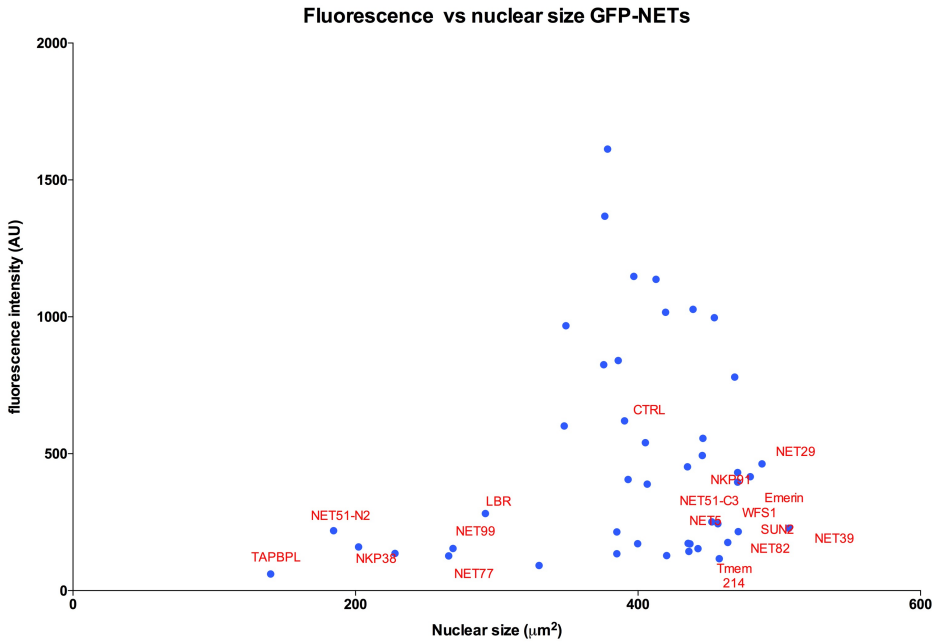

Figure 13 ***Nuclear size and fluorescence intensity correlation.*** *The plot presents the correlation between nuclear size and the fluorescence intensity of each NET in the screen. It might be argued that NETs showing a strong correlation of size changes with fluorescence intensity could be discarded as artefactual; however, no such general correlation was observed.*

The initial screen was performed in the HeLa cervical cancer epithelial cell line due to its generally high transfection efficiencies and the tendency for HeLa cells to have bigger nuclei that result in better detection by the script. However, the qualitative and quantitative differences in nuclear size changes in different tissue cancer types together with the tissue-specific expression of a majority of NETs suggested the possibility that different NETs might affect nuclear size only in particular cancer cell lines. Therefore, we also tested NET effects on nuclear size in prostate adenocarcinoma (PC3) and breast cancer (MCF7) cell lines. Transfection levels for the PC3 cell line were comparable with HeLa cells allowing a sufficient number of cells to be analysed for statistical significance based on the HeLa distributions, while for the MCF7 cell line transfection efficiency did not reach a satisfactory level. Analysis of the data from running the screen in the PC3 prostate cancer line revealed significant differences in the NETs with effects, indicating that NET effects on nuclear size are tissue specific. A few NETs had similar effects on both lines

(e.g. NET29 and WFS1), but the majority had effects on one cell line but not the other and vice versa. Interestingly, the proteins NET39/PPAPDC3 and LBR show alteration of nuclear size in two different directions in the two cell lines, with an increase of nuclear size for HeLa cells and a decrease in size for PC3 cells, suggesting that the same protein if targeted in different pathologies might have opposing outcomes.

Several other NETs with potential effect on nuclear size, as for example Nesprins, could be added on the screen but were left out due to their large cytoplasmic domain that would make the cloning of this proteins for this type of screen unsuccessful.

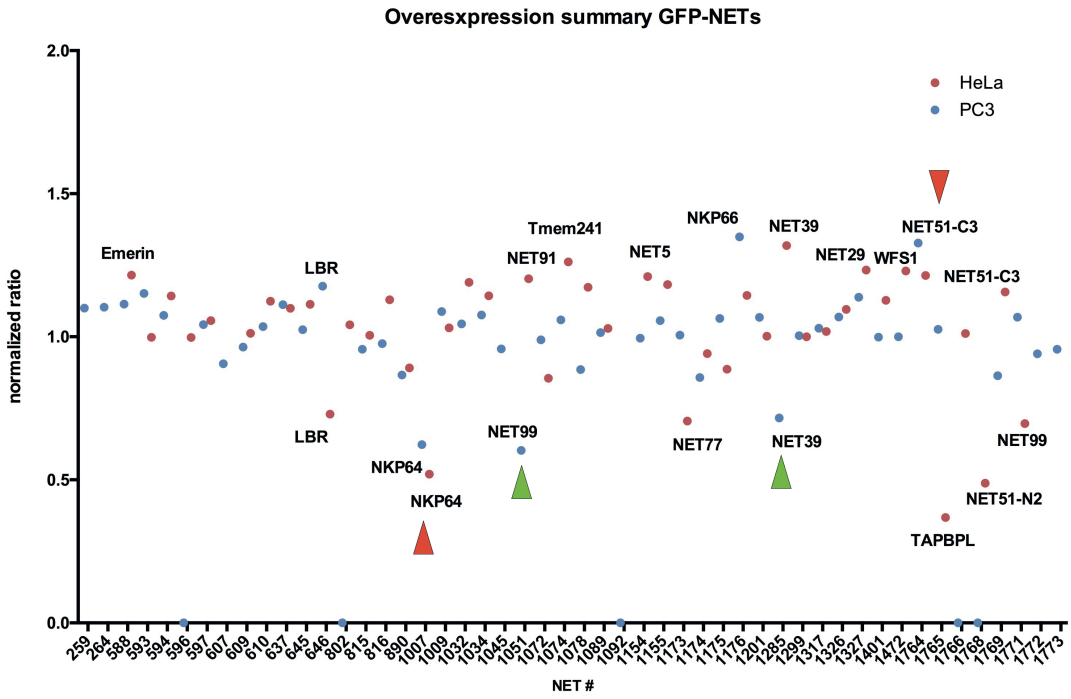

Figure 14 ***Nuclear size alteration driven by NETs in different type of cancer.*** *Normalized ratio of GFP-NET overexpression in two different systems, HeLa and PC3 cell lines. The ratio between untransfected and transfected nuclear size for each NET has been normalized against the internal NLS-GFP control. Alterations greater than 20% has been highlighted. NETs having effect in different direction in the two cell lines are highlighted with a green arrow (NET99 and NET39) where NETs having the same directionality are marked with a red arrow (NKP64 and NET51).*

3.6.1 NETs with effects on nuclear size have altered gene copy numbers in different cancers

Some of the NETs identified with a potential role in nuclear size regulation have correlative changes in gene copy number in different cancer types according to the direction of size changes in each cancer. Analysis of data kindly provided by Erica Golemis at the Fox Chase Cancer Center (Philadelphia) identified at least 6 different NETs with such correlations in gene copy number: WFS1, NKP91/TMEM41A, TMEM214, NET77/SQTRM1, NET82/RHBDD1 and NET39/PPAPDC3.

For example, WFS1 overexpression increased nuclear size in HeLa cells. In 59% of lung squamous cell carcinoma patients, where a decrease in nuclear size correlates with worse prognosis, there is a hemizygous deletion of the gene encoding WFS1. In the opposite direction 41% of adrenocortical carcinoma patients, where bigger nuclei correlate with increased metastatic potential, exhibit a hemizygous amplification of the gene (table 9). Thus, the directionality of nuclear size changes in the cancers matches the NET expression and nuclear size directionality. These results suggest a correlation for tissue specificity of the same protein in different types of cancer, with directionality of nuclear size changes dependent of in which tissue the protein is expressed and active.

Table 9 ***Gene copy number alteration in NETs altering nuclear size.*** *NETs identified in the screen have altered gene copy number in different cancer where the directionality of nuclear size alteration correlate with worst grade for patients is opposite. Hemi or homo gene amplification (green) and hemi or homo gene deletion (red) are presented for each type of cancer. Data provided by Erica Golemis based on the TCGA cancer database.*

NET	Cancer type	Type of alteration	Percentage of patients
WFS1	Adrenocortical Carcinoma	Hemi amplification	41%
	Lung Squamous Cell Carcinoma	Hemi deletion	59%
NKP91	Lung Squamous Cell Carcinoma	Homo and Hemi amplification	43% and 46%
	Pheochromocytoma and Paraganglioma	Hemi deletion	59%
	Cervical Squamous Cell Carcinoma and Endocervical Carcinoma	Hemi amplification	59%
TMEM214	Lung Squamous Cell Carcinoma	Hemi Deletion	70%
	Kidney Chromophobe	Hemi amplification	50%

NET	Cancer type	Type of alteration	Percentage of patients
NET77	Adrenocortical Carcinoma	Hemi amplification	63%
	Lung Squamous Cell Carcinoma	Hemi deletion	69%
NET82	Kidney Chromophobe	Hemi deletion	74%
	Bladder Urothelial Carcinoma	Hemi deletion	44%
	Lung Squamous Cell Carcinoma	Hemi amplification	26%
NET39	Ovarian Serous Cystadenocarcinoma	Hemi deletion	58%
	Ovarian Serous Cystadenocarcinoma	Hemi deletion	70%

A pool of these NETs was transiently transfected in different tissue cancer cell lines: prostate cancer (PC3 cell line), breast cancer (MCF7 cell line) and adrenocortical carcinoma (HCT116 cell line), to further test if alteration of nuclear size is tissue specific. A widely expressed NET, Emerin, and a muscle tissue-restricted NET, NET39, were chosen to determine if tissue specificity of the expression could influence in different ways the nuclear size regulation. Z-stacks were taken at 0.2 µm each step for each cell nucleus, but they were analysed in 2D by taking the nuclear area from the step with the largest area that should represent the middle of the nucleus. Effects on nuclear size are distinct in each cancer background, with even the same NET (e.g. Emerin and

NET39) having a different directionality in the nuclear size alteration depending on the type of cancer (Fig 15).

Emerin is a particular interesting NETs as is not tissue restricted and involved in the Emery-Dreyfuss muscular dystrophy (EMDM) (Brown et al. 2008) and has been already implicated in alteration of the nuclear size in muscle cells (Shimojima et al. 2017). Moreover, this protein binds directly several transcriptional regulators and epigenetic remodellers, such HDAC3 and HP1 (Demmerle et al. 2012; Rowat, Lammerding, and Ipsen 2006), therefore could influence several layers of nuclear size regulation and would be an interesting target to pursue further as target for development of new drugs.

This result shows that NET-directed nuclear size regulation is highly tissue specific and dependant on other factors in the tissue background, arguing that further investigation of these tissue specific players for different cancer types might lead to approaches to increase the effectiveness of treatments.

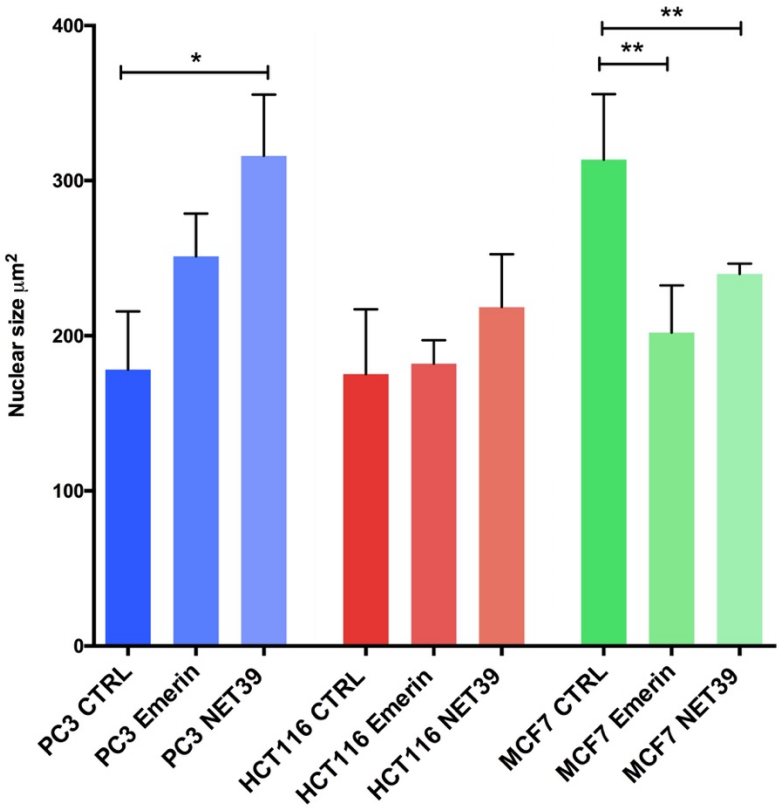

Figure 15 ***NETs nuclear size alteration effects in different cell lines.*** *Nuclear size alteration due to different NETs overexpression in prostate cancer (PC3), adrenocortical carcinoma (HCT116) and breast cancer (MCF7) cell lines. Cells were transiently transfected with either a NLS.GFP control or the GFP tagged NET emerin or NET39. Nuclear mid-plane measurements were taken and analysed with ImageJ to calculate the mean nuclear size for each sample.*

3.7 Screening for compounds altering nuclear size

Along with the identification of potential proteins regulating the nuclear size, this project aims at the identification of novel compounds that can induce nuclear size alteration. These new compounds can be used to restore defects in nuclear size and might be used as novel chemotherapeutic agents in the treatment of cancers. For this reason a high throughput screening of the Prestwick library was performed to identify potential new drugs affecting the nuclear size that have already been approved by different drug agencies (FDA and EMA).

An adapted Acapella script, reported in the appendix, was used to determine the nuclear and cytoplasm areas. The nuclear area was measured

from the H2B-RFP staining and for the cytoplasmic staining all area within the delineated plasma membrane stain was first measured and then the nuclear area was subtracted. These two numbers were used to determine the karyoplasmic ratio for each cell in the images obtained. Over 3,000 cells were analysed for each condition and the distributions for the individual nuclear areas and karyoplasmic ratios were used to determine an average size and ratio for each condition.

With the parameters decided for this pre-screen, we were able to detect even 20% nuclear size changes with statistical significance ($p<0.001$, Wilcoxson non-parametric test for matched pairs). However, there were a number of cases where false positives were detected due to apoptosis in the sample, therefore images of positive hits were manually checked for all samples showing significant changes in nuclear size or the karyoplasmic ratio (Fig 16).

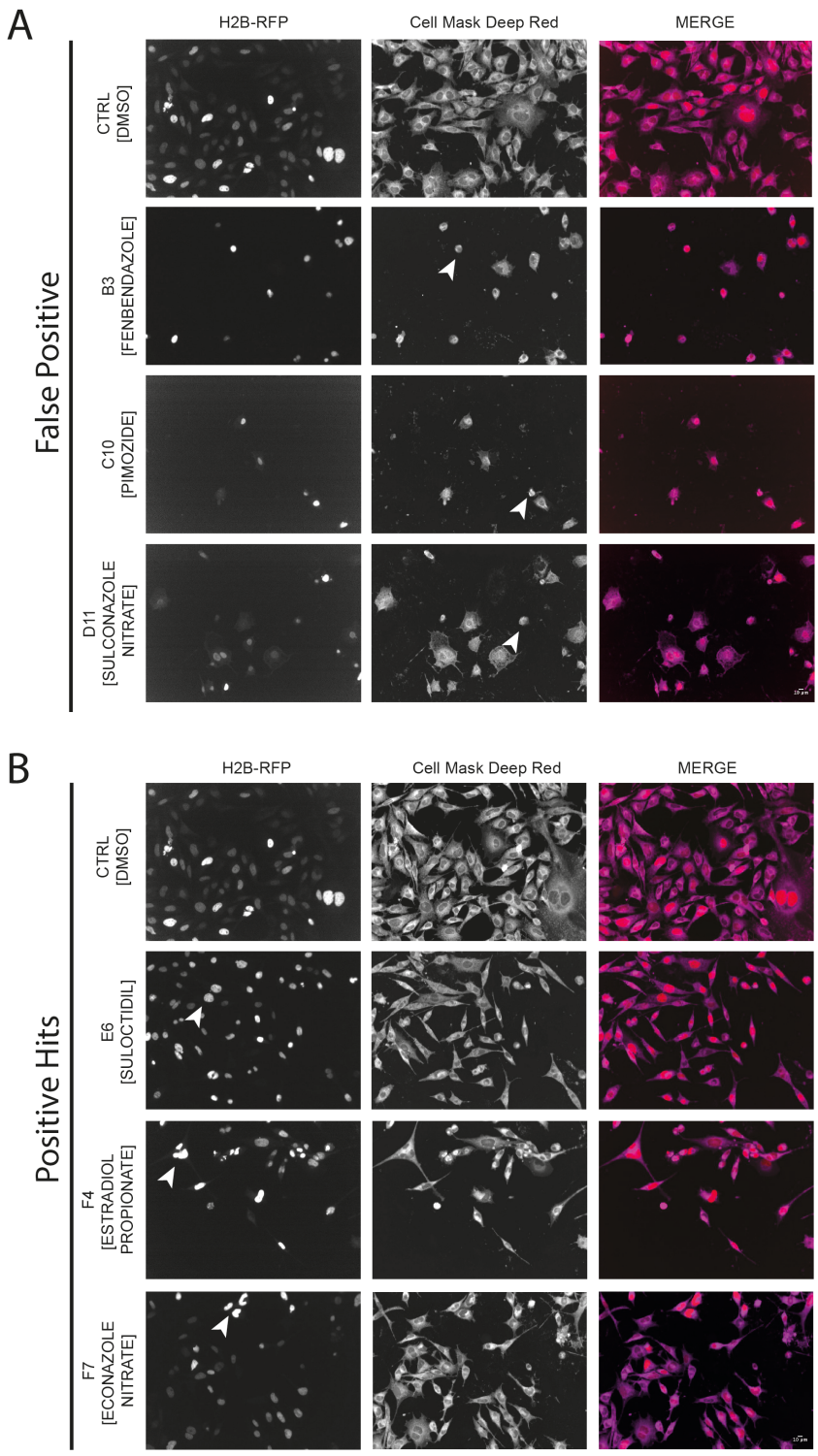

Figure 16 ***Positive hits in the pre-screen for the identification of compounds altering nuclear size.*** *A. Representative images of false positives, deriving from cytotoxicity of the compounds. Images were taken from the Opera high content screen of PC.H2B.mRFP (red) cell line stained with Cell Mask Deep red dye (magenta) staining for the cytoplasm after 24 h treatment. B. Representative images of positive hits. Cells were treated as above. Scale bar 10 μm.*

3.7.1 Compounds altering the karyoplasmic ratio show tissue specificity

The screen was performed in three different cell lines: PC3, HCT116 and H1299. These three cell lines were chosen in order to both compare two lines with the same directionality for the nuclear size change correlating with worst prognosis and also compare lines where the directionality is opposite. For prostate and colorectal cancers (PC3 and HCT116 cell lines) increased nuclear size and volume correlate with higher grade tumours, where in lung cancer (H1299 cell line) a reduction of nuclear size is associated with higher tumour grades. For each cell line 2 time points were screened: 6 and 36 h. The 6 h time point was chosen to identify early and fast effects of drugs and to be able to distinguish if a nuclear size change occurred independently of the cell dying for compounds with high cytotoxicity. The 36 h time point was important to determine if a compound had a cytotoxic effect and also to allow cells to undergo at least one complete cell cycle in case the NE would need to be disassembled and reformed at the end of mitosis in order to achieve the change in nuclear size. The first screen was conducted in biological triplicates for the PC3 cell line to determine its reproducibility. Having observed that it was reasonably reproducible, with a 17% probability to obtain a false positive, the screen was then performed in duplicate for the remaining cell lines and time points (Fig 17).

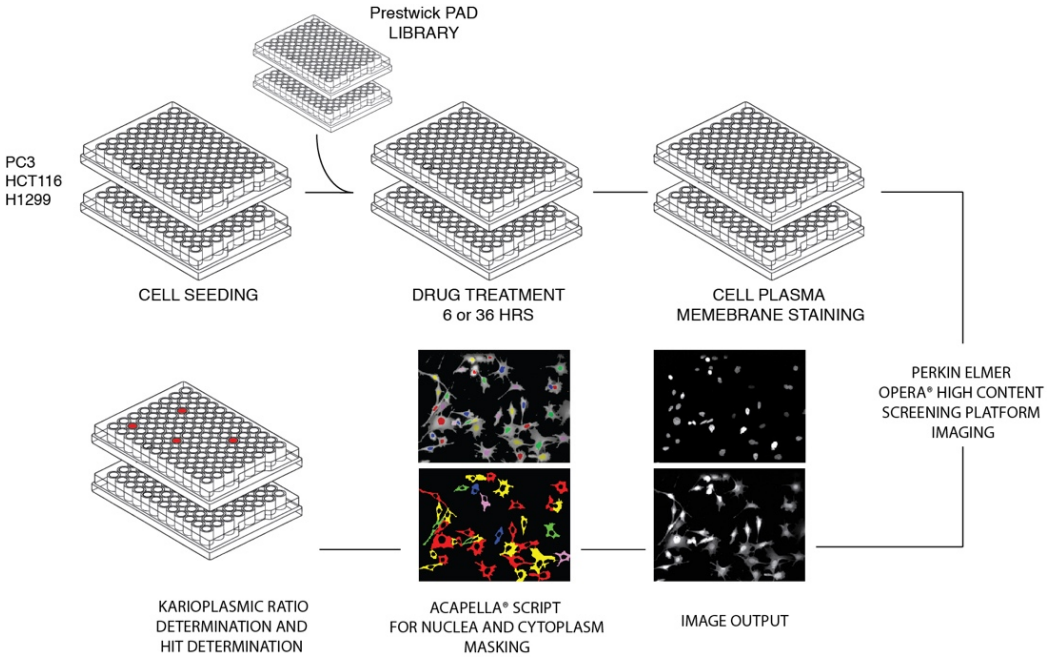

Figure 17. ***Schematic representation of the screen for determining compounds with influence on nuclear size.*** *Three cell lines (PC3, HCT116 and H1299) were seeded into optical clear bottom 96 well plates prior to addition of the Prestwick PAD library compounds. Cell were incubated with compounds for 6 or 36 hours before fixation and staining. Plates were imaged on the Perkin Elmer OPERA system, analysed using a specially written script in Acapella, and a list of hits with >20% change in nuclear size or karyoplasmic ratio generated.*

The karyoplasmic ratio was assessed using two different metrics. First, single cell karyoplasmic ratio was calculated and then averaged over all cells of a given condition. Each plate carries two internal DMSO control columns used to for the average values of the control and each of the remaining wells treated individually as represent a single compound. The mean N/C ratio (together with the associated standard error on the mean, SEM) was then compared across conditions (Fig 18A). While such an analysis method is, in principle, sufficient to detect overall shifts in the N/C ratio distribution across a cell population, it might be insufficient to detect conditions that either mis-regulate the N/C ratio (and therefore broaden N/C ratio distribution without affecting the mean value), or strongly affect the N/C ratio in a small percentage of the cells in a population. To complement the analysis of the mean N/C ratio, we proceeded with a second analysis designed to reveal how treatment with a specific compound enriches the fractions of cells with abnormally large or

small N/C ratio. Specifically, we first assessed upper (M+3*(Q3-M)) and lower (M-3*(M-Q1)), threshold values of the N/C ratio using the median (M), first and third quartiles (Q1 and Q3) of the distribution for N/C ratios of in-plate DMSO controls. As expected, due to cell population variation and as the screen is performed with one fixed focus plane, there was a minor percentage (3-5% depending on plates) of those DMSO-treated control cells that displayed a N/C ratio beyond those thresholds. Then, for each compound well, we quantified the percentage of cells that displayed a N/C ratio beyond those control cells-derived thresholds. Those fractions of cells with abnormally large or small N/C ratio are expected to increase upon a global shift of a N/C ratio distribution following compound treatment, but also to respond to either a broadening of the N/C ratio distribution (loss of N/C ratio regulation in most individual cells) or all-or-none response of the N/C ratio to the drug in a small percentage of cells.

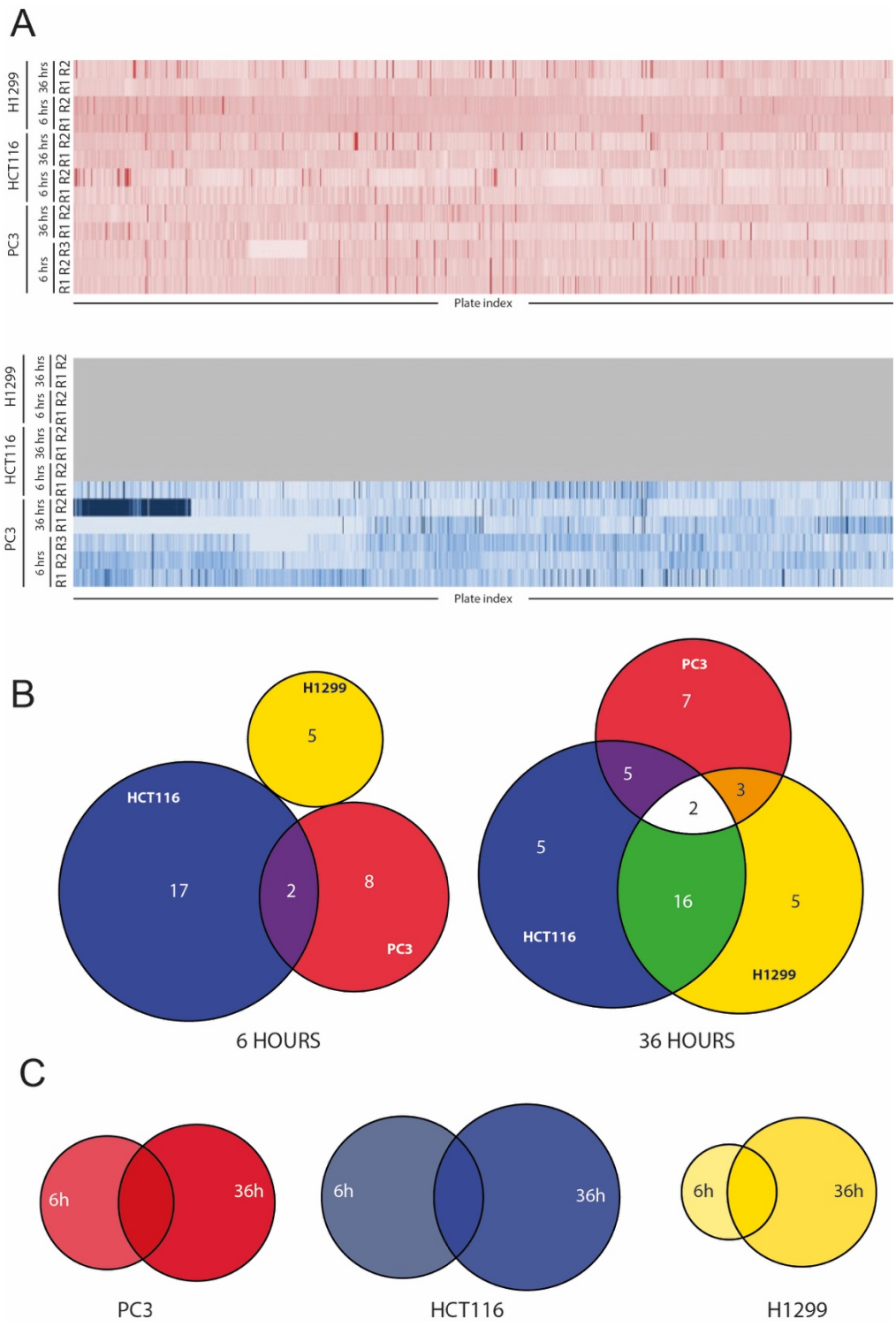

Figure 18 ***Sum of screening results for compounds altering the karyoplasmic ratio.*** *A. Heat map for larger and smaller karyoplasmic ratio. Results are presented with a darker colour for high alteration of the karyoplasmic ratio after normalization against the controls. Compounds increasing the karyoplasmic ratio are presented in red and compounds reducing the karyoplasmic ratio are presented in blue. Replicates for each cell line are indicated with the label R1, R2 or R3. B. Eluero-Venn diagrams for compounds altering the karyoplasmic ratio. Diagrams are divided by cell line screened (PC3, HCT116 and H1299) and time point (6 and 36 hours). C. Eulero-Venn diagram by cell line for the different time points. Diagrams show the overlapping compounds altering the karyoplasmic ratio for the two time points (6 and 36 hours) in the three different cell lines screened.*

One of the compounds able to alter the karyoplasmic ratio that is noticeable on the hit results is paclitaxel, also known as taxol, because this is one of the most used chemotherapeutic agents to treat different types of cancer (table 10). It has an antimitotic activity against cancer cells that can explain the alteration of nuclear size. Taxol, however, was not present as a hit at 36 hours of treatment due to the cytotoxicity effects on the cell lines. Another interesting compound was podophyllotoxin that has been shown to have effects on the growth of carcinoma cells, especially the PC3 cell line (Xu et al. 2011). Many of the hits have previously been used to treat cancer, suggesting that targeting actively the karyoplasmic ratio in cancer could contribute effectively to treatment.

Table 10 ***Hits altering the karyoplasmic ratio in different cell lines for the two time points****. Hits identified in the screen altering the karyoplasmic ratio for PC3 (red), HCT116 (blue) and H1299 (yellow) cell lines, with respective known function. Minus (-) indicates reduction in nuclear size and plus (+) indicates increment in nuclear size.*

Compound	Function	6 HRS			36 HRS		
		PC3	HCT116	H1299	PC3	HCT116	H1299
Gallamine triethiodide	Muscarinic antagonist			-			-
Alexidine dihydrochloride	Detergent			+			+
Cantharidin	Serine protease releaser		-			-	
Primaquine diphosphate	Heme polymerase inhibitor		+			+	
Paclitaxel	microtubule polymerisation inhibitor		-			-	
Anisomycin	Acetylcholine esterase inhibitor		+			+	
Oxyphenbutazone	cyclooxygenase inhibition		-			-	
Podophyllotoxin	Microtubule polymerization inhibitor	+			+		+
Cilostazol	Phosphodiesterase inhibitor	+			+		
Emetine dihydrochloride	Protein synthesis inhibitor	+			+		

Roxatidine Acetate HCl	Histamine antagonist (H2)	-			-	-	-
Cilostazol	Phosphodiesterase inhibitor	+			+	+	+
Paclitaxel	microtubule polymerisation inhibitor	+	+	+			
Mycophenolic acid	Antineoplastic				+		+
Prenylamine lactate	Ca2+ channel stimulation				+		+
Piperlongumine	Antifungal	-	-		+		+
Emetine dihydrochloride	Protein synthesis inhibitor				+	+	+
Primaquine diphosphate	Heme polymerase inhibitor				+	+	+

3.7.2 Nuclear size vs karyoplasmic ratio

Data were also analysed to identify alteration of just the nuclear size as this is the main morphological alteration analysed by cytopathologists when staging and grading different cancer types. Results showed more compounds identified with the nuclear size as the parameter compared with analysing the hits for the karyoplasmic ratio, with 45% more hits identified for PC3, HCT116 and H1299 for both the time points (Fig 19A).

Comparing the hits that are above the threshold of a statistical significance analysing the nuclear size or the karyoplasmic ratio, it results that if nuclear size is chosen as the parameter for the detection of positive hits, more compounds are identified compared with karyoplasmic ratio analysis, with some of these compounds not having an effect on the karyoplasmic ratio at all (Fig 19B). This could be explained as the regulation of cytoplasmic and nucleoplasmic volume is a multi-variable and complex regulation, therefore identify drugs that influence most of the pathways to detect an effect is more difficult. Moreover, the data were analysed in the second methodology to identify compounds that either increase or decrease the nuclear size, allowing to generate a pool of compounds that can be interesting in the follow up experiments depending on the type of cancer considered. For example, drugs decreasing the nuclear size are more interesting for prostate cancer and

adrenocortical carcinoma where an increase of the nuclear size correlates with the worst prognosis. These drugs could be useful to restore the original nuclear size and result in a better outcome for the patient.

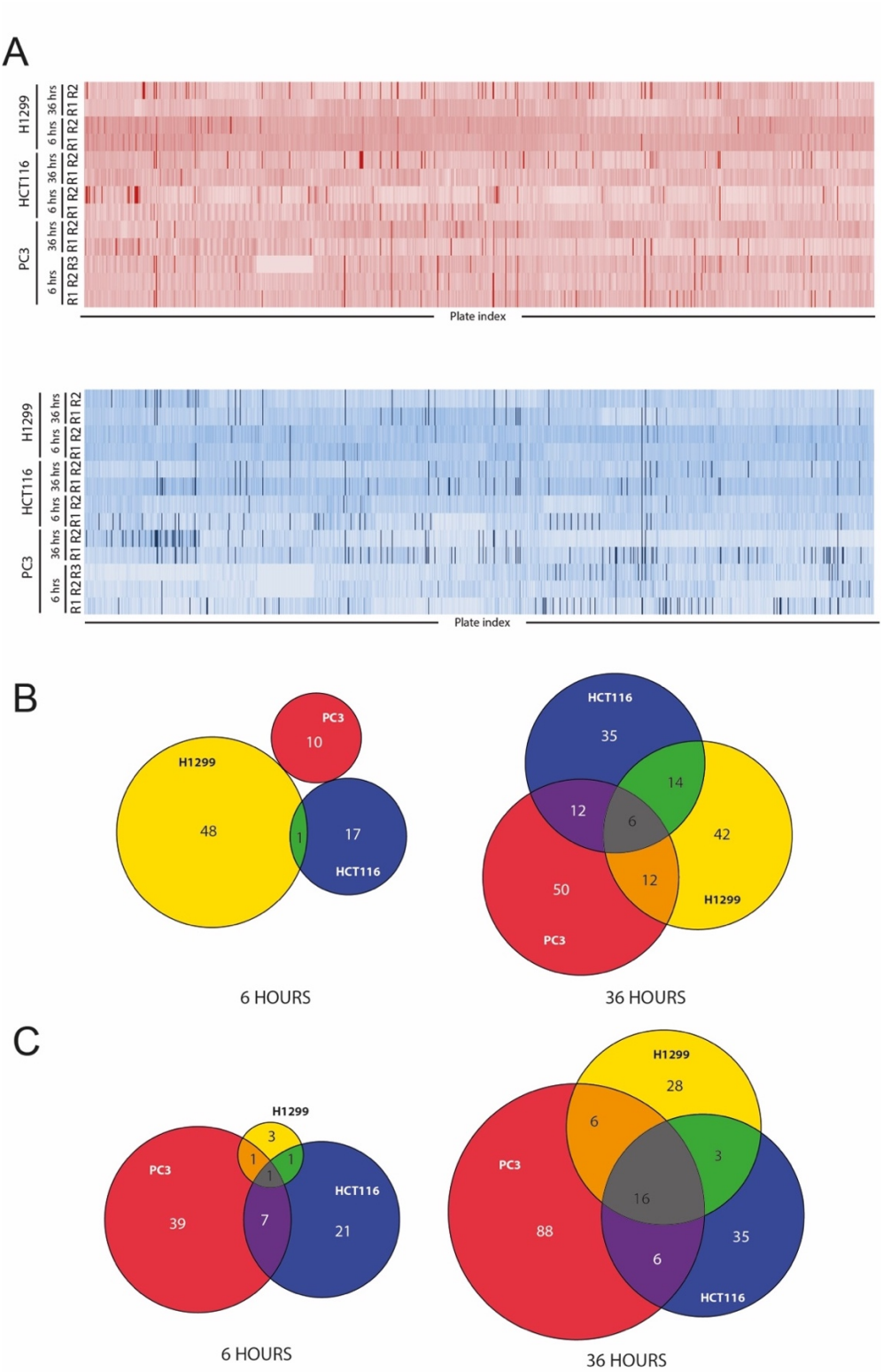

Figure 19 ***Sum of screening results for compounds altering the nuclear size.*** *A. Heat map for larger and smaller nuclear size. Results are presented with a darker color for high alteration of the nuclear size after normalization against the controls. Compounds increasing nuclear size are presented in red and compounds reducing nuclear size are presented in blue. B. Eluero-Venn diagrams for compounds reducing nuclear size. Diagrams are divided by cell line screened (PC3, HCT116 and H1299) and time point (6 and 36 hours). C. Eluero-Venn diagrams for compounds increasing nuclear size. Diagrams are divided by cell line screened (PC3, HCT116 and H1299) and time point (6 and 36 hours).*

3.7.3 Cluster analysis reveals classes of compounds altering nuclear size or the karyoplasmic ratio of cells

Data were also analysed by type of compound and their therapeutic group to identify if there is any correlation between nuclear size regulation and therapeutic group or the molecular targets of these compounds. Clustering analysis revealed that some therapeutic groups, such as adrenergic receptor antagonists or Na+/K+ ATPase inhibitors, tend to cluster together, leading to an increase of the nuclear size more in the H1299 cell line compared to the other cell lines. Other compounds instead have a wider effect on all the cell lines such as microtubule inhibitors or MAP kinase inhibitors (Fig 20A). For compounds specifically decreasing the nuclear size, 5-HT serotonin uptake and cyclo-oxygenase inhibitors affect the nuclear size in most of the cell lines with some stronger effects on the PC3 cell line (Fig 20B).

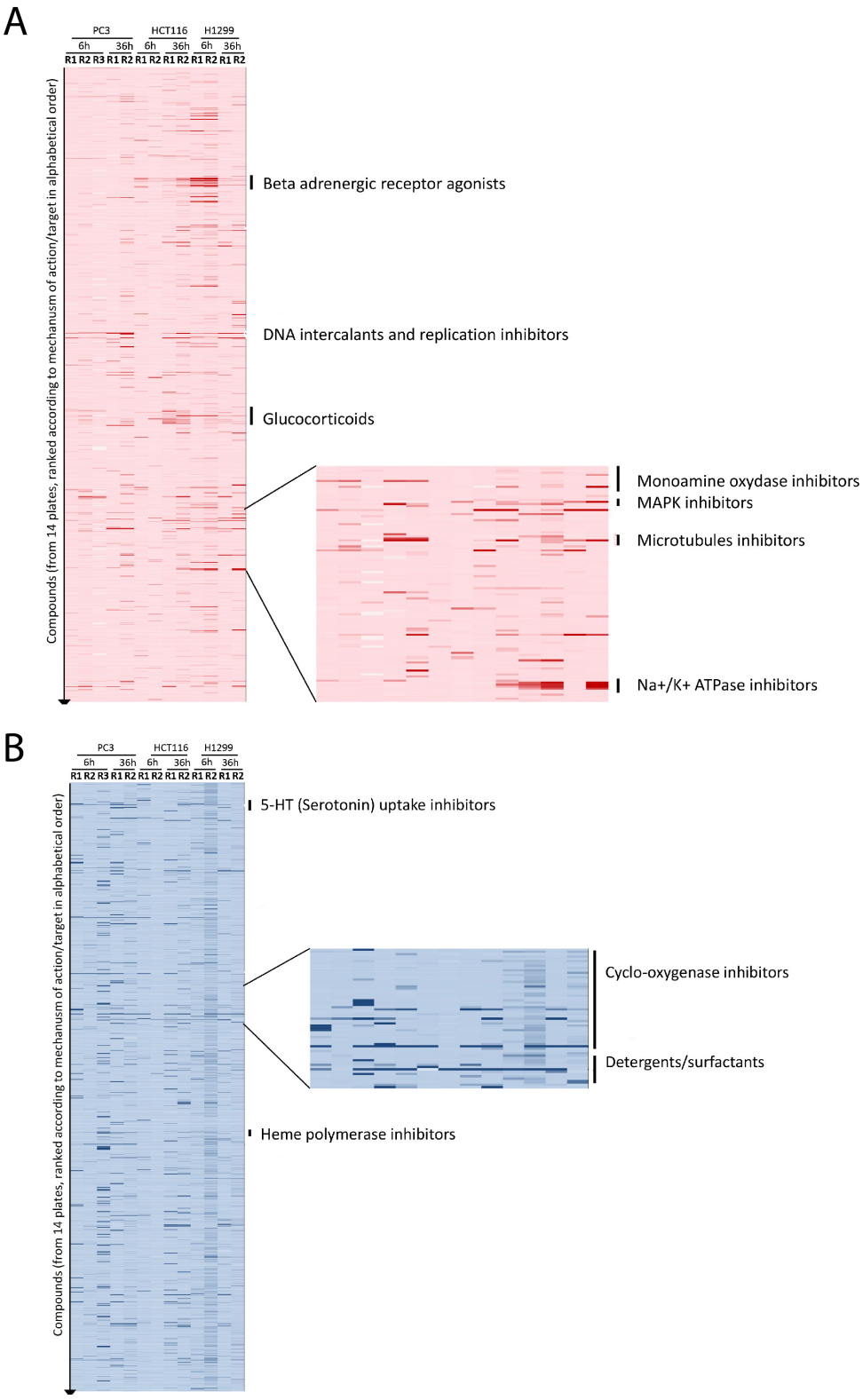

Figure 20 ***Cluster analysis for compounds altering the nuclear size.*** *A. Heat map cluster analysis for compounds increasing nuclear size. Data are plotted based on the therapeutic effects of the drugs in the library, dark red compounds represent stronger effect on nuclear size compared with the DMSO controls. B. Heat map cluster analysis for compounds decreasing nuclear size. Same analysis as above was performed for this set, where dark blue indicate positive effects on decreasing nuclear size.*

Interestingly, analysing the therapeutic groups clusters it results that some compounds can alter the nuclear size both in the nuclear size aspect and the karyoplasmic ratio (e.g. Na+/K+ ATPase and COX inhibitors and microtubule depolymerisation agents), where other compounds such as β-adrenergic receptor inhibitors increase only the nuclear size with no effects on the karyoplasmic ratio, indicating an activity on the general scaling of the cells of those compounds (Fig 21).

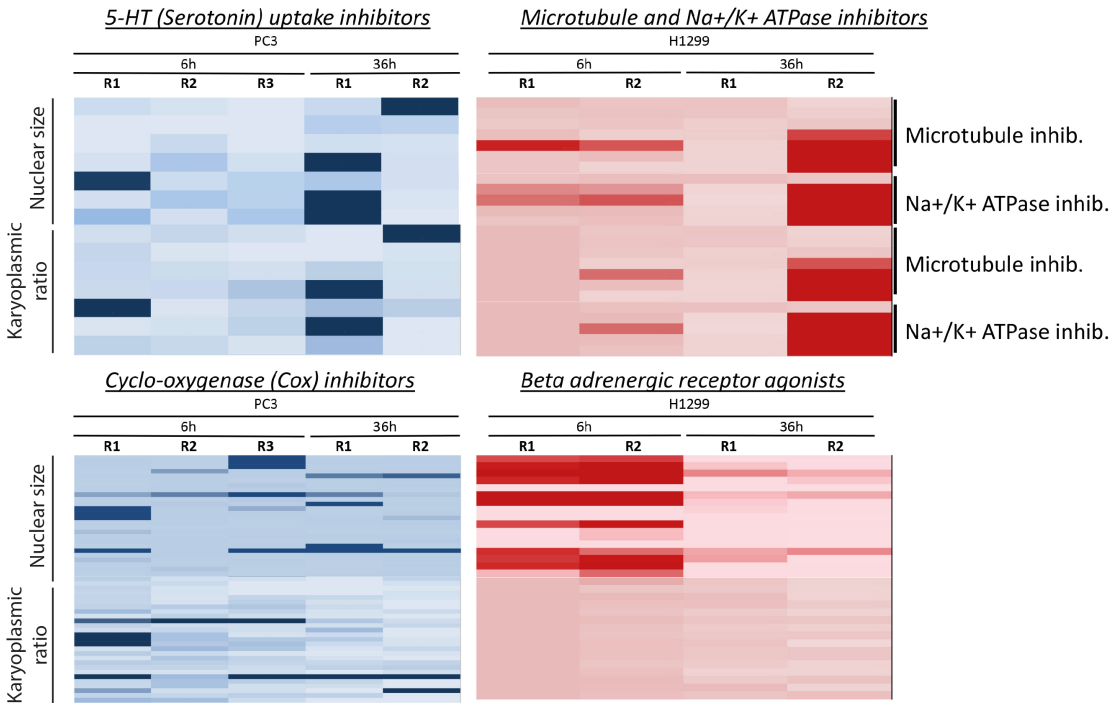

Figure 21 ***Comparison of nuclear size and karyoplasmic ratio alteration in cluster analysis.*** *Heat map of the cluster analysis for nuclear size and karyoplasmic ratio are presented side by side. Data in blue represent reduction of the parameter analysed and red represent increase of the parameter with the darkest colours indicating a stronger effect.*

Analysing compounds that affect nuclear size leading to an increase, and therefore potentially benefitting the lung cancer model (H1299 cell line) in re-establishing a normal and more physiological nucleus, we can identify some classes of compounds that have effects at the 6 h time point such as β-adrenergic agonists and on the longer incubation at 36 h such as microtubule

polymerization inhibitors. Bronchodilatators and Na+/K+ ATPase inhibitors instead have an increased nuclear size effect on the H1299 cell line in both of the time points and therefore flag these classes of compounds as potentially interesting for follow up characterization.

For compounds decreasing nuclear size, and therefore potentially beneficial for cancers in which enlargement of the nuclear size correlates with worse prognosis such as prostate cancer (PC3 cell line) and adrenocortical carcinoma (HCT116 cell line), the classes of compounds that generated more hits are 5-HT serotonin uptake, cyclo-oxygenase inhibitors and microtubule depolymerisation agents, with a strong effect on both the nuclear size as well as the karyoplasmic ratio. These classes of compounds are the most promising for further analysis in these cancer types and could provide interesting compounds to be tested and translated into the clinic.

3.8 Chapter summary

As targeting nuclear size and shape in addition to already existing chemotherapy regimens could result in less aggressive/metastatic tumours, it is of particular interest to identify potential new protein targets and drugs and to understand the potential mechanisms and factors that lead to loss of nuclear size during cancer progression. In this chapter I analysed roughly 50 NETs for their ability to change nuclear size when overexpressed in different cell lines with a high throughput approach. The approach allowed the fast analysis of multiple proteins at the same time resulting in identification of 18 potential NETs that can now be further characterized in detail for their roles in nuclear size regulation. Although the screen benefited from several high-throughput aspects, it also had some drawbacks. Firstly, it is possible that some NETs were missed due to the difficulty in obtaining high transfection efficiencies in a 96 well format. If the screen were to be repeated this could be overcome with the establishment of stable cell lines overexpressing each of the proteins analysed in this study, although their generation would be a large amount of work so that the cost-benefit ratio might not be very high. There also might

have been more NETs identified if we had performed knockdown of the NETs as well, and especially as in doing both we could have identified NETs where overexpression had one effect on nuclear size and knockdown had the opposing effect. This was not done initially because, as transmembrane proteins, NETs we have targeted in the past do not tend to turn over as fast as soluble proteins and we have also had much lower success rates even with commercially designed siRNA pools than others report for soluble proteins in knocking NETs down. Therefore, the initial investment in the time to develop these reagents would have potentially limited outcomes in the timeframe of the PhD. This, however, would have definitely had a strong benefit as it would allow us to investigate what likely happens physiologically in cancers where NETs are downregulated as is often observed in the TGCA database for NETs. Now that CRISPR approaches are getting much more successful and efficient this would perhaps be an even better way of generating lines with different NET knockouts for a future screen. Another limitation on the screen is the use of a single plane to measure nuclear area as opposed to measuring volume from taking z-sections and generating 3D reconstructions. Nonetheless, to minimise this defect, the plane decided for the screen represented the middle plane section for all the cells and any error made was likely minimized by the high numbers of cells analysed. With the current screen configuration, positive hits can be subsequently tested in more detail with 3D volume reconstructions on a higher resolution microscope to prove or discard the NET influence in nuclear size regulation.

The fact that in two different cell lines we observe different proteins affecting nuclear size is consistent with the idea that tissue specific effects seen in different cancers for nuclear size changes are due to functions of different pools of proteins differently expressed in each tissue. This argues that, instead of using more generalised drugs in chemotherapeutic procedures such as taxol, incorporating compounds with more tissue specific effects might be applied to reduce toxic side effects and produce a more effective response against a particular tumour type. If indeed tissue-specific NETs are responsible for nuclear size changes, the size changes contribute to the increased

metastasis, and drugs identified in the compound screen target those NETs, then this approach could work, though much groundwork is still needed to determine these points. Nonetheless, this interpretation is consistent with bioinformatics analysis of cancer genotypes in the TCGA database where the same NET had gene amplifications in one cancer type and loss in another that both corresponded to the nuclear size changes observed in culture for the NET effects. It is nonetheless important to remember that this analysis is on the gene copy number and the second allele could theoretically overcompensate at the protein level for the loss of one gene copy or alterations in the mechanism of protein clearance and degradation can compensate for aberrant amplification of a gene. However, in general the indication of differential alteration of gene numbers, for these specific proteins, is consistent with the idea of tissue specificity of phenotypes and alterations due to tissue-specific NETs with effects on nuclear size.

Along with the identification of potential new proteins that can be used as targets to specifically restore normal nuclear size in cancer cells and thus potentially reduce aspects of the increased metastasis associated with the nuclear size defects, these screens identified several repurposed drugs that can also alter nuclear size. The choice of using a pre-approved drug library should allow for more rapid translation of the identified drugs into clinical studies. The results showed that targets of nuclear size alterations are tissue specific, with small or in some cases barely any overlap within compounds identified in different cell lines. Among the identified compounds there are some that are already being used as effective anti-tumour treatments or other drugs that alter the nuclear size for obvious reasons such as anti-mitotic or microtubule depolymerizing drugs. The success in compound identification suggests that nuclear size as a readout for larger chemical libraries could identify even higher specificity and affinity compounds for cancer treatments. No particular class of drug emerged as strongly predominant in the screen that would have led to focus future studies on a more specific class of compound, but any of the identified compounds could be studied individually for changes in effectiveness with slight chemical modifications. This idea will be of interest

with some experiments in the next chapter where some of the strong and interesting hits identified in this chapter will be further characterized.

4. Characterization of compounds altering the nuclear size

4.1 Introduction

The idea that targeting nuclear size might be beneficial for treating patients will be explored in detail with this chapter. The main hypothesis is that targeting nuclear size with small compounds might lower the metastatic potential of that given cancer. Thus we tested the identified compounds in the high throughput screen in vitro in standard cell culture assays and in vivo for reduction of motility and reduction of the tumour size in xenografts models. The different compounds were chosen due to their tissue specificity identified during the screening process, namely oxyphenbutazone, paroxetine hydrochloride, parbendazole, piperlongumine and digitoxigenin (Table 11).

Oxyphendutazione is a nonsteroidal anti-inflammatory drug (NSAID) that has been shown to be a cancer chemopreventive agent in skin carcinogenesis (Kapadia et al. 2010) and able to induce cytotoxicity in hepatocellular carcinoma model systems via inhibition of Wnt-β-catenin pathway (Saleem et al. 2017). Paroxetine hydrochloride is an antidepressant of the selective serotonin reuptake inhibitor (SSRI) class and is used for treatment of different mental disorders as major depressive and obsessive-compulsive disorders. It interacts with different enzymes of the cytochrome P450 complex (Sanchez, Reines, and Montgomery 2014), and it causes altered influx of calcium in astrocytes inducing mitochondrial-induced

apoptosis (Then et al. 2017). Parbendazole is a substitute 2-ammino derivative showing a broad spectrum anthelminthic activity. It has been proved as an extremely potent microtubule assembly inhibitor by direct binding to tubulin (Havercroft, Quinlan, and Gull 1981; Quinlan et al. 1981). Digitoxigenin is a cardenolide, the aglycone of digitoxin. Digitoxigenin has been shown to induce cytotoxic effects on non-small cell cancer cells, inhibiting the Na,K-ATPase activity and effective chemotherapeutic against metastatic uveal melanoma (Fagone et al. 2017; Schneider et al. 2018). Piperlongumine is a natural alkaloid produced by the plant of long pepper (*Piper longum*). This compound has been analysed in different studies due to its anticancer activity. The mechanism of action of piperlongumine is a strong interaction with the glutathione S-transferase Pi 1 that inactivates the enzyme generating a reduction of free glutathione and increase in ROS thus triggering apoptosis responses (Harshbarger et al. 2017; Raj et al. 2011). Piperlongumine has also been successfully used to treat breast cancer in xenograft models, showing reduction of the tumour volume and no metastasis (Bharadwaj et al. 2015; Raj et al. 2011).

Table 11 ***Main characteristics of compounds tested in this chapter.*** *The compounds were identified in the high throughput screen for their ability to alter the karyoplasmic ratio in different cancer cell lines*

Compound name	Structure	Molecular Weight	Therapeutic group
Oxyphenbutazone	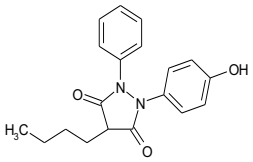	324.38285	Anti-inflammatory
Paroxetine Hydrocloride	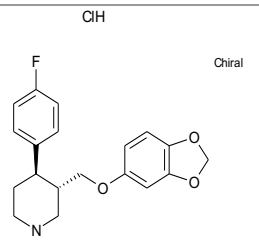	365.83552	Antidepressant
Parbendazole	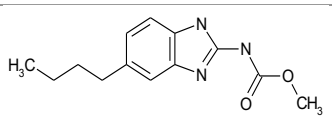	247.29934	Anthelmintic
Piperlongumine	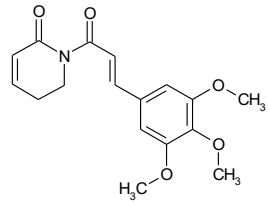	317.34468	Antifungal
Digitoxigenin	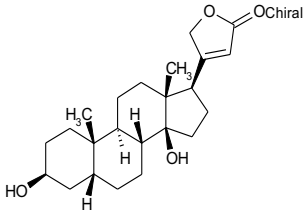	374.52503	Cardiotonic

4.2 Drugs altering nuclear size can impact cell motility

Scratch wound healing assays are standard assays to establish effects on cell movement typically from protein knockdowns or chemical/drug treatments. A single monolayer of cells is typically mechanically disrupted by scratching with a teflon block though the cells can also be electrically wounded. This generates an area that is free of cells which is monitored until wound

closure. If drug treatment is affecting the ability of cells to migrate, this will result in a longer time for wound closure.

To be sure the measurement of wound closure is only dependent on the mobility of cells and not on cell division, cells are usually starved with 1% FBS containing medium and we did this 16 h before the scratch. Cells were treated with 6 different concentrations of the selected compounds in four replicates, immediately following the scratch and were recorded every 3 h for at least 48 h. Analysis of the wound closure times against the controls revealed that only paroxetine hydrochloride had no effect on the migration of the cells at any of the concentrations tested. Oxyphenbutazone reduced the migration in a dose/concentration dependent manner until a concentration of 100 nM of the compound, where parabendazole has effects on the migration at higher concentrations (up to 1uM) but no statistical significant effects at the lower concentrations.

(Fig 22A)

Cell morphology was visibly altered in the oxyphenbutazone samples, with cells mostly rounded and marginally attached to the plate. This could mean a cytotoxic effect of the drug inducing apoptosis or necrosis in the sample. While this potentially increases its value as an anti-cancer compound, it makes it difficult to separate its effects specifically on cell migration. Nonetheless, such as effect seems logical as Oxypenbuatazone is known to actively depolymerize microtubules, which would inhibit cell migration. This also blocks mitosis and can be the explanation for a high number of cells with a rounded shape as opposed to the cells directly initiating apoptosis. To further elucidate the real effects of the drugs on cell proliferation and apoptosis additional tests for viability and cytotoxicity will be described in the following sections of this chapter.

Piperlongumine and digitoxigenin were separately tested for wound healing assays in both the PC3 cells and the H1299 line. These wound healing assays showed a peculiar pattern with one drug having an effect on wound closure in one cell line and not the other and vice versa. Piperlongumine had a strong effect in the nuclear size screen at the two highest concentrations of

the serial dilutions used in the assay (10μM and 1μM) in PC3 and H1299 cells, but piperlongumine had no effects on nuclear size in H1299 until 36 hours of incubation. Digitoxigenin instead increased wound closure time in H1299 until a concentration of 100 nM, but had no effect in the PC3 cell line (Fig 22B-C). These results altogether indicate a high tissue specificity in targeting nuclear size while at the same time reducing the migration of cells.

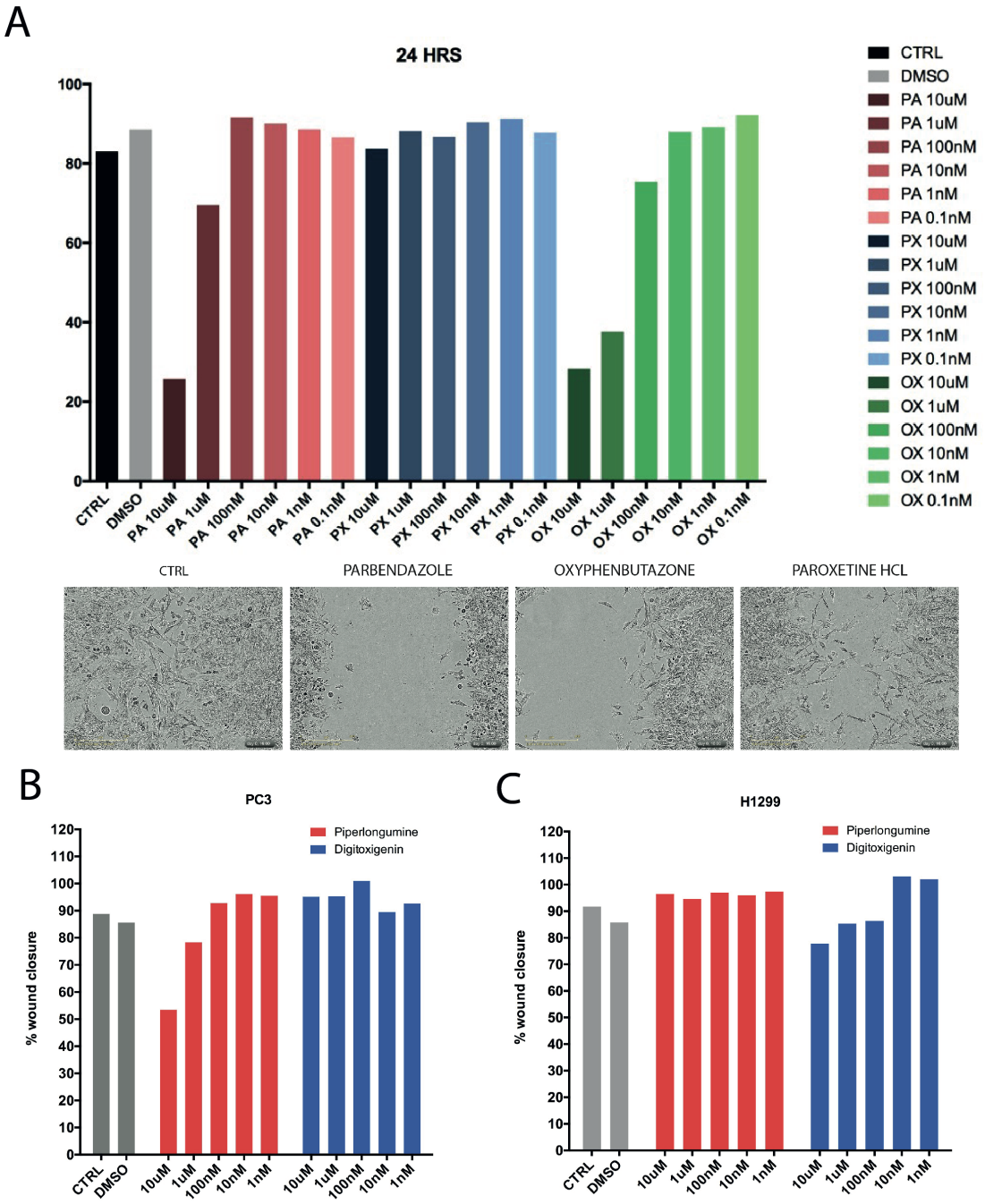

Figure 22 ***Wound closure assays for compounds altering nuclear size.*** *A. Percentage of wound closure for parbendazole, paroxetine HCl and oxyphenbutazone. The PC3 cell monolayer was scratched with a 96 well plate scratcher and medium was replaced with serial dilution of the compounds of interest. Cells and wound area was monitored with an Incucyte system, scanning every 3 hours for 3 days. Data in the graph are for the 24 hour time point when control wound was completely closed. Representative images of the wound closure were taken with and Incuyte (Essen Bioscience). B. Percentage of wound closure for piperlongumine and digitoxigenin in the PC3 cell line. The same assay was carried out for the last 2 drugs identified in the PC3 cell line following the same protocol. C. Percentage of wound closure for piperlongumine and digitoxigenin in H1299 cell line. The assay was carried out also in the H1299 cell line for direct comparison with the PC3 cell line.*

4.3 Drugs altering nuclear size can trigger apoptotic cascades

One of the variables that is not always easy to distinguish in the wound healing assays is if the effects seen on the migration are directly due to reduction of motility or to induction of cell death impeding cell movement. This can be done using Annexin V labelling if the wound healing assay setup includes an immunofluorescence setup. However, in our case to avoid misinterpretation of the wound healing assays, I separately performed apoptosis and necrosis detection by FACS and viability assays. A good cancer therapy from our approach should be able to target motility and therefore the metastatic potential, but also not induce necrosis that triggers inflammation reactions. If the drug also induces apoptosis this would increase the efficacy of the treatment as it will act on the main tumour site, reducing the tumour size or growth, and if coupled with reduced migration and extravasation would prevent metastatic spread. Drugs could also reduce cell proliferation and not just induce apoptosis or necrosis, this would result as a not proliferative tumour without tumour growth. This effects will be tested later on in this chapter to gain a comprehensive view of the effects of each single drugs.

The apoptosis or necrosis induction was detected with a standard Annexin V/Propidium Iodide staining before FACS detection. In the early stages of apoptosis one of the first events happening is the translocation of phosphatidylserine from the inner lipid layer of the plasma membrane to the outer. Annexin V has a high affinity for phosphatidylserine and cannot get through the lipid bilayer, which makes it a great marker to follow early stages of apoptosis as this outer plasma membrane staining appears. Propidium Iodide is also impermeable to the plasma membrane and so only gets into cells that have lost membrane integrity, thus allowing detection of cells in late stages of apoptosis and necrosis. The co-staining results in 4 different populations of cells, living healthy cells with no staining, early stage apoptotic cells positive only for Annexin V, late stage apoptotic cells positive for Annexin V and propidium iodide, and necrotic cells positive only for propidium iodide.

PC3 cells were incubated with drugs for 24 or 36 h, refreshing the medium every 24 h, and gating strategies for the analysis were decided for detection only in singlets and intact cells (Fig 23A). PC3 cells were chosen as the cell line to test as this was the first cell line screened and for which results were available first, and to keep consistency with the other analyses performed through this study.

Analysis revealed that oxyphenbutazone has a strong effect on triggering apoptosis processes with 10% of cells being in an early stage and around 70% of cells in late stages of the apoptotic cascade. Parbendazole showed a lower ability to trigger the apoptotic process with around 20% of the cell population being in early and late stages of apoptosis. Paroxetine had no effect in inducing either apoptosis or necrosis, in line with no strong effect on migration in the wound healing assays. For this reason, this drug was removed from further analysis. Piperlongumine had a strong effect in inducing apoptosis, but not necrosis, to the same extent of oxyphenbutazone. Finally, digitoxigenin induced apoptosis and necrosis in this cell line with almost 70% of cells exhibiting necrosis or in in late stages of the apoptotic cascade (Fig 23B). All together these apoptosis analyses show promising effects for oxyphenbutazone, parbendazole, piperlongumine and digitoxigenin to be further characterised and tested in more detailed assays to try and translate them into clinical drugs.

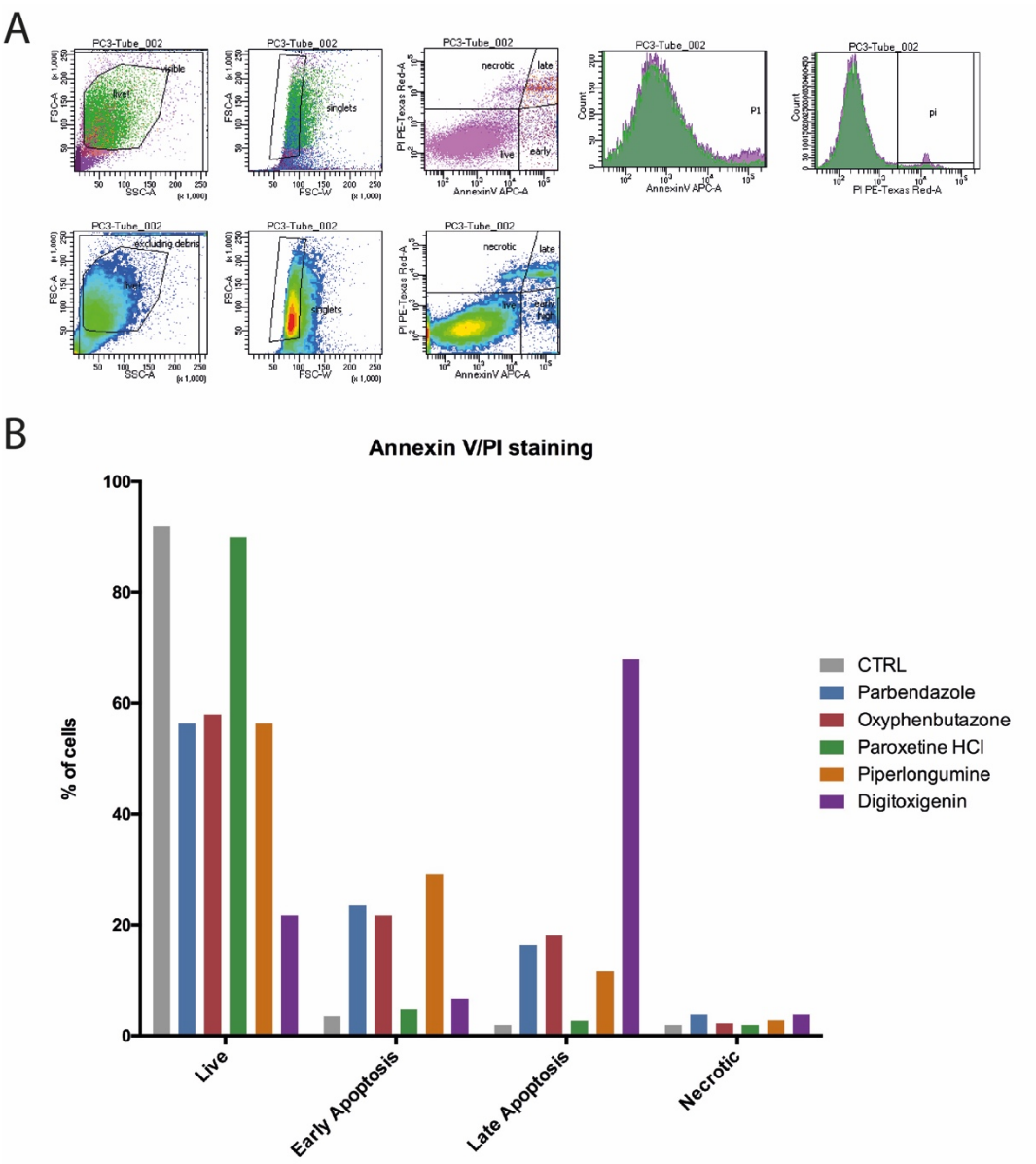

Figure 23 ***Apoptosis/Necrosis analysis for compounds that alter nuclear size.*** *A. Gating strategies for AnnexinV/Propidium Iodide FACS analysis. Cells were gated to take into account only live, intact and single cells (first 2 gating). Detection of Annexin V and propidium iodide fluorescence allows detection of live, early apoptosis, late apoptosis and necrosis depending on the presence of no, one of both florescence signal. Live cells are not positive at any of the stainings, early apoptotic cells present fluorescence only for Annexin V, late apoptotic cells are positive for both of the staining and necrotic cells are positive only for propidium iodide staining. B. FACS results at 36 hours for drugs altering nuclear size analysed in this study. PC3 cells were treated with a concentration of 10μM for each compound for 36 hours, refreshing the medium every day. Cells were stained with the protocol mentioned in material and methods and run through the FACS for detection of the two dyes.*

For viability analysis, a resazurine-based assay was performed. This assay allows quantification of live cells due to reduction of the resazurine to resorufine, a red and highly fluorescent compound, in healthy cells. The detection of either the absorbance or fluorescence of the coupled

resazurine/resorifine allows the determination of live cells numbers compared with controls. All cells were incubated for 24 h with serial dilution of the drugs to generate a curve dose-response.

In line with the apoptosis/necrosis assay parbendazole and oxyphenbutazone reduce cell proliferation in all three cell lines at high concentration with low effects at the lower dilutions (Fig. 24A). Piperlongumine and digitoxigenin, on the contrary, have different effects on the three cell lines tested. Where piperlongumine has mainly the same IC50 in all three cell lines, digitoxigenin has much stronger effects on the prostate cancer PC3 cell line and less toxicity in the lung and colon cancer cell lines (Fig 24B).

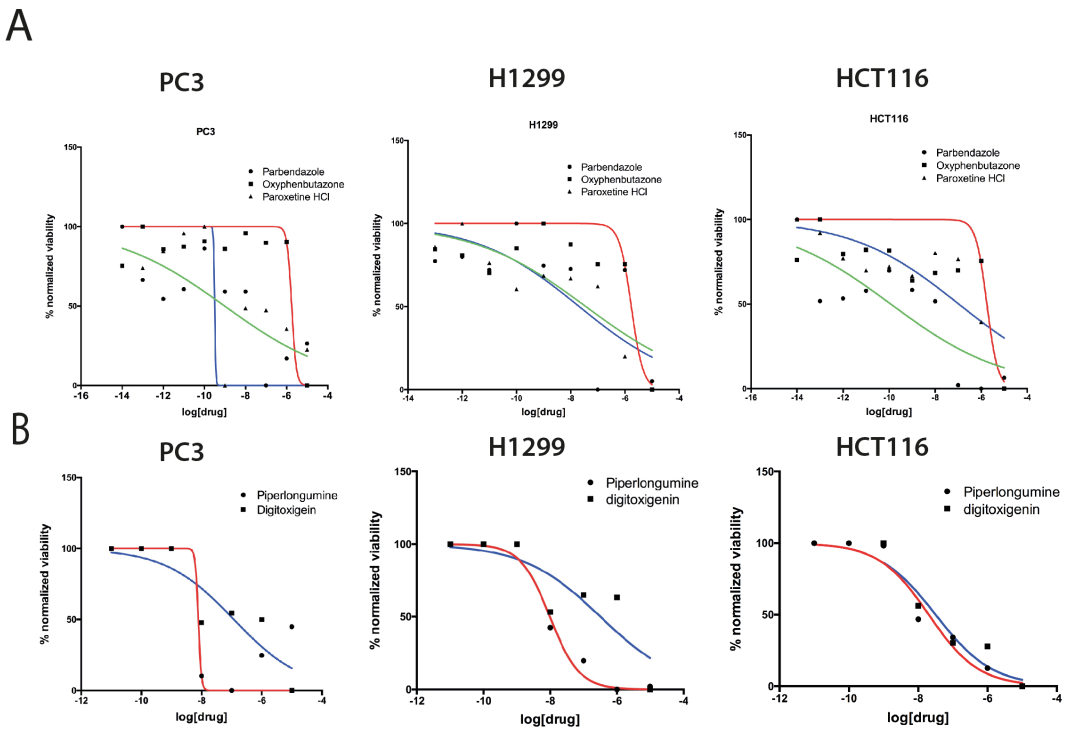

Figure 24 ***Curve dose response (viability assays) for compounds altering nuclear size.*** *A. Oxyphenbutazone, parbendazole and paroxetine curve dose/response in PC3, HCT116 and H1299 cell lines. Cells were incubated for 24 h with serial dilution of the drugs of interest. Alamar blue cell viability solution was added to each well of a 96 well plate and cell were incubated for 3 h to allow development of the fluorescent dye. Plates were read with a fluorescent multi-well plate reader and normalized to the controls (DMSO). B. Piperlongumine and digitoxigenin curve dose/response in PC3, HCT116 and H1299. The same protocol was used to determine curves dose/response for the drugs piperlongumine and digitoxigenin.*

4.4 In vivo studies

As most of the drugs in the PAD library are already approved by different government bodies for use in humans the drugs identified in my screens should have an easier translation to the clinic. To test if any of the compounds identified in the screen have a therapeutic effect in reducing the proliferation of tumours and spread of metastasis in a living organism, a xenograft mouse model was engaged. One of the main problems encountered in analysing the literature for the drugs taken into consideration in this chapter was to identify the IC50 for mice so that we could determine concentrations and dosage to be used for treatment in the xenograft models. Oxypehenbutazone and parbendazole have never been used *in vivo* for treatment of any xenograft models, therefore a control group with different concentrations and dosage was needed making these two drugs less attractive for initial *in vivo* experiments. Moreover, as these drugs have never been used and concentrations are not known, a negative result in xenograft models could miss a promising compound that simply needed a higher concentration used.

The most promising drug that from literature and previous characterization could have effects on tumour growth is piperlongumine. This drug has been already been used in *in vivo* models and concentration and dosage have been tested with a strong effect in reducing tumour growth in different type of cancers, such as breast and bladder cancer. A prostate cancer xenograft mouse model was generated by injection of PC3 cells carrying a luciferase marker for detection of tumour size and spread in both flanks of male nude mice. The tumours were then allowed to grown and once tumours reached the size between 0.02 cm^3 to 0.05 cm^3, mice were randomized and treated daily through the weekdays either with a control solution of 10% DMSO or 15 mg/kg piperlongumine for three weeks.

Tumours showed considerable growth the first week after injection, but were too soft for start the actual treatment. In the beginning of the second week there was a small reduction of the volume due to the matrigel dissolving. At the end of the second week tumours looked solid and ready for treatment (Fig 25) Unfortunately, by the second week of treatment tumours in both the control

and the treatment group started declining due either apoptosis or necrosis, making reading of tumour size hard to perform and rendering the experiment a failure. However, differences in size were observed between the control and piperlogumine treated tumours with the piperlongumine treated smaller. This suggests that it is worth repeating the experiment, but in the next repeat of this xenograft model the tumour should allowed to grow for at least three weeks before starting the drug treatment and I will increase the amount of cells injected to account for possible cell death of this particular cell line. This repeat will unfortunately not be available until after submission of this thesis.

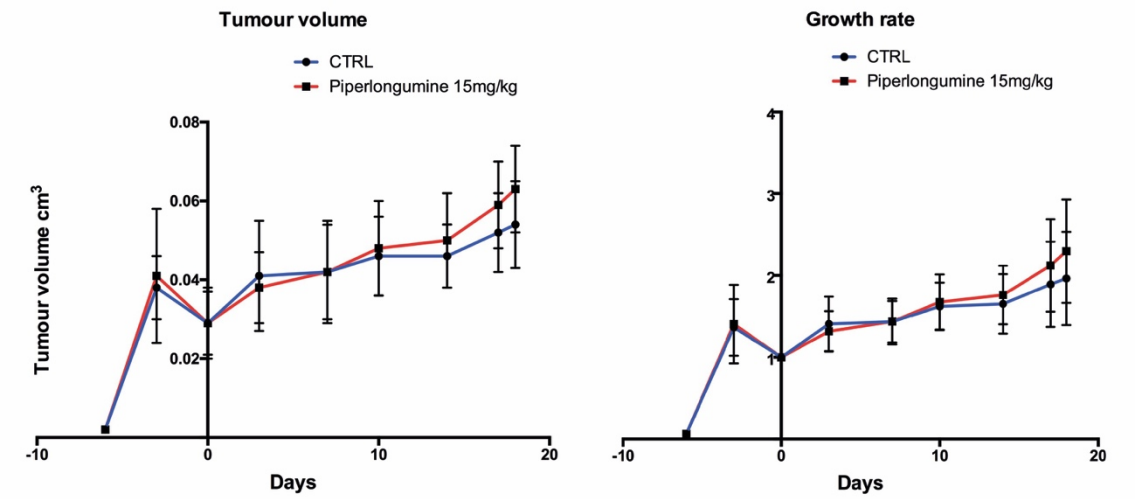

Figure 25 ***Tumour volume and growth curve for DMSO and piperlongumine xenograft models.*** *Average tumour volume and growth curve for control group treated with 10% DMSO (5 mice, 10 tumours) and 15 mg/kg piperlongumine (5 mice, 10 tumours). Tumours were monitored by calliper measurements at the beginning and end of each week of the experiment.*

Pipelongumine has been shown to reduce tumour size in breast cancer and an inhibition of STAT3, binding the pY-peptide ligand reducing the nuclear translocation, inhibition of ligand-induced and consecutive STAT3 phosphorylation. This results in modulation of pre and anti-apoptotic genes leading to reduced tumour growth (Bharadwaj et al. 2015). To test if this can transpose into prostate cancer we performed ELISA assay for the total and phosphorylated STAT3. Results shown that there is a statistical significant reduction in pSTA3 between the control and the treated mice groups, but not

for the tSTAT3 (Fig 26). This suggests an activity of the compounds in possibly inducing apoptosis in prostate cancer tumours as well, arguing for a necessary repeat of the xenograft models to validate the data with a normal growing tumour.

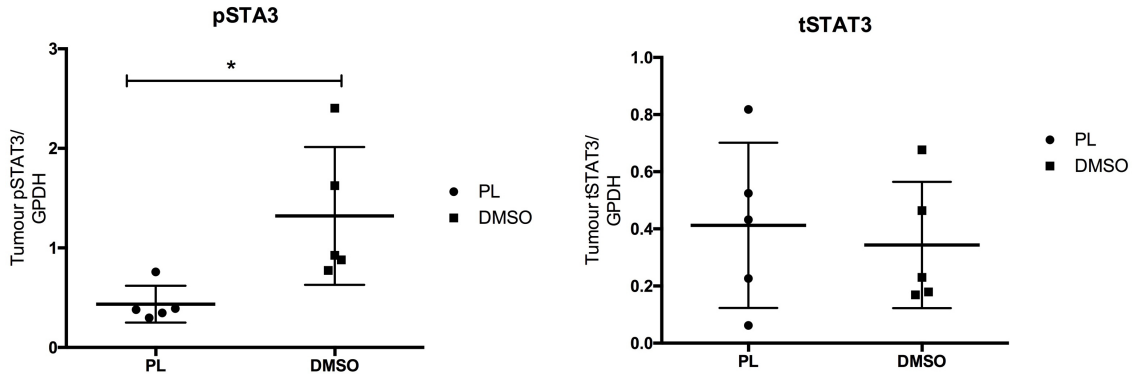

Figure 26 ***Reduction of pSTAT3 induced by piperlongumine in xenograft models.*** *Whole cell lysates from tumour tissue treated with DMSO or piperlongumine (PL). GAPDH normalize pSTAT3 and tSTAT3 are plotted alog the Y-axis. Statistical significance calculated with an unpaired t test with Welch's correction, **: p<0.01, ****: p<0.0001.*

4.6 Chapter summary

In this chapter I have shown that compounds identified in the screens of the preceding chapter have effects on different aspects of cell viability, motility and cytotoxicity, besides the ability of alter the karyoplasmic ratio. Taken together these results show that the targeting of nuclear size can lead to reduction of migration and therefore potentially less metastatic tumours. Note that effects on nuclear size alteration are tissue specific as well as the effects in migration, where a drug can have an effect on a particular cell line, - e.g. piperlongumine reducing cell motility in the PC3 cell line but not in the H1299 line. At the same time, drugs having effects on nuclear size might not have an effect on cell migration at all as per the compound paroxetine hydrochloride. This might be due to alterations of nuclear size that do not alter nucleoskeleton-cytoskeleton interactions or activation of a pathway that leads to nuclear size alteration without affecting motility function. In general, most of the drugs identified in the screen altering the karyoplasmic ratio or nuclear size and tested in this chapter have direct effects on cell migration.

Moreover, the compound treatments mostly resulted in the triggering of apoptotic cascades instead of inducing necrosis. This is extremely important in the development or repurposing of drugs as apoptosis cascades are preferred to necrosis as apoptosis does not induce inflammation processes in the tissue that are induced by necrosis and might have undesired effects on the patients. The induction of apoptosis is particularly interesting in light of some aggressive tumours where the detection of metastasis is already to an advanced state than in most cases is not curable. Compounds with tissue-specific effects that combine inhibition of metastatic spread with killing of the tumour without also inducing inflammation are the theoretically most ideal for treating patients.

In this chapter, I have performed a number of both cell culture and in situ assays to determine compound effects on cell migration, proliferation, viability and their effects on tumour growth. There are a number of additional assays that would be useful to further characterise these compounds, such 3D invasion assays that represent a great model for extravasation processes in vitro and give a better insight on the real migratory capacity and invasiveness potential of cancer cells and how this is altered by drug treatment.

Using a pre-approved drug library in the screen will hopefully allow a faster translation into clinical usage, therefore the PAD library was chosen as the main library to perform the screen. Before translation into clinical usage of the identified drugs a xenograft mouse model is critical to assess potential benefits of drugs identified in the screen in reducing tumour growth and metastasis. Even though the drug used in our first xenograft model, piperlongumine, was known to reduce tumour growth in different other cancer types, a quick remission of the tumours in both treated and control mice during the treatment period made the result hard to interpret and a repeat of the xenograft model is required to prove the efficacy of piperlongumine in reducing tumour growth for prostate cancer. This will elucidate the real potential of nuclear size targeting as a new and effective targeting strategy to reduce metastatic potential of highly aggressive cancers and provide a tool for development of new drugs to be added as part of actual chemotherapeutic regimens.

5. Regulation of nuclear size driven by NETs and compounds: NET50 in prostate cancer

5.1 Introduction

The idea that adding compounds targeting nuclear size to other drugs in current chemotherapy regimens could be an effective treatment to reduce the metastatic potential of certain tumour types while reducing toxicity due to the tissue-specific effects has been the driving force behind this study and is strongly supported by the results of the previous two chapters. However, such treatments could be even more targeted and directed if the specific targets involved in the nuclear size changes to begin with were known. The NET screen identified several such candidate targets and suggests the hypothesis that some of the drugs may act on these NETs; however this hypothesis is as yet unproven. If nuclear size changes contribute to that increased metastatic potential and the tissue specificity of nuclear size changes in the different tumour types is driven by these tissue-specific NETs, then these NETs can be directly targeted in future screens for drug development. In this chapter I will investigate one of the proteins identified as a promising nuclear size regulator in the early and late stages of prostate cancer LNCaP and PC3 cells models, NET50. The chapter will explore in more detail the NET50 effect on nuclear size and then investigate both its potential interaction with a compound identified for correcting the nuclear size defect in the PC3 cancer model,

estradiol propionate, and the role of nuclear size changes in metastatic characteristics of the later stage prostate cancer.

5.2 Prostate cancer progression

Prostate cancer is the most non-skin cancer in men in the Western world (Jemal et al. 2010). The progression through the disease is sustained by circulating androgens acting on the androgen receptor (AR). Levels of androgens are regulated through the hypothalamic-pituitary-adrenal-gonadal axis and at the diagnosis of the disease the androgen-deprivation therapy is used to reduce the androgens circulating to reduce the growth and sustainment of the tumour (Tsao et al. 2012). This results in most of the cases as temporary regression of the pathology in most patients, but the therapy or surgical castration tend to fail resulting in a new growth of the tumour. Several, despite castration, are the reasons allowing androgens to circulate and sustain the new growth of the tumour such as AR gene amplification or residual testosterone in the prostate microenvironment (Visakorpi et al. 1995).

5.2.1 Current treatments for castration recurrent prostate cancer

One of the current chemotherapy treatments for castration recurrent prostate cancer (CRPC) is estradiol (E2) which is believed to downregulate androgen production via a negative feedback control (Bosland 2005). Several studies on estradiol as an effective treatment for CRPC lead to different results and the literature is quite controversial on the topic; however, this is particularly interesting considering the dehydrogenase function of NET50/DHRS7 and the fact that estradiol was reported as one of its substrates (Skarka et al. 2014). Estradiol seems to be more effective than the currently used diethylstilbestrol in killing early and late stages of prostate cancer models *in vitro*, with the ability to activate different MAPs generating signalling cascades for the production of reactive oxygen species (ROS) or induction of caspase cleavage leading to either necrosis or apoptosis (Koong and Watson 2014). Estrogens, and in particular estradiol, have been shown to reduce CRPC growth in

orchiectomized mice xenograft models. The inhibition is related to the ability of estradiol to reduce intratumoural androgen levels and is not dependent on the presence or activation of the estrogen receptor (Montgomery et al. 2010). For these reasons estradiol has been proposed as a potential treatment for further investigation for targeting different aspects on steroidogenesis in prostate cancer.

During the set-up of the parameters for the compounds high throughput screen, one of the compounds that shown alteration on the karyoplasmic ratio was and estradiol derivative, estradiol propionate. The set-up was performed with some plates form the Microsurce Spectrum library and estradiol propionate showed effects where other estradiol derivatives showed no alteration of the karyoplasmic ratio. Estradiol propionate is a direct estradiol derivative, bearing a carbonyl group instead of a single oxygen at C17β, and is a chemically synthetized compound not present in nature. As it has been shown that NET50 has activity against steroid-like molecules and molecules carrying a carbonyl group (Štambergová et al. 2016) we postulated that the protein and the compound can potentially cooperate in regulating nuclear size

5.3 Subcellular localization of NET50

NET50, also known as DHRS7, retSDR4, and SDR34C1, is an orphan member of the short chain dehydrogenase/reductase (SDR) family. It was first isolated from retinal pigment epithelium cells (Haeseleer and Palczewski 2000), but is expressed in a small subset of different tissues and most highly in prostate (Romanuik et al. 2010; Štambergová et al. 2016). Although DHRS7 was separately identified as NET50 in a proteomic study of nuclear envelopes (Schirmer et al. 2003), it has also been reported as an ER-membrane bound protein (Skarka et al. 2014). Direct testing reveals it to be in both compartments (Fig 26). The topology of the protein is still debated as it was first postulated that the catalytic domain would face the lumen of the ER according to Štambergová et al., but as NET50 activity is not stimulated by ER-luminal H6PDH-mediated NADPH generation, the protein needs an alternative ER-

luminal source of NADPH and a different orientation to gain access to the cofactor. Through the use of a digitonin permeabilization assay and based on similarity with other members of the SDR family a cytoplasmic orientation of the catalytic moiety has also been proposed by Araya and colleagues (Araya et al.).

As poor titration of digitonin can lead to incorrect interpretations in digitonin permeabilization assays and the Schirmer lab has considerable expertise with this assay, I decided to directly test which of these studies is correct by myself determining NET50 topology with a digitonin assay. First, using the transmembrane span prediction TMHMM Server v. 2.0 identified a single region at the N-termini that is predicted as a hydrophobic helix to be inserted in the double lipid layer, in line with the other proteins of the SDR family. The assay allows to selectively permeabilize with digitonin the plasma membrane of cells previously transfected with the protein of interest tagged with a fluorescent protein. Antibodies against the fluorescent protein are used to detect the orientation for the protein of interest, if the fluorescent protein is exposed on the cytoplasmic side this will be detected by fluorescence signal as opposed to the protein not being accessible because presented in the nucleoplasmic side of the nucleus. Controls permeabilized with Triton X-100 are used to asses that the antibody is effectively recognizing the fluorescent protein and known orientation proteins can be used as comparison. The digitonin assays revealed that the catalytic domain of the protein is facing the nucleoplasm/cytoplasm in line with experiments performed in Araya et al. 2017 (Fig 27). As previous microscopy studies found NET50 co-localized with Nup153 and not with Nup358 (Malik, Zuleger, and Schirmer 2010), this places the protein at the inner nuclear membrane; therefore the catalytic domain is facing the nucleoplasm (Fig 20) and its dehydrogenase/reductase activity could potentially contribute to nuclear functions.

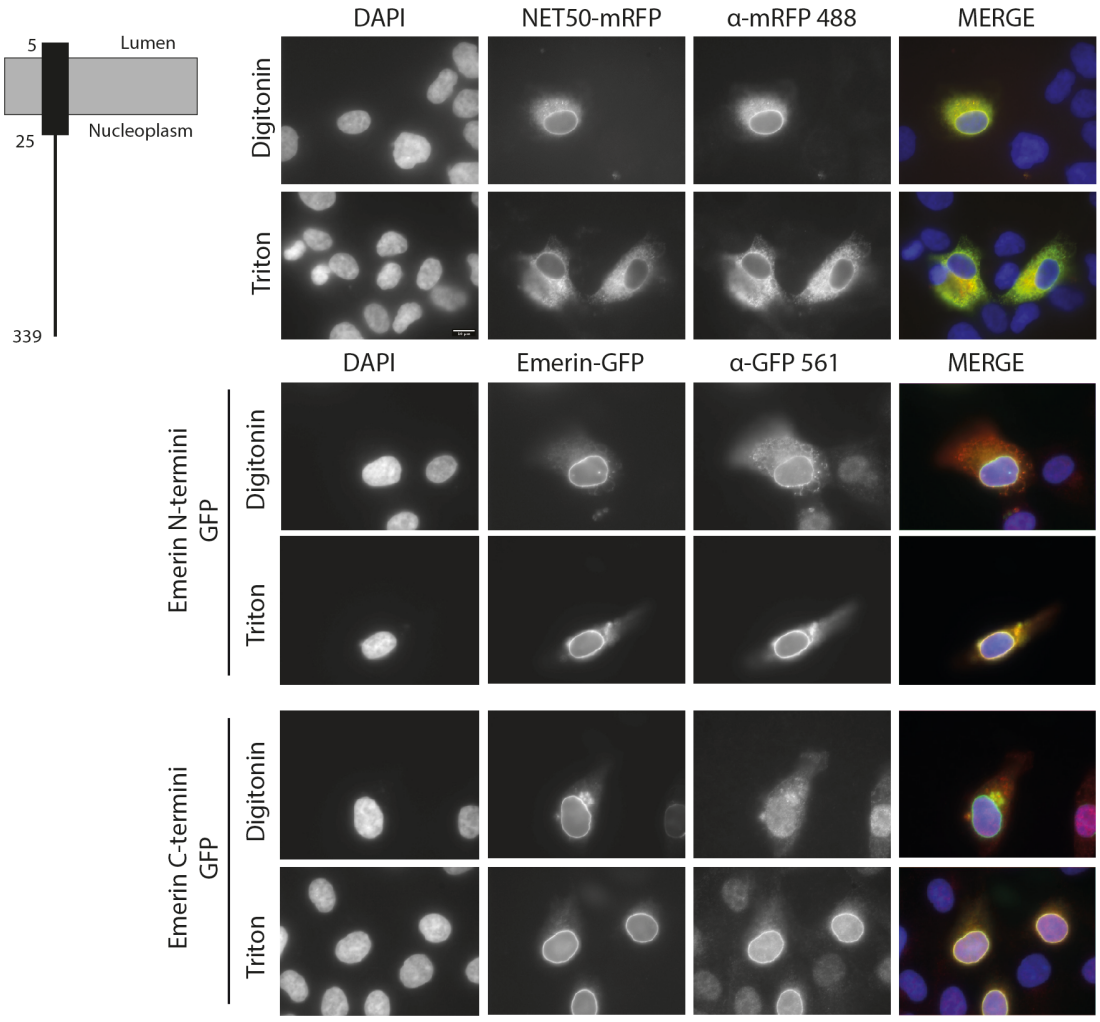

Figure 27 ***Topology of NET50.*** *The model of the protein was generated through transmembrane topology prediction with TMHMM server 2 and orientation through digitonin assay. Antibody against mRFP can recognise the fluorescent protein in digitonin treated cells placing the C-terminus of the protein in the nucleoplasm. Emerin GFP tagged on the C and N-termini is used as control for the assay. Scale bar 10 μm.*

5.4 Function of NET50

5.4.1 Screens for NET50 activity

As the Schirmer lab is interested in understanding the functions of tissue-specific NETs and NET50 is very preferentially expressed in prostate they included it in several screens. The screens are based on the fact that ONM proteins likely affect the cytoskeleton and INM likely chromatin NET50 has been tested in several screens performed in the lab and showed no great alteration of the cell cycle when overexpressed, although causing a slight delay

this was not considered relevant in the context of cell cycle alteration (Korfali et al. 2011). Alteration of cell cycle progression would explain the importance of this protein in cancer progression as one of the hallmark of cancer is unconditioned proliferation, allowing cells to master their own densities. Moreover, NET50 displays a localization at the nuclear envelope that is lamin A dependant as targeting of the protein is lost in lamA -/- cells (Malik, Korfali, et al. 2010) and no particular cytoskeleton defects when overexpressed in HT1080 cells (Malik, Korfali, et al. 2010). As the protein has multiple potential functions based on these studies, it is possible that the ER and NE populations have distinct functions and/or could have a similar function but on different substrates.

5.4.2 Enzymatic activity of NET50

Little is known about the reducing/dehydrogenase enzymatic role of NET50 in the cell, but biochemical studies on lipid-reconstituted purified NET50 protein revealed that it is a functional sterol dehydrogenase. Its substrate specificity in vitro highlighted an activity against normal cellular substrates such as all-trans retinal and steroids such as A-dione and cortisone. The protein seems to have activity also against non-endogenous substrates bearing a carbonyl group such as 1,2- naphtoquinone, 9,10- phenanthren equinone, benzoquinone, and nitrosamine 4- (methyl- nitrosamino)- 1- (3- pyridy l)- 1- butanone (Skarka et al. 2014; Štambergová et al. 2016). All these activity measures were inferred by indirect chromatographic analysis of the co-factor NADPH:$NADP^+$ ratio after incubation of the protein with the different substrates. Other evidence suggests NET50 to be involved in the inactivation of 5α-dihydrotestosterone, implying a role for the modulation of the AR transcriptional activity and therefore the importance of the protein as an anti-cancer player (Araya et al. 2017). Most of prostate cancer starts with an androgen-dependant growth, but as the cancer progresses cells are able to activate androgen receptor elements and response even in presence of a blockade of androgens. NET50, with a role in modulating and inactivate a

precursor of testosterone might be a crucial protein in control of prostate cancer progression.

5.4 NET50 as biomarker for prostate cancer

Several recent studies have shown a reduction in the expression of NET50 in prostate cancer (Romanuik et al. 2010; Seibert et al. 2015), leading to the hypothesis that the downregulation of NET50/DHRS7 can be used as an effective biomarker for prostate cancer prognosis.

Staining normal prostate tissues and prostate cancer tissues with a polyclonal DHRS7 antibody highlighted a progressive loss of the protein during cancer progression with the lowest staining associated with the specimens with worse Gleason level scores (Seibert et al. 2015). Gleason level is the score system for prostate cancer that associates a grade depending on the appearance of cancer tissues under the microscope that includes both nuclear shape and size changes. For prostate cancer prognosis, the specimen is first associated with one of five progressively worse microscopic patterns to assign the Gleason score. Primary, secondary and tertiary grades, depending on the percentage of the pattern in the specimen, are then decided and the final grade results as the sum of the pattern score of the primary grade and the highest pattern between secondary and tertiary allowing a final grade score from 2 to 10 with 2 representing the lowest score and most well differentiated tumours oppose to 10 associated with least differentiated tumours (Humphrey 2004). In addition to demonstrating the correlation between loss of NET50 and cancer severity, the authors of this study knocked down NET50 in earlier stage prostate cancer cell lines that still expressed it resulting in increased proliferation, invasiveness and less adhesion to the substrate (Seibert et al. 2015). This was assessed with a proliferation assay and Ki67 staining for proliferating cells, measuring the growth curve and intensity of Ki67 staining of siRNA depleted cells phenocoping the increased and uncontrolled proliferation of cancer cells. Trans-well migration and fibronectin adhesion assays were used for invasiveness and adhesion, to test motility and ability of cancer cells

to extravase from the primary tumour and spread in different sites, another important feature of more metastatic tumour cells (Seibert et al. 2015). All together these results suggested an important role of this protein in prostate cancer progression for which loss correlates with more aggressive cancer cells. Studies on the transcriptome of LNCaP cell line, the model cell line for early stages of prostate cancer where NET50 is still expressed, suggested a key role for NET50 in leading to the reactivation of the androgen receptor (AR). This is because NET50, likely through its dehydrogenase activity, sustains de novo androgen synthesis and/or metabolism in castration recurrent prostate cancer (CRPC), flagging the protein as an important anti-cancer protein in this type of cancer (Romanuik et al. 2010). Thus, reactivating NET50 in late stage prostate cancer might help the patient through its function with androgen. We wondered if its function in nuclear size regulation might also be relevant.

5.7 NET50 can regulate nuclear size in prostate cancer

Although NET50 reduced the normal nuclear size of HeLa nuclei when overexpressed in our screen, we had not tested for volume changes or if knockdown also affected nuclear size. We specifically confirmed these results in HT1080 cells both in 2D, analysing the mid cross sectional area of several nuclei, and in 3D with nuclear volume reconstructions of z-stack images from the nuclei of NET50 overexpressing cells.

To determine if NET50 nuclear size alteration is maintained in a prostate cancer model I used two different prostate cancer cell lines representing different stages of cancer progression, LNCaP and PC3. The LNCaP prostate cancer cell line, isolated from lymph node metastasis, resembles the early stages of prostate cancer development and expresses the androgen receptor so is therefore androgen sensitive. On the other hand, the PC3 prostate cancer cell line, isolated from lumbar metastasis, resembles a late stage of prostate cancer, is androgen insensitive due to the lack of expression of the androgen receptor, and has a higher metastatic potential. This cell line being a highly metastatic cell line established form a grade IV tumour, presents characteristics morphological features of a poorly differentiate tumour with

different sub-phenotypes, comprising epithelial like and neuroendocrine cells (Kaighn et al. 1979).

Immunofluorescence and Western blotting with a monoclonal antibody targeting the C-terminal region of NET50 were used to assess the presence of the protein in the LNCaP and PC3 cell lines. As expected the cell line resembling the early stages of prostate cancer progression (LNCaP) shows the presence of the protein at a NE subcellular localization where the cell line resembling the late stage of prostate progression (PC3) shows downregulation of protein expression and no localization at the NE or in the ER (Fig 29A-B). Though no degradation products were observed in the PC3 cells with this antibody it is unclear whether the nucleoplasmic staining is background for the antibody in the absence of antigen, if there is a cleavage product that is still recognised by the antibody, or if there is cross reactivity of the antibody with other close members of the protein family.

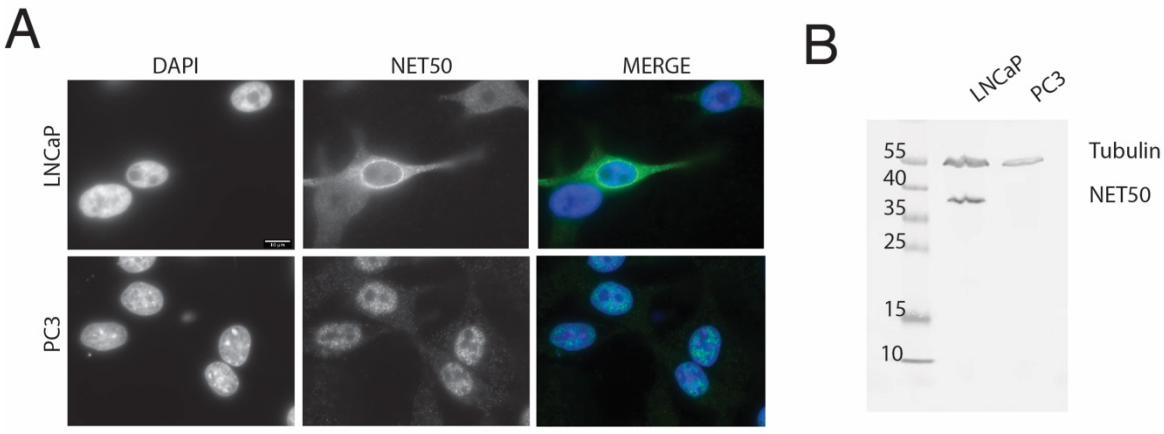

Figure 28 ***Characterization of NET50 in prostate cancer models*** *A. Immunostaining with primary antibody targeting the C-terminal region of the protein in two different systems, LNCaP and PC3. LNCaP shows staining of the protein at the NE, where staining is absent for the protein in PC3 cell line. Staning is not present in all the LNCaP cells as is an early stage prostate cancer model therefore cells already started losing some protein. Staning in the PC3 cells is weak and considered to be background or aspecific bining of the antibody. B. Western blot for the expression of NET50 in LNCaP and PC3 cell lines. In line with the immunostaining NET50 is expressed in early stages of prostate cancer (LNCaP) and progressively lost through cancer progression, with no expression in late stages (PC3). Scale bar 10 μm.*

To investigate the role of NET50 in nuclear size regulation, transient overexpression of a mRFP fluorescently labelled NET50 was performed and this resulted in reduction of the nuclear volume of ~60% for both cell lines with

statistical significance for both samples. Roughly 100 PC3 nuclei for each condition were analysed to take into account the different sub-phenotypes that the cell line develops in culture. By contrast, knocking down NET50 via transient transfection of a pool of siRNAs against its mRNA transcript resulted in a statistically significant increase of the nuclear volume in the LNCaP cell line. (Fig 30A-B) Cells were analysed if a clear nuclear envelope ring of fluorescence was detected for the overexpression samples, or if completely negative for antibody staining for the knockdown samples.

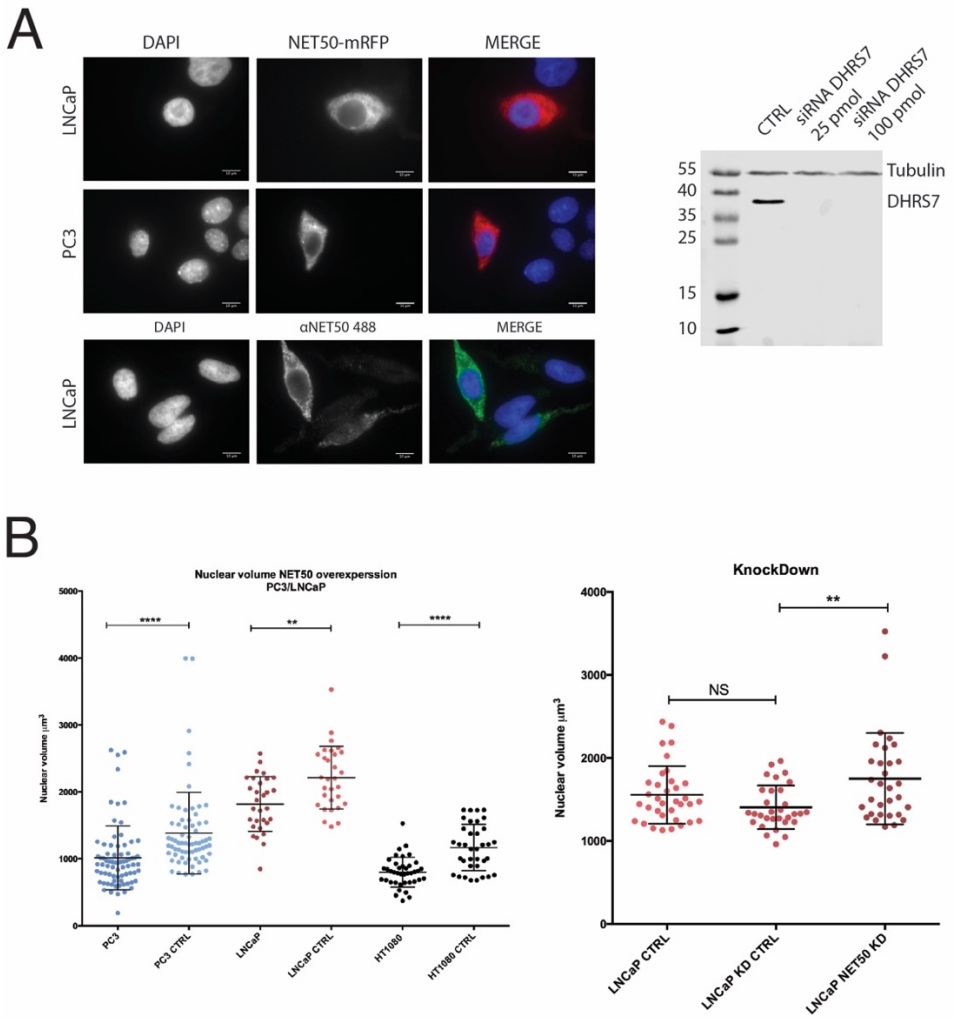

Figure 29 ***Effect of NET50 overexpression and knockdown on nuclear volume.*** *A. Representative images for the overexpression and knockdown of NET50. Cells expressing NET50-mRFP were analysed for nuclear volume in both LNCaP and PC3 cell lines. Cell not positive for antibody stain were analysed for nuclear volume in LNCaP cell line only. Western blot showing the effective knockdown of the protein in the LNCaP cell line. B. Nuclear volume reconstruction for overexpression of the protein shows a decrease for the control cell line HT1080 and both prostate cancer cell lines LNCaP and PC3. NET50 knockdown in the LNCaP cell line results in an increase of the nuclear volume. Statistical significance calculated with an unpaired t test with Welch's correction, **: p<0.01, ****: p<0.0001. Scale bar 10 µm.*

5.8 Estradiol propionate reduces nuclear volume

Since estradiol has been used as an effective remedy for CRPC, and because estradiol propionate was one of the hit compounds in the pre-screen optimization with the Spectrum Library for compounds altering nuclear size, we were interested in testing the effects of this compound in a prostate cancer system. Both cell lines were treated with 2 different concentrations (10μM and 3μM) of the compound for the whole duration of the transfection protocol and thereafter, replacing the medium with freshly added compound every 24 h. Compound treatment resulted in a decrease of nuclear volume of ~70% for the PC3 cell line where the protein is not expressed and no statistical significant alteration in the LNCaP cells, where the protein is still expressed (Fig 31A).

To establish if it is the presence or the catalytic activity of the protein that is required to disrupt the nuclear volume reduction by the compound, NET50 was ectopically overexpressed with transient transfection in the PC3 cell line where the protein is not normally expressed and knocked down in the LNCaP cell line where it is normally expressed. Treating these cells with two different concentrations of estradiol propionate resulted in the reduction of the nuclear volume only where NET50 is not expressed (Fig 31B).

This suggested either a mechanism of suicide inhibition by the estradiol propionate on NET50, that binding to the catalytical pocket neutralizes the action on nuclear size regulation for both the protein and the compound, or both NET50 and estradiol propionate are part of the same pathway that lead, when both are present, to no alteration of the nuclear volume.

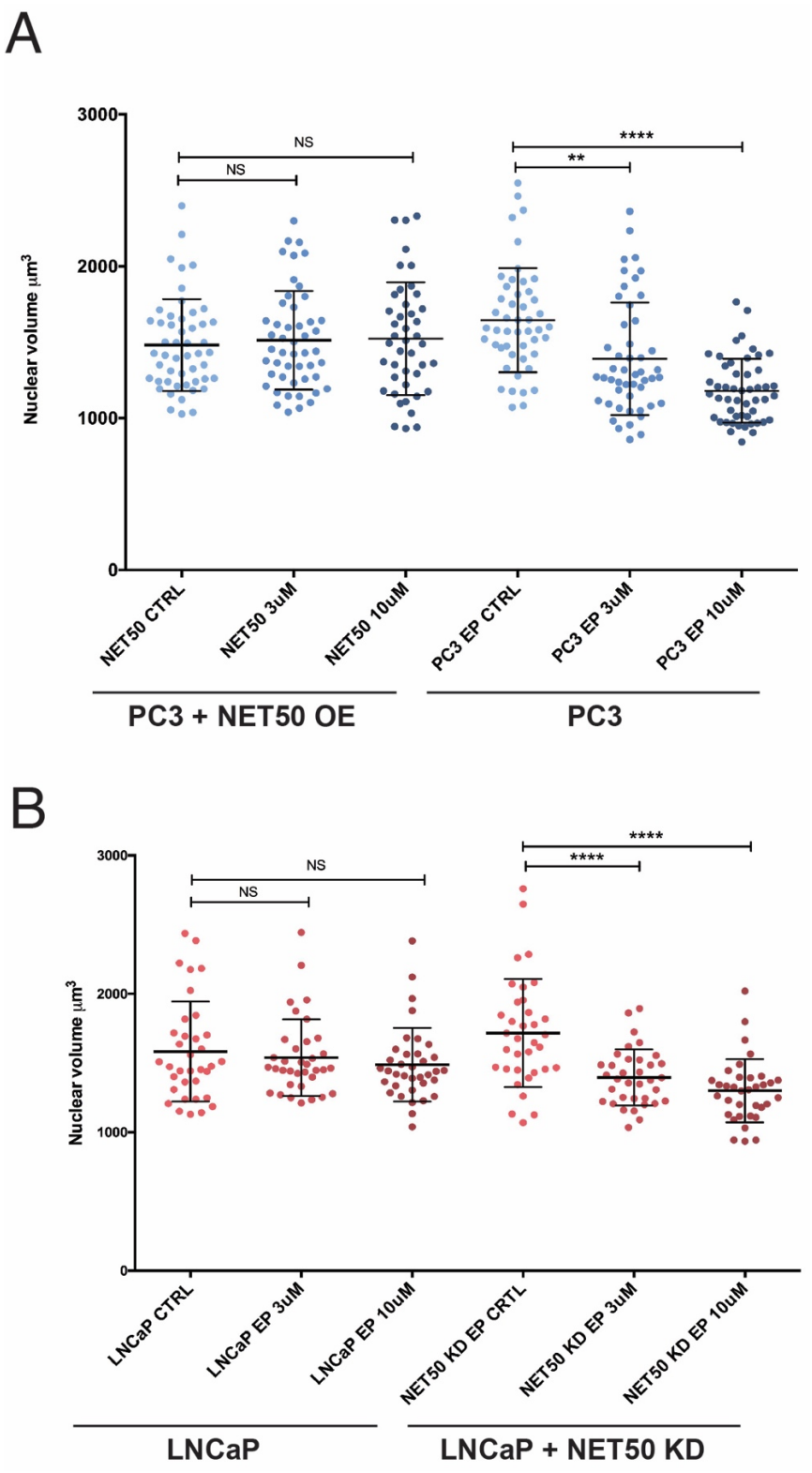

Figure 30 ***Effect of estradiol propionate on nuclear volume.*** *A. PC3 cell line treated with estradiol propionate shows reduction of the nuclear volume when NET50 is not expressed (left) but the effect of volume reduction is lost if the protein is ectopically expressed (right). B. LNCaP cell line treated with the same compound shows no reduction of the nuclear volume (left) but the effects are gained back when the protein is knocked down (right). Statistical significance calculated with an unpaired t test with Welch's correction, **: p<0.01, ****: p<0.0001.*

5.9 NET50 predicted catalytic site mutations block its nuclear size effects

To determine if the catalytic activity of NET50 is required to direct nuclear volume alterations, site directed mutagenesis to generate point mutations of the protein was performed. As crystal structures of the protein have not yet been solved, the protein sequence was run on the Phyre 2 server to identify similar domains in an already crystalized member of the superfamily. One of the most similar structures predicted by the server with a 100.0% confidence is the human 17-beta-hydroxysteroid-dehydrogenase type 1 (PDB 1FDV), a closely related member of the SDR family (Fig 32A). Following a bioinformatics study on the whole SDR family by Bray and colleagues (Bray, Marsden, and Oppermann 2009) the key residue coordinating the cofactor NADP was identified as arginine R38 in 17-beta-hydroxysteroid-dehydrogenase type 1 and the predicted residue for NET50 is arginine R82. By aligning the sequences of the two proteins with proper numeration, arginine R82 was confirmed as a potential residue to mutate and the mRFP-NET50-R82E mutant was designed and generated (Fig 32B).

Transient overexpression of the mutant construct using the PC3 cell line as a NET50 null background resulted in a statistically significant increment of the nuclear volume, phenocopying the increment of nuclear volume in knock down of the protein in the LNCaP cell line (Fig 32C). This suggested a minimal residual protein is still expressed in PC3 cell line, despite not being able to detect this on a western blot, with a dominant negative inhibition of NET50. Cells were then treated with 2 concentrations of estradiol propionate in the presence of the mutant protein leading to a volume reduction as if the protein was not expressed at all, suggesting a catalytically dead mutant as fluorescence was detected but no reduction of the nuclear volume occurred as did occur with overexpression of the wild-type protein. (Fig 32D).

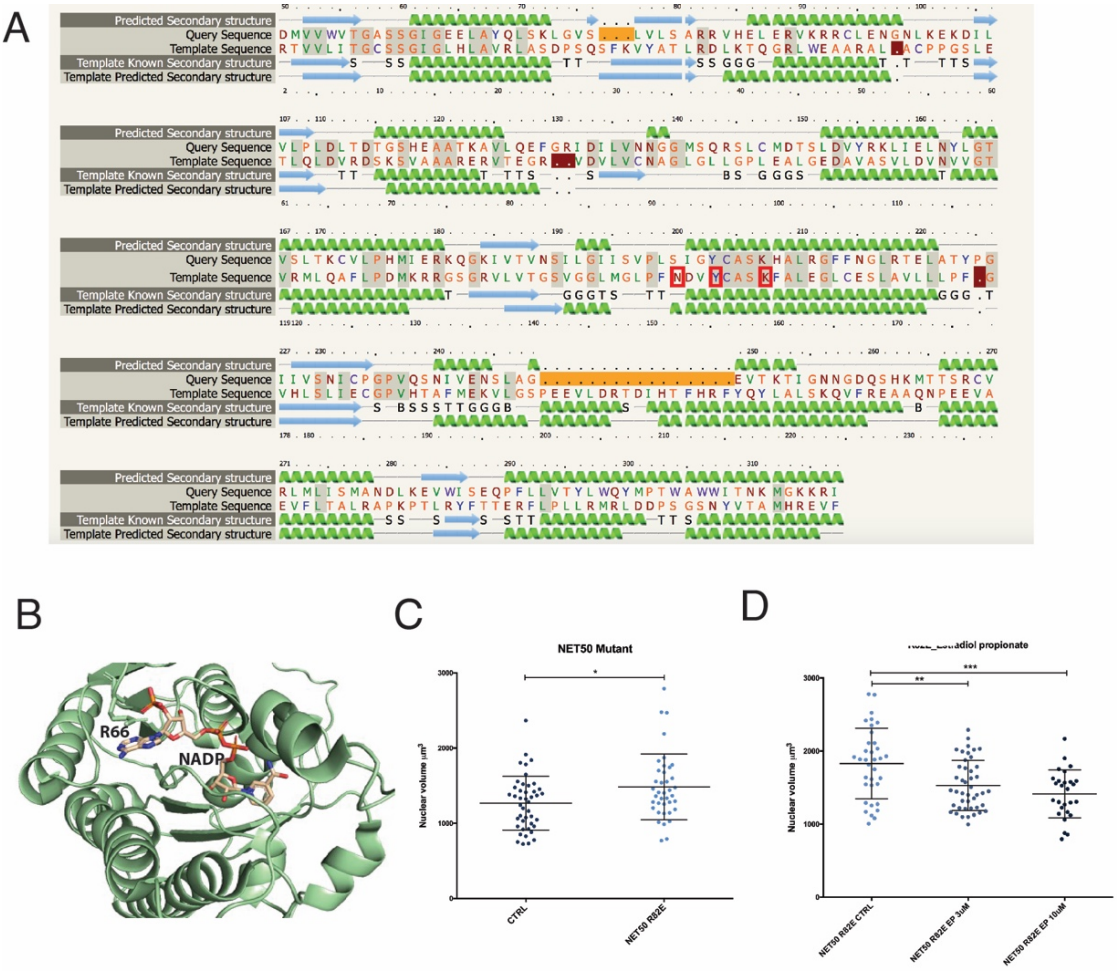

Figure 31 ***NET50 enzymatically dead mutation prevents its nuclear size effects and allows the estradiol propionate effects on nuclear volume in presence of the mutated protein.*** *A. Sequence alignment of NET50 against 17-beta-hydroxysteroid-dehydrogenase type 1 (17β-HSD1) generated by the Phyre2 server. B. Cartoon representation of NET50 with the cofactor NADP. The residue R66 in the 17-beta-hydroxysteroid-dehydrogenase type 1 was chosen as potential mutation as is the key residue coordinating the cofactor. Allignment of NET50 and 17β-HSD1 determined the residue R82 to be the residue coordinating the cofactor. C. Overexpressing the NET 50 mutant R82E in PC3 cell line results in increased nuclear volume, resulting in the same phenotype as the knockdown of the protein. D. Treating PC3 cells overexpressing the mutant version of the protein with estradiol propionate results in a reduction of nuclear volume as if the protein was not expressed. Statistical significance calculated with an unpaired t test with Welch's correction, **: p<0.01, ****: p<0.0001.*

5.10 Chapter summary

In this chapter a new NET, NET50/DHRS7, has been shown to have an effect on nuclear size regulation in a prostate cancer in vitro cell system. The observations of loss of the protein expression in cancer progression as shown

in other studies (Romanuik et al. 2010; Seibert et al. 2015) and the fact that increased nuclear size is a diagnostic feature for the later stages and higher grades of prostate cancer are now linked through our data showing that NET50 loss causes an increase in nuclear size. It is unclear what are the factors that lead to the downregulation of the protein during the later stages of prostate cancer, but these correlations raise the possibility that restoring normal nuclear size might reduce the cancer severity. One hypothesis is that regulation of nuclear size by the protein can involve the catalytic activity of the protein. Given the similarity with different members of the SDR family NET50 could be involved in the regulation of steroidogenesis, with steroids being fundamental molecules for the maintenance of healthy prostate tissues and regulators of uncontrolled proliferation of cancer cells. For example, NET50 could process small molecules into active compounds that can directly influence the transcription of different genes involved in the maintenance of normal nuclear size. Another mechanism by which the protein could act in nuclear size regulation is by association with other proteins at the NE that are able to anchor and repress oncogenes that, in absence of the protein, get released from the NE and cause the nuclear size alteration and progression of prostate cancer. As NET50 has not been linked with genome repositioning and organization activity in the screens performed in the Schirmer lab so far, the only possible explanation for a possible involvement of the protein in influencing genome organization is if it is able to form a complex with other NETs with genome organisation properties. Considered together these results are consistent with NET50 being a key regulator of nuclear size, at least in prostate cancer development, and that it might be used as biomarker for earlier and better identification of early stages of this pathology, as suggested by Seibert and colleagues, or as an effective target for new anticancer drug target.

Further investigation into whether alteration of the nuclear size is dependent of the enzymatic activity of the protein or dependent on the association of the protein with other partners to from a complex is required. Interestingly, the effects on nuclear size alteration from the loss of the protein are reversed if cells are treated with estradiol propionate, having the same

nuclear size reduction effect. In the other direction, overexpression of NET50 to reduce nuclear size is not augmented when also treating the cells with estradiol propionate. This might be explained by a catalytic alteration of estradiol propionate by NET50, resulting in a non-active metabolite rendered unable to affect nuclear size. Estradiol propionate, being a hormone, has the characteristic steroid structure as A-Dione and testosterone for which activity has been shown for NET50 and other members of the SDR protein family. Moreover, estradiol propionate carries a carbonyl group, a key chemical group shown to be a substrate of NET50 enzymatic activity (Štambergová et al. 2016). Another explanation for the lack of an additional effect on nuclear size if both protein and compound are present is suicidal inhibition of the protein by the compound. Influence on the nuclear size regulation is most likely related to the catalytic activity of the protein, as the catalytically dead mutant (R82E) showed reduction of nuclear volume when treated with estradiol propionate.

6. Discussion

6.1 Nuclear size in cancer

Nuclear size and shape alterations are one of the most evident morphologic aberrations visible in cancer tissues and have been used for decades to stage and grade cancer in an effective and precise way (Cibas and Ducatman 2014). These alterations could be a direct cause of the worsening patient outcomes or may be an indirect consequence of other factors that affect outcomes. For example, upregulation of chromatin compacting proteins due to aberrant gene expression can lead to a state of compaction of the genome resulting in the shrinking of the nucleus, or alteration of lipid synthesising enzymes at the NE might lead to the insertion of excessive amounts of lipids in the NE membranes resulting in an enlargement of the nuclear size. In this study, we investigate the regulation of nuclear size as a new potential approach to effectively target tumour progression and lower the metastatic potential of highly aggressive cancers.

There are certainly many ways that a nuclear size change itself or associated changes in NE-chromatin or NE-cytoplasmic filament connections can provide direct advantages to cancer cells. These range from aspects of metastasis such as increased cell migration and an enhanced ability to squeeze through cell junctions in invading other tissues to an increased proliferative capacity and altered gene expression. Therefore, understanding the basic mechanisms or the factors that can influence these morphological

alterations is a first step to specific targeted approaches for treatments based on nuclear size changes. That these changes are tissue-specific may allow for such targeted approaches to focus toxicity in the particular tissue and so not only allow for chemotherapeutic treatments resulting in better patient outcomes, but also reduce the side effects of chemotherapy and improve quality of life during these stages of the cancer. The current focus of the cancer community is to target central pathways and signal cascades, especially kinases, in cancer treatments, arguing that the metastatic process is just a secondary effect and cannot be properly controlled or targeted effectively (Fidler and Kripke 2015; Steeg and Theodorescu 2008). There are currently many studies being carried out trying to target several kinases in the hope to identify or repurpose drugs to be effective in treating both primary tumours and metastasis (Collins et al. 2019; Miao et al. 2019).

Here we propose a more phenotypic approach, targeting one of the more evident morphological alterations, nuclear size, detected in cancer progression in several tumour types.

6.2 NETs involved in nuclear size regulation are tissue specific

The hypothesis that different phenotypes for nuclear size and shape detected in different type of cancers could be driven by tissue-specific nuclear membrane proteins has been central for this study. Researchers focused on nuclear size regulation until now have focused on trying to identify a communal factor or factors that could explain the nuclear size alteration in all the different cancer types. This has yielded deep understanding of factors that can influence or regulate nuclear size, such as lamins that have been implicated in direct nuclear size regulation in a concentration dependent manner (Jevtić et al. 2015) or protein like Nesprins directly involved in nuclear size regulation (Luke et al. 2008). Despite the effort and research on these factors no clear answer has been identified to explain the differences of nuclear size alteration detected in the different cancer types. We here shift the focus, arguing that a

more tissue specific view could be the answer to identify potential regulators of nuclear size. It makes sense that nuclear membrane proteins would be involved in nuclear size regulation as control of nuclear size requires the regulated growth of the nuclear membrane and production of its component proteins. These in turn have many connections to chromatin and the cytoskeleton and so maintaining nuclear mechanical characteristics through the cell cycle requires that this process be tightly regulated so that the balance of connections to both chromatin and the cytoskeleton is maintained. As recent years have found that the NE is in fact a highly-specialized organelle rich with tissue-specific proteins (Schirmer et al. 2003), it further follows that the tissue-specificity in the characteristic degree and directionality of nuclear size changes would likely be directed by tissue-specific NETs. In this study, several NETs were screened for their ability to potentially regulate nuclear size variation in different cancer models.

As the results suggested there is a tissue specificity in how these proteins influence the nuclear size, with some proteins (e.g. Emerin or NET39) having different directionality in altering the nuclear size depending on the tissue in which they are expressed. This result even more interesting when considered in light of the gene copy number alterations of these NETs in cancer patients. Some NETs that increase nuclear size when overexpressed and when knocked down yield decreased nuclear size were hemi-amplified in a type of cancer in which the increased nuclear size correlates with worse grade and hemi-deleted in cancer where decreased nuclear size correlates with a more severe and aggressive cancer. This suggest that these NETs might have the ability to regulate the nuclear size changes during cancer progression.

There are many mechanisms by which changes in nuclear size may lead to even more severe tumour progression. An abnormal increase of nuclear size can disrupt important connections between the chromatin and the NE, thus releasing large portions of the genome into the nucleoplasm. This could cause genes in these regions that are normally kept tightly shut off in the repressive environment characteristic of the NE to become active. If such

genes included oncogenes or cell cycle proteins that increase proliferation, this would result in a more metastatic tumour. Activation of kinases could have many pleiotropic effects on cells ranging from affecting nuclear import of critical transcription factors to phosphorylation of structural elements such lamins leading of disassembly of the main structural element of the nucleus (Lee et al. 2007). Kinases are also part of complex cascade responses, alterations of early responding proteins can easily result in activation or repression of several final actuators. These final actuators could be genes and proteins that allows advantages to the tumour cells such us unconditioned proliferation or better cell motility favouring the spread of the tumour in secondary sites. For example, the nuclear envelope is linked to the Wnt pathway through different proteins (Jamieson, Sharma, and Henderson 2014; Luke et al. 2008b), therefore the loss or overexpression of these proteins in cancer can lead to incorrect activation or inhibition of oncogenes that could potentially result in altered nuclear size. Abnormal nuclear size alteration might also effect cytoskeletal connections via disruption of connection between the nucleus and plasma membrane, potentially resulting in alteration of cell migration giving cancer cells an advantage in the process of metastatic spread. Cytoskeletal connections can also be altered by gene expression changes that alter the amount of key proteins involved in nucleoskeletal-cytoskeletal connections. For example, a reduction of expression of proteins of the LINC complex due to repression induced by reduction of the nuclear size, and therefore more compact and silenced chromatin, would lead to less proteins available at the NE for proper connections with intermediate filaments and microtubules.

My screen focused on the overexpression of proteins mimicking an upregulation of that particular protein during cancer progression. This would have been better if we had also performed the screen knocking down the pool of proteins. This would both have allowed determination if overexpression and knockdown of these NETs have opposing effects and this analysis may also give an even deeper understanding in the contribution of NETs in nuclear size regulation. We did not do the knockdown in the first place for all NETs screened because of difficulties in removing NETs that appear to generally

have a longer half-life than soluble proteins. However, now that CRISPR/Cas9 technologies are well established and can obtain knockdown of proteins in a reasonable amount of time, performing the screen to knockout NETs at the NE might help identify more proteins involved in nuclear size regulation and thus provide more candidates that will be worth considering as targets for cancer therapies. Another reason the knockdowns were not undertaken in the first analysis is that several of the NETs have protein pools in both the ER and in the NE. In these cases for the knockdown it would be difficult to determine whether the effects were more direct due to loss of the NE pool or indirect from a separate function of the ER pool. With further investigations of NETs in general it might be possible to identify splice differences or post-translational modifications that differentially direct the protein to the ER or NE. With this information, CRISPR/Cas9 could be used to replace the wild-type gene for example with one that has a phosphomimic mutation that keeps the entire pool in the NE or a phosphonull mutation that keeps it all in the ER. This would allow a better determination of roles and mechanisms behind the nuclear size changes for particular NETs.

The NET screen was only performed with 50 NETs, but there are several hundred in each tissue tested and because the majority are tissue specific the total number is closer to 1,000. Thus if further screening could be done it would likely identify many additional nuclear size factors if this larger set of proteins could be screened.

There are also some caveats to the methodology of the screening. High throughput screening has the major benefit that it allows the analysis of a large amount of variables once parameters and conditions are set up, but it can harbour different types of false positives. In particular, for this type of screen one of the more problematic variables is that high transfection efficiency is more difficult to achieve in 96 well format than in standard tissue culture plates while the cytotoxicity is often higher. This is likely due to several factors including: 1) the fact that cells do not adhere and spread as well on optical plates as standard tissue culture coated plates and it is not possible to coat the glass with most substrates that would enhance adherence and spreading

without compromising the optical qualities for screening, 2) capillary action in the small wells prevents an even distribution of cells, 3) the ratio of volume to surface area is greatly perturbed in small wells, 4) difficulties in changing the medium, as cells tend to adhere less, making frequent media changes not a valid option. These changes could result in erroneous measurements of the nuclear area due to a low number of transfected cells or low expressing cells. Moreover, cells might undergo apoptosis during the transfection procedure for several reasons, such as high cytotoxicity of the transfection reagent or impurity in the DNA used for the transfection, and this can result in erroneous nuclear size readout. To remove false positives in the screening process due to these issues, positive hits should be furtherer investigated with a more detailed approach as 3D volume reconstructions to confirm the accuracy of readings for nuclear size effects. We did this for NET50 because of its preferential expression in prostate and our focus on prostate cancer, but there were many other potentially interesting candidate NETs that should be further evaluated with 3D analysis.

6.3 Compounds targeting nuclear size show tissue specificity

Similar to the tissue specificity observed for NETs, the drugs affecting nuclear size also were tissue-specific in their effects. This suggests that they can be more effective against one particular type of cancer by specifically targeting that tissue type and accordingly have less toxic side effects on patients by not doing systemic damage. Targeting nuclear size alterations in a tissue specific manner can be a valuable direction for the discovery or repurposing of drugs. Screening for drugs altering this feature in different cancer cell lines revealed that only a subset of drugs is shared between all the cell lines, where most of the hits are indeed cell line restricted and therefore cancer type specific.

Comparing karyoplasmic ratio and nuclear size as the method of analysis for the identification of new compounds revealed that the

karyoplasmic ratio harboured less hits. In the early stages of use of nuclear changes in cancer diagnosis the karyoplasmic ratio was used, but this was quickly replaced with simply nuclear size because it is much easier to stain just for the nucleus for quantification of size changes (Fischer 2014; Taira et al. 2012b; Veta et al. 2012). Thus, it is not even clear for all cancer types using nuclear size changes diagnostically whether the karyoplasmic ratio also changes. This is nonetheless an important distinction because a cell with a nuclear size increase could also have the cytoplasm increase so that the karyoplasmic ratio is unchanged. Such a cancer type would likely be different in cause than one in which the sensing mechanism that links the nuclear size increases to cell size increases breaks down. Correspondingly, it will be important to determine clearly for all these cancer types if the nuclear size increases used for grading involve a disruption of the karyoplasmic ratio as if the karyoplasmic ratio is disrupted a smaller group of compounds can be focused on. It is noteworthy that another benefit of the high-throughput Opera screening platform is that with multiple parameters determined the analysis can be adapted in many ways and just as treatments yielding a change in the karyoplasmic ratio can be determined so can treatments that exhibit an equivalent change in both nuclear and cytoplasmic volume.

As mentioned for the NETs screen, high throughput screening might harbour erroneous hits that need to be verified with more focused approaches. For the drug screen one of the most problematic aspects is cytotoxicity of the drugs that might trigger apoptotic or necrotic responses that would result in false-positive hits as both nuclear size and karyoplasmic ratio will be altered in necrotic and apoptotic cells. Adding a different apoptotic or necrotic marker would facilitate the removal of potential compounds highly toxic for the cells. The compounds inducing apoptosis would be still a valuable hit that can be used in follow up analysis due to their potential in being useful to reduce tumour growth in vivo and highly toxic compounds may be used for shorter treatment times, which is why the screen was performed at both 6 and 36 h.

The screen identified several classes of compounds as strong hits in all the cell lines and with different directionality for the nuclear size alteration such

as 5-HT serotonin uptake and cyclo-oxygenase inhibitors or Na+/K+ ATPase and COX inhibitors. Microtubule depolymerising agents were identified both as increasing and decreasing the nuclear size in different cell lines, this might be a case of an erroneous read out as cells will be blocked in mitosis due to the lack of proper spindle formation leading to cell death, but represent a good example of how compounds leading to apoptosis or cell death can interfere with the assay readout. At the same time, this is a good example of how the assay identified compounds that can be used to target tumours based on a range of criteria with the high-throughput data collection and supporting these hits several studies have shown the efficacy of the microtubule depolymerizing agents in being effective against cancer cells (Dumontet and Jordan 2010; Jordan and Wilson 1998).

To improve further the screen, it would be interesting to follow different variables and sizing of different organelles within the cell. This was the original idea of the compound screen in which we intended to monitor four different organelles at the same time through fluorescent proteins fused to signal sequences, namely the nucleus, the nucleoli, the ER and mitochondria. Screening for different parameters would have generated a more comprehensive view of mechanism of action of different compounds in scaling different compartments of the cell and allowed for the identification of drugs with different clinical or industrial benefits. For example, identification of compounds inducing increase size in ER could be benefit for industrial purpose in mammalian protein production. The actuation of this type of screening was not successful due to several problems with cloning and the impossibility to obtain a final working lentiviral vector, but with recent improvements and development of plasmid DNA synthesis it would be a viable option for the generation of this vector and stable cell lines.

Finally, as the screen results in a more manageable number of compounds compared to the initial numbers of the library, it would be useful to characterise deeper the effects of the compounds affecting nuclear size with volume 3D reconstructions to fully understand the size, and possibly shape, alteration effects.

6.4 Protein and compounds influencing nuclear size can interact

Although the NET and compound screens were engaged independently, we expected that some compounds would be specifically targeting the NETs that alter nuclear size for their effects. Accordingly, we had planned a third screen involving biochemical and biophysical screening techniques on recombinant produced proteins. These comprise assays such as plate based size exclusion chromatography that is a miniaturized screening method for homogeneous in-solution affinity selection. Target proteins are first incubated with compound pools and protein-compound complexes are separated by size exclusion chromatography. The eluted fractions are then analysed by Liquid Chromatography-Mass Spectrometry (LC-MS/MS) for the identification of compounds binding to the target. Another approach that could be used to identify compounds interacting with recombinant proteins is the on beads CONA screening where fluorescent labelled proteins are incubated with an on beads library and interaction between compounds and protein can be detected by a fluorescent ring around a bead. The positive beads can be picked and analysed by mass spectrometry to identify the interacting compound.

Even without getting the CONA assay off the ground, we nonetheless did find at least one compound that acts on a NET that regulates nuclear size changes. In this case, NET50 and the compound estardiol propionate cooperated in altering nuclear size. NET50 had an effect in reducing nuclear size when overexpressed in prostate cancer models, suggesting an active involvement of this protein, progressively lost during cancer progression, in maintaining a normal nuclear size in healthy tissues. Mutation of the coordinating residue for the cofactor of the protein results in loss of decrease effect on nuclear volume arguing for an involvement of the catalytic function of the protein in the process of nuclear size regulation.

As per the compound side of the nuclear size regulation, estradiol propionate had an effect of nuclear size reduction in a concentration

dependant manner. This decrease in nuclear size is lost or masked when NET50 is expressed in the cell. There are several hypotheses that could explain the mutual exclusive nuclear size effect, such as process of suicide inhibition in which the compound interacts with the catalytic pocket of the protein, thus blocking the normal catalytic function of the protein. This is supported by the activity of close members of the SDR family, active against steroid like substrates (Lidén and Eriksson 2006; Marchais-Oberwinkler et al. 2011), and as estradiol propionate is not a circulating hormone, derivate from a potential natural substrate of the protein, might have the correct conformation and charge to be accommodate in the catalytic pocket, but impeding the normal catalytical mechanism of NET50. Estradiol derivatives have been shown to effectively inhibit the 17β-Hydroxysteroid dehydrogenase, a close member of the SDR family to NET50, in cell-free assay by blocking the substrate pocket (Bérubé and Poirier 2009; Qiu et al. 2002). Another explanation for the absence of nuclear size effects when both protein and compound are present at the same time is for NET50 to actually use estradiol propionate as a substrate, generating a new compound that can not longer induce nuclear volume reduction in the cell. This can be explained with the identification of activity of the protein against carbonyl groups (Štambergová et al. 2016), for which estradiol propionate is an example, flagging the compound as potential substrate that gets modified losing the nuclear size reduction when the protein is still expressed in the cell.

Several and deeper investigations of the relationship between the estradiol propionate and NET50 are required to fully elucidate the mechanisms of nuclear size regulation. But this work provides an example of how selectively targeting a single protein involved in nuclear size, for which loss of expression during cancer progression is associated with more severe tumours, could provide new way for drug development.

6.5 Targeting nuclear size might reduce metastasis and tumour growth

Targeting nuclear size, either via targeting a protein or through an independent effect of a compound, might result in reduction of the metastatic potential of tumours. This was the case for most of the compounds tested where in addition to their action in altering nuclear size they induced apoptosis and inhibit cell migration in wound healing assays. These effects could be the result of different functions targeted by the compounds as, for example, microtubule de-polymerising agents could alter the cytoskeleton connections resulting in less migration as already proven as effective anti cancer therapy (Dumontet and Jordan 2010; Jordan and Wilson 1998).

Another potential mechanism is that nuclear size changes could either influence chromatin compaction leading to a smaller or harder nucleus and likewise increase in nuclear size can lead to less chromatin contacts, allowing a more malleable nucleus. In the former case the smaller nucleus might be able to migrate easier by fitting through tight junctions, but the same time could derive from the increased nuclear size in the latter case because a more malleable nucleus could deform to squeeze through the tight junctions. Drugs that tend to restore the normal nuclear size have been the focus of this study, but even drugs that further increased or decreased nuclear size could lead to an imbalance in connections between the nucleus and the cytoskeleton so that the cell migration capacity might be mitigated. In addition to directly affecting migration, these changes in chromatin contacts could results in deregulation of cancer gene expression patterns, as for example affecting the Wnt or Tgfβ pathways as the nuclear envelope is directly linked to the regulation of these pathways (Jamieson et al. 2014; Markiewicz et al. 2006; Neumann et al. 2010). Thus, the compounds affecting nuclear size in both directions could potentially actually have beneficial treatment effects for reducing metastasis.

The mouse model presented in this study had problems with the control tumours not growing and so have not been useful thus far to gain insights *in*

vivo on how compounds affect nuclear size targeting and reduction of tumour growth and metastatic spread. However, previous literature has shown successful tumour growth reduction in other cancer types for piperlongumine (Bharadwaj et al. 2015; Raj et al. 2015), suggesting a possible efficacy of the nuclear size targeting strategy. The xenograft model needs to be performed again allowing the tumour to develop properly before starting with drug treatment, making sure the effects of the drug are not masked by the progressive degeneration of the tumour in both control and treated groups. This will allow to establish if targeting nuclear size can be effective against tumour growth and can be further translate into clinic for effective treatment of patients.

Once the effects of identified compounds are confirmed in vivo in xenograft models, would be interesting translate them in a more clinical perspective. Many questions arise when administering new drugs to patients, for example if the compounds identified can be just add to pre-existing chemotherapeutic regiments or the drug can be used to substitute an existing one reducing the side effects. In theory, as the aim of this project has been to reduce the metastatic potential of highly aggressive tumours by targeting the nuclear size, adding the identified compounds could result in a containment of the tumour within its primary site, while the already in use chemotherapeutic treatment acts on killing the primary tumour. One of the main downside of treatments after the tumour metastasize is an effective delivery of the drugs in all sites and chemotherapeutic regiments are often useless at this stage of the pathology. Moreover, the identified drugs may have a better effects in treatment of particular cancers as based on the tissue specificity of that particular cancer, resulting in less toxic side effects for the patients or allowing the reduction of concentrations of other drugs used in conjunction with the tissue specific drug.

6.6 Future perspectives

There are many remaining questions that must be answered regarding nuclear size regulation during cancer progression and its potential targeting to reduce the metastatic potential of tumours. Deeper investigation of the mechanisms by which several different NETs can contribute to maintaining a normal nuclear size is crucial to understand the role of the NE both for normal functioning and what happens in a complex disease such as cancer. These mechanisms can range from potential enzymatic activities of these proteins, for which little is known, to complex interactions with the cytoskeleton that can be lost if the protein is down regulated in its expression during cancer progression. Understanding these mechanisms and interactions can provide new insights on new targets for drug development or repurposing.

Along with new targets, targeting nuclear size as a macroscopic phenotype can be a valuable approach in developing new drugs that can reduce the metastatic potential of particularly aggressive tumours. As shown with this study, targeting nuclear size as a phenotype can result in a less migratory effect on different cancer types and in a type-specific manner and can separately reduce tumour growth via selectively triggering apoptosis. These identified compounds can be translated in the clinic as additional drugs to reduce metastatic spread of the tumour and if proven particularly effective *in vivo* might result in lower dosages and toxicity for the patients.

Finally, one of the most important aspects identified in this study is that effects on nuclear size are tissue specific and therefore causes of alteration of this morphological feature and its regulation should be focused on more tissue specific elements such as NETs. Moreover, this tissue specificity is transpose also in drug treatments with compounds identified being cell line specific, suggesting that drug screening and identification of new drugs should focusing

on a selected type of cancer, rather than trying to target multiple diseases at the same time.

6.7 Final remarks

The work presented herein and the recent interest in nuclear size regulation and factors that can influence it, allow to hypothesise the involvement of this phenotypic feature as possible targeting strategy for highly aggressive cancer. This study focused on the identification of proteins involved in the process of regulate the nuclear size and compounds that can alter or restore it, presenting phenotypic screening procedures that can be a used and implemented for identification of new targets or compounds. By the understanding and further investigation on both mechanism and interaction of proteins resident at the NE will open new directions in drug discovery and repurposing. In particular, NET50 results as interesting new target influencing the nuclear size in prostate cancer due to the ability to alter the nuclear size, and could be a new protein to both identify mechanisms of nuclear size regulation and as a new drug target.

Moreover, this study points out a more tissue specific direction where compounds and proteins can have completely different, and sometime opposite, effects on the phenotype detected, suggesting an alternative aspect in which focus future researches. Finally, targeting nuclear size with compounds results a tissue specific process, in which drugs have different effects depending on the cancer type they are administered, pointing out that more focused screen on tissue specificity can improve the successful identification of new drugs able to reduce the metastatic potential of highly metastatic cancers.

7. References

Abdalla, Fathi B. Elmabrou., Rabia Markus, Abdelbaset Buhmeida, Jamela Boder, Kari Syrjanen, and Yrjo Collan. 2012. “Estrogen Receptor, Progesterone Receptor, and Nuclear Size Features in Female Breast Cancer in Libya: Correlation with Clinical Features and Survival.” *Anticancer Res* 32:3485–93.

Agrelo, Ruben, Fernando Setien, Jesus Espada, Maria Jesus Artiga, Maria Rodriguez, Alberto Pérez-Rosado, Abel Sanchez-Aguilera, Mario F. Fraga, Miguel Angel Piris, and Manel Esteller. 2005. “Inactivation of the Lamin A/C Gene by CpG Island Promoter Hypermethylation in Hematologic Malignancies, and Its Association with Poor Survival in Nodal Diffuse Large B-Cell Lymphoma.” *Journal of Clinical Oncology* 23(17):3940–47.

Akhtar, Waseem, Johann De Jong, Alexey V Pindyurin, Ludo Pagie, Wouter Meuleman, Jeroen De Ridder, Anton Berns, Lodewyk F. A. Wessels, Maarten Van Lohuizen, and Bas Van Steensel. 2013. “Resource Chromatin Position Effects Assayed by Thousands of Reporters Integrated in Parallel.” *Cell* 154(4):914–27.

de Andrea, Carlos E., Antonio Sergio Petrilli, Reynaldo Jesus-Garcia, Luiz F. Bleggi-Torres, and Maria Teresa S. Alves. 2011. “Large and Round Tumor Nuclei in Osteosarcoma: Good Clinical Outcome.” *International*

Journal of Clinical and Experimental Pathology 4(2):169–74.

Araya, Selene, Denise V. Kratschmar, Maria Tsachaki, Simon Stücheli, Katharina R. Beck, and Alex Odermatt. 2017. “DHRS7 (SDR34C1) – A New Player in the Regulation of Androgen Receptor Function by Inactivation of 5α-Dihydrotestosterone?” *Journal of Steroid Biochemistry and Molecular Biology* 171(March):288–95.

Barnhart, Erin L., Greg M. Allen, Frank Jülicher, and Julie A. Theriot. 2010. “Bipedal Locomotion in Crawling Cells.” *Biophysical Journal* 98(6):933–42.

Beale, L. S. 1860. “Examination of Sputum from a Case of Cancer of the Pharynx and the Adjacent Parts.” *Arch. Med. Lond.* 2(44).

Bell, Emily S. and Jan Lammerding. 2016. “Causes and Consequences of Nuclear Envelope Alterations in Tumour Progression.” *European Journal of Cell Biology* 95(11):449–64.

Benavente, Ricardo, Georg Krohne, and Werner W. Franke. 1985. “Cell Type-Specific Expression of Nuclear Lamina Proteins during Development of Xenopus Laevis.” *Cell* 41(1):177–90.

Van Berlo, J. H., J. W. Voncken, N. Kubben, J. L. V. Broers, R. Duisters, R. E. W. van Leeuwen, H. J. G. M. Crijns, F. C. S. Ramaekers, C. J. Hutchison, and Y. M. Pinto. 2005. “A-Type Lamins Are Essential for TGF-B1 Induced PP2A to Dephosphorylate Transcription Factors.” *Human Molecular Genetics* 14(19):2839–49.

Bérubé, Marie and Donald Poirier. 2009. “Improved Synthesis of EM-1745, Preparation of Its C17-Ketone Analogue and Comparison of Their Inhibitory Potency on 17β-Hydroxysteroid Dehydrogenase Type 1.” *Journal of Enzyme Inhibition and Medicinal Chemistry* 24(3):832–43.

Bharadwaj, U., T. K. Eckols, M. Kolosov, M. M. Kasembeli, A. Adam, D. Torres, X. Zhang, L. E. Dobrolecki, W. Wei, M. T. Lewis, B. Dave, J. C.

Chang, M. D. Landis, C. J. Creighton, M. A. Mancini, and D. J. Tweardy. 2015. “Drug-Repositioning Screening Identified Piperlongumine as a Direct STAT3 Inhibitor with Potent Activity against Breast Cancer.” *Oncogene* 34(11):1341–53.

Bosland, Maarten C. 2005. “The Role of Estrogens in Prostate Carcinogenesis: A Rationale for Chemoprevention.” *Rev Urol* 7 Suppl 3(3):S4–10.

Bray, James E., Brian D. Marsden, and Udo Oppermann. 2009. “The Human Short-Chain Dehydrogenase/Reductase (SDR) Superfamily: A Bioinformatics Summary.” *Chemico-Biological Interactions* 178(1–3):99–109.

Broers, J. L. V, Barbie M. Machiels, H. J. H. Kuijpers, Frank Smedts, Ronald Van Den Kieboom, Yves Raymond, and F. C. S. Ramaekers. 1997. “A- and B-Type Lamins Are Differentially Expressed in Normal Human Tissues.” *Histochemistry and Cell Biology* 107(6):505–17.

Broers, Jos L. V, Emiel A. G. Peeters, Helma J. H. Kuijpers, Jorike Endert, Carlijn V. C. Bouten, Cees W. J. Oomens, Frank P. T. Baaijens, and Frans C. S. Ramaekers. 2004. “Decreased Mechanical Stiffness in LMNA-/- Cells Is Caused by Defective Nucleo-Cytoskeletal Integrity: Implications for the Development of Laminopathies.” *Human Molecular Genetics* 13(21):2567–80.

Brown, Susan C., Richard J. Piercy, Francesco Muntoni, and Caroline A. Sewry. 2008. “Investigating the Pathology of Emery–Dreifuss Muscular Dystrophy.” *Biochemical Society Transactions* 36(6):1335–38.

Buch, Charlotta, Robert Lindberg, Ricardo Figueroa, Santhosh Gudise, Evgeny Onischenko, and Einar Hallberg. 2009. “An Integral Protein of the Inner Nuclear Membrane Localizes to the Mitotic Spindle in Mammalian Cells.” *Journal of Cell Science* 122:2100–2107.

Busse, Dorothea, Na Li, Gunnar Dittmar, Johannes Schuchhardt, Jana Wolf, Wei Chen, and Matthias Selbach. 2011. “Corrigendum: Global Quantification of Mammalian Gene Expression Control.” 473:337–42.

Cai, Mengli, Ying Huang, Rodolfo Ghirlando, Katherine L. Wilson, Robert Craigie, and G. Marius Clore. 2001. “Solution Structure of the Constant Region of Nuclear Envelope Protein LAP2 Reveals Two LEM-Domain Structures: One Binds BAF and the Other Binds DNA.” *EMBO Journal* 20(16):4399–4407.

Cai, Mengli, Ying Huang, Jeong Yong Suh, John M. Louis, Rodolfo Ghirlando, Robert Craigie, and G. Marius Clore. 2007. “Solution NMR Structure of the Barrier-to-Autointegration Factor-Emerin Complex.” *Journal of Biological Chemistry* 282(19):14525–35.

Callan, H. G., J. T. Randall, and S. G. Tomlin. 1949. “An Electron Microscope Study of the Nuclear Membrane.” *Nature* 163(4138):280.

Cavalier-Smith, T. 1978. “Nuclear Volume Control by Nucleoskeletal DNA, Selection for Cell Volume and Cell Growth Rate, and the Solution of the DNA C-Value Paradox.” *Journal of Cell Science* 34(1):247–78.

Cavalier-Smith, Thomas. 2005. “Economy, Speed and Size Matter: Evolutionary Forces Driving Nuclear Genome Miniaturization and Expansion.” *Annals of Botany* 95(1):147–75.

Cibas, Edmund S. and Barbara S. Ducatman. 2014. *Cytology: Diagnostic Principles and Clinical Correlates*. Vol. 34.

Collins, Conlon, Kannan, Verma, Eli, Lalani, and Crown. 2019. “Preclinical Characteristics of the Irreversible Pan-HER Kinase Inhibitor Neratinib Compared with Lapatinib: Implications for the Treatment of HER2-Positive and HER2-Mutated Breast Cancer.” *Cancers* 11(6):737.

Crisp, Melissa, Qian Liu, Kyle Roux, J. B. Rattner, Catherine Shanahan, Brian Burke, Phillip D. Stahl, and Didier Hodzic. 2006. “Coupling of the

Nucleus and Cytoplasm: Role of the LINC Complex." *Journal of Cell Biology* 172(1):41–53.

Croft, Jenny A., Joanna M. Bridger, Shelagh Boyle, Paul Perry, Peter Teague, and Wendy A. Bickmore. 1999. "Differences in the Localization and Morphology of Chromosomes in the Human Nucleus." *Journal of Cell Biology* 145(6):1119–31.

Czapiewski, Rafal, Michael I. Robson, and Eric C. Schirmer. 2016. "Anchoring a Leviathan: How the Nuclear Membrane Tethers the Genome." *Frontiers in Genetics* 7(MAY):1–13.

Dahl, Edgar, Glen Kristiansen, Kathrin Gottlob, Irina Klaman, Elke Ebner, Bernd Hinzmann, Klaus Hermann, Christian Pilarsky, Matthias Dürst, Monika Klinkhammer-Schalke, Hagen Blaszyk, Ruth Knuechel, Arndt Hartmann, André Rosenthal, and Peter J. Wild. 2006. "Molecular Profiling of Laser-Microdissected Matched Tumor and Normal Breast Tissue Identifies Karyopherin A2 as a Potential Novel Prognostic Marker in Breast Cancer." *Clinical Cancer Research* 12(13):3950–60.

Davidson, Patricia M., Celine Denais, Maya C. Bakshi, and Jan Lammerding. 2014. "Nuclear Deformability Constitutes a Rate-Limiting Step during Cell Migration in 3-D Environments." *Cellular and Molecular Bioengineering* 7(3):293–306.

Demmerle, Justin, Adam J. Koch, and James M. Holaska. 2012. "The Nuclear Envelope Protein Emerin Binds Directly to Histone Deacetylase 3 (HDAC3) and Activates HDAC3 Activity." *Journal of Biological Chemistry* 287(26):22080–88.

Denais, C. M., R. M. Gilbert, P. Isermann, A. L. McGregor, M. te Lindert, B. Weigelin, P. M. Davidson, P. Friedl, K. Wolf, and J. Lammerding. 2016. "Nuclear Envelope Rupture and Repair during Cancer Cell Migration." *Science* 352(6283):353–58.

Dumontet, Charles and Mary Ann Jordan. 2010. “Microtubule-Binding Agents: A Dynamic Field of Cancer Therapeutics.” *Nature Reviews Drug Discovery* 9(10):790–803.

Edens, Lisa J., Karen H. White, Predrag Jevtic, Xiaoyang Li, and Daniel L. Levy. 2013. “Nuclear Size Regulation: From Single Cells to Development and Disease.” *Trends in Cell Biology* 23(4):151–59.

Eynard, Hector G., Elio a. Soria, Eduardo Cuestas, Roberto a. Rovasio, and Aldo R. Eynard. 2009. “Assessment of Colorectal Cancer Prognosis Through Nuclear Morphometry.” *Journal of Surgical Research* 154(2):345–48.

Fagone, Paolo, Rosario Caltabiano, Andrea Russo, Gabriella Lupo, Carmelina Daniela Anfuso, Maria Sofia Basile, Antonio Longo, Ferdinando Nicoletti, Rocco De Pasquale, Massimo Libra, and Michele Reibaldi. 2017. “Identification of Novel Chemotherapeutic Strategies for Metastatic Uveal Melanoma.” *Scientific Reports* 7:44564.

Fidler, Isaiah J. and Margaret L. Kripke. 2015. “The Challenge of Targeting Metastasis.” *Cancer and Metastasis Reviews* 34(4):635–41.

Fidorra, J., Th Mielke, J. Booz, and L. E. Feinendegen. 1981. “Cellular and Nuclear Volume of Human Cells During the Cell Cycle.” 214(215):205–14.

Fischer, Andrew H. 2014. “The Diagnostic Pathology of the Nuclear Envelope in Human Cancers.” Pp. 571–91 in *Cancer Biology and the Nuclear Envelope*. Vol. 773.

Franz, Cerstin, Rudolf Walczak, Sevil Yavuz, Rachel Santarella, Marc Gentzel, Peter Askjaer, Vincent Galy, Martin Hetzer, Iain W. Mattaj, and Wolfram Antonin. 2007. “MEL-28/ELYS Is Required for the Recruitment of Nucleoporins to Chromatin and Postmitotic Nuclear Pore Complex Assembly.” *EMBO Reports* 8(2):165–72.

Frost, J. K. 1986. “The Cell in Health and Disease. An Evaluation of Cellular Morphologic Expression of Biologic Behavior. 2nd, Revised Edition.” *Monographs in Clinical Cytology* 2:1–304.

Fujitomo, Takashi, Yataro Daigo, Koichi Matsuda, Koji Ueda, and Yusuke Nakamura. 2012. “Critical Function for Nuclear Envelope Protein TMEM209 in Human Pulmonary Carcinogenesis.” *Cancer Research* 72(16):4110–18.

Fukuzawa, S., T. Hashimura, M. Sasaki, H. Yamabe, and O. Yoshida. 1995. “Nuclear Morphometry for Improved Prediction of the Prognosis of Human Bladder Carcinoma.” *Cancer* 76(10):1790–96.

Gant Luxton, G. W., Edgar R. Gomes, Eric S. Folker, Howard J. Worman, and Gregg G. Gundersen. 2011. “TAN Lines: A Novel Nuclear Envelope Structure Involved in Nuclear Positioning.” *Nucleus* 2(3):173–81.

Ghosh, Kaustabh, Charles K. Thodeti, Andrew C. Dudley, Akiko Mammoto, Michael Klagsbrun, and Donald E. Ingber. 2008. *Tumor-Derived Endothelial Cells Exhibit Aberrant Rho-Mediated Mechanosensing and Abnormal Angiogenesis in Vitro*.

Giorgadze, T., R. Kanhere, C. Pang, C. Ganote, L. E. Miller, P. Tabaczka, E. Brown, and M. Husain. 2012. “Small Cell Carcinoma of the Cervix in Liquid-Based Pap Test: Utilization of Split-Sample Immunocytochemical and Molecular Analysis.” *Diagnostic Cytopathology* 40(3):214–19.

Gluz, Oleg, Peter Wild, Robert Meiler, Raihana Diallo-Danebrock, Evelyn Ting, Svjetlana Mohrmann, Gerhart Schuett, Edgar Dahl, Thomas Fuchs, Alexander Herr, Andreas Gaumann, Markus Frick, Christopher Poremba, Ulrike Anneliese Nitz, and Arndt Hartmann. 2008. “Nuclear Karyopherin A2 Expression Predicts Poor Survival in Patients with Advanced Breast Cancer Irrespective of Treatment Intensity.” *International Journal of Cancer* 123(6):1433–38.

Gomes, Edgar R., Shantanu Jani, and Gregg G. Gundersen. 2005. “Nuclear Movement Regulated by Cdc42, MRCK, Myosin, and Actin Flow Establishes MTOC Polarization in Migrating Cells.” *Cell* 121(3):451–63.

Grossman, Einat, Ohad Medalia, and Monika Zwerger. 2012. “Functional Architecture of the Nuclear Pore Complex.” *Annual Review of Biophysics* 41:557–84.

Haeseleer, Françoise and Krzysztof Palczewski. 2000. “[24] Short-Chain Dehydrogenases/Reductases in Retina.” *Methods in Enzymology* 316(1994):372–83.

Harada, Takamasa, Joe Swift, Jerome Irianto, Jae-Won Shin, Kyle R. Spinler, Avathamsa Athirasala, Rocky Diegmiller, P. C. Dave P. Dingal, Irena L. Ivanovska, and Dennis E. Discher. 2014. “Nuclear Lamin Stiffness Is a Barrier to 3D Migration, but Softness Can Limit Survival.” *The Journal of Cell Biology* 204(5):669–82.

Harris, H. 1967. “THE REACTIVATION OF THE RED CELL NUCLEUS.” *J. Cell Sci* 2(1):23–32.

Harshbarger, Wayne, Sudershan Gondi, Scott B. Ficarro, John Hunter, Durga Udayakumar, Deepak Gurbani, William D. Singer, Yan Liu, Lianbo Li, Jarrod A. Marto, and Kenneth D. Westover. 2017. “Structural and Biochemical Analyses Reveal the Mechanism of Glutathione S-Transferase Pi 1 Inhibition by the Anti-Cancer Compound Piperlongumine.” *Journal of Biological Chemistry* 292(1):112–20.

Havercroft, J. C., R. A. Quinlan, and K. Gull. 1981. “Binding of Parbendazole to Tubulin and Its Influence on Microtubules in Tissue-Culture Cells as Revealed by Immunofluorescence Microscopy.” *Journal of Cell Science* 49:195–204.

Helander, K., P. A. Hofer, and G. Holmberg. 1984. “Karyometric Investigations on Urinary Bladder Carcinoma, Correlated to

Histopathological Grading." *Virchows Archiv. A, Pathological Anatomy and Histopathology* 403(2):117–25.

Ho, Chin Yee, Diana E. Jaalouk, Maria K. Vartiainen, and Jan Lammerding. 2013. "Lamin A/C and Emerin Regulate MKL1/SRF Activity by Modulating Actin Dynamics." *Nature* 497(7450):1–13.

Holaska, James M., Soroush Rais-Bahrami, and Katherine L. Wilson. 2006. "Lmo7 Is an Emerin-Binding Protein That Regulates the Transcription of Emerin and Many Other Muscle-Relevant Genes." *Human Molecular Genetics* 15(23):3459–72.

Holland, Andrew J. and Don W. Cleveland. 2012. "Losing Balance: The Origin and Impact of Aneuploidy in Cancer." *EMBO Reports* 13(6):501–14.

Humphrey, Peter A. 2004. "Gleason Grading and Prognostic Factors in Carcinoma of the Prostate." *Modern Pathology* 17(3):292–306.

Ikeguchi, M., S. Oka, H. Saito, A. Kondo, S. Tsujitani, M. Maeta, and N. Kaibara. 1999. "Computerized Nuclear Morphometry: A New Morphologic Assessment for Advanced Gastric Adenocarcinoma." *Annals of Surgery* 229(1):55–61.

Ishimura, Akihiko, Jennifer K. Ng, Masanori Taira, Stephen G. Young, and Shin-Ichi Osada. 2006. "Man1, an Inner Nuclear Membrane Protein, Regulates Vascular Remodeling by Modulating Transforming Growth Factor Beta Signaling." *Development (Cambridge, England)* 133(19):3919–28.

Jamieson, Cara, Manisha Sharma, and Beric R. Henderson. 2014. "Targeting the β-Catenin Nuclear Transport Pathway in Cancer." *Seminars in Cancer Biology* 27:20–29.

Jemal, Ahmedin, Rebecca Siegel, Jiaquan Xu, and Elizabeth Ward. 2010. "Cancer Statistics, 2010." *CA: A Cancer Journal for Clinicians*

60(5):277–300.

Jenkins, Hazel, Thomas Höfken, Carol Lyon, Brigitte E. Lane, Reimer Stick, and Christopher J. Hutchison. 1993. “Nuclei That Lack a Lamina Accumulate Karyophilic Proteins and Assemble a Nuclear Matrix.” *J Cell Sci* 106 (Pt 1:275–85.

Jevtić, Predrag, Lisa J. Edens, Xiaoyang Li, Thang Nguyen, Pan Chen, and Daniel L. Levy. 2015. “Concentration-Dependent Effects of Nuclear Lamins on Nuclear Size in Xenopus and Mammalian Cells.” *Journal of Biological Chemistry* 290(46):27557–71.

Jevtic, Predrag and Daniel L. Levy. 2015. “Nuclear Size Scaling during Xenopus Early Development Contributes to Midblastula Transition Timing.” *Current Biology* 25(1):45–52.

Johnson, Brett R., Ryan T. Nitta, Richard L. Frock, Leslie Mounkes, David A. Barbie, Colin L. Stewart, Ed Harlow, and Brian K. Kennedy. 2004. “A-Type Lamins Regulate Retinoblastoma Protein Function by Promoting Subnuclear Localization and Preventing Proteasomal Degradation.” *Proceedings of the National Academy of Sciences of the United States of America* 101(26):9677–82.

Jordan, Mary Ann and Leslie Wilson. 1998. “Microtubules and Actin Filaments: Dynamic Targets for Cancer Chemotherapy.” *Current Opinion in Cell Biology* 10(1):123–30.

Jorgensen, Paul, Nicholas P. Edgington, Brandt L. Schneider, Ivan Rupes, Mike Tyers, and Bruce Futcher. 2007. “The Size of the Nucleus Increases as Yeast Cells Grow.” *Molecular Biology of the Cell* 18(8):3523–3532.

Kaighn, M. E., K. S. Narayan, Y. Ohnuki, J. F. Lechner, and L. W. Jones. 1979. “Establishment and Characterization of a Human Prostatic Carcinoma Cell Line (PC-3).” *Investigative Urology* 17(1):16–23.

Kapadia, Govind J., Magnus A. Azuine, Yuuko Shigeta, Nobutaka Suzuki, and Harukuni Tokuda. 2010. “Chemopreventive Activities of Etodolac and Oxyphenbutazone against Mouse Skin Carcinogenesis.” *Bioorganic and Medicinal Chemistry Letters* 20(8):2546–48.

Kau, Tweeny R., Jeffrey C. Way, and Pamela A. Silver. 2004. “Nuclear Transport and Cancer: From Mechanism to Intervention.” *Nature Reviews. Cancer* 4(2):106–17.

Kaufmann, Scott H., Mack Mabry, Rajani Jasti, Cancer Cell Lines, and Joel H. Shaper. 1991. “Differential Expression of Nuclear Envelope Lamins A and C in Human Lung Cancer Cell Lines Differential Expression of Nuclear Envelope Lamins A and C in Human Lung.” 581–86.

Kim, S. H., P. G. McQueen, M. K. Lichtman, E. M. Shevach, L. A. Parada, and T. Misteli. 2004. “Spatial Genome Organization during T-Cell Differentiation.” *Cytogenetic and Genome Research* 105(2–4):292–301.

Koong, Luke Y. and Cheryl S. Watson. 2014. “Direct Estradiol and Diethylstilbestrol Actions on Early- versus Late-Stage Prostate Cancer Cells.” *The Prostate* 74(16):1589–1603.

Korfali, Nadia, Vlastimil Srsen, Martin Waterfall, Dzmitry G. Batrakou, Vanja Pekovic, Christopher J. Hutchison, and Eric C. Schirmer. 2011. “A Flow Cytometry-Based Screen of Nuclear Envelope Transmembrane Proteins Identifies NET4/Tmem53 as Involved in Stress-Dependent Cell Cycle Withdrawal.” *PloS One* 6(4):e18762.

Korfali, Nadia, Gavin S. Wilkie, Selene K. Swanson, Vlastimil Srsen, Dzmitry G. Batrakou, Elizabeth a L. Fairley, Poonam Malik, Nikolaj Zuleger, Alexander Goncharevich, Jose de Las Heras, David a Kelly, Alastair R. W. Kerr, Laurence Florens, and Eric C. Schirmer. 2010. “The Leukocyte Nuclear Envelope Proteome Varies with Cell Activation and Contains Novel Transmembrane Proteins That Affect Genome Architecture.” *Molecular & Cellular Proteomics : MCP* 9:2571–85.

Korfali, Nadia, Gavin S. Wilkie, Selene K. Swanson, Vlastimil Srsen, Jose de Las Heras, Dzmitry G. Batrakou, Poonam Malik, Nikolaj Zuleger, Alastair R. W. Kerr, Laurence Florens, and Eric C. Schirmer. 2012. “The Nuclear Envelope Proteome Differs Notably between Tissues.” *Nucleus (Austin, Tex.)* 3(6):552–64.

Kuzmina, S. N., T. V Buldyaeva, S. B. Akopov, and I. B. Zbarsky. 1984. “Protein Patterns of the Nuclear Matrix in Differently Proliferating and Malignant Cells.” *Molecular and Cellular Biochemistry* 58(1–2):183–86.

Ladekarl, M., T. Boek-Hansen, R. Henrik-Nielsen, C. Mouritzen, U. Henriques, and F. B. Sorensen. 1995. “Objective Malignancy Grading of Squamous Cell Carcinoma of the Lung: Stereologic Estimates of Mean Nuclear Size Are of Prognostic Value, Independent of Clinical Stage of Disease.” *Cancer* 76(5):797–802.

Lammerding, Jan, Loren G. Fong, Julie Y. Ji, Karen Reue, Colin L. Stewart, Stephen G. Young, and Richard T. Lee. 2006. “Lamins A and C but Not Lamin B1 Regulate Nuclear Mechanics.” *Journal of Biological Chemistry* 281(35):25768–80.

Lammerding, Jan, P. Christian Schulze, Tomosaburo Takahashi, Serguei Kozlov, Teresa Sullivan, Roger D. Kamm, Colin L. Stewart, and Richard T. Lee. 2004a. “Lamin A / C Deficiency Causes Defective Nuclear Mechanics and Mechanotransduction.” *Journal of Clinical Investigation* 113(3):370–78.

Lammerding, Jan, P. Christian Schulze, Tomosaburo Takahashi, Serguei Kozlov, Teresa Sullivan, Roger D. Kamm, Colin L. Stewart, and Richard T. Lee. 2004b. “Lamin A / C Deficiency Causes Tema Grupo Defective Nuclear Mechanics and Mechanotransduction.” *Journal of Clinical Investigation* 113(3):370–78.

de Las Heras, Jose I., Dzmitry G. Batrakou, and Eric C. Schirmer. 2013. “Cancer Biology and the Nuclear Envelope: A Convoluted Relationship.”

Seminars in Cancer Biology 23(2):125–37.

de Las Heras, Jose I., Peter Meinke, Dzmitry G. Batrakou, Vlastimil Srsen, Nikolaj Zuleger, Alastair Rw Kerr, and Eric C. Schirmer. 2014. “Tissue Specificity in the Nuclear Envelope Supports Its Functional Complexity.” *Nucleus* 4(6):460–77.

de Las Heras, Jose I. and Eric C. Schirmer. 2014. “The Nuclear Envelope and Cancer: A Diagnostic Perspective and Historical Overview.” Pp. 571–91 in *Cancer Biology and the Nuclear Envelope*. Vol. 773.

De Las Heras, Jose I., Nikolaj Zuleger, Dzmitry G. Batrakou, Rafal Czapiewski, Alastair R. W. Kerr, and Eric C. Schirmer. 2017. “Tissue-Specific NETs Alter Genome Organization and Regulation Even in a Heterologous System.” *Nucleus* 8(1):81–97.

Lee, Jerry S. H., Christopher M. Hale, Porntula Panorchan, Shyam B. Khatau, Jerry P. George, Yiider Tseng, Colin L. Stewart, Didier Hodzic, and Denis Wirtz. 2007. “Nuclear Lamin A/C Deficiency Induces Defects in Cell Mechanics, Polarization, and Migration.” *Biophysical Journal* 93(7):2542–52.

Lehner, C. F., R. Stick, H. M. Eppenberger, and E. a. Migg. 1987. “Differential Expression of Nuclear Lamin Proteins during Chicken Development.” *Journal of Cell Biology* 105(1):577–87.

Lidén, Martin and Ulf Eriksson. 2006. “Understanding Retinol Metabolism: Structure and Function of Retinol Dehydrogenases.” *Journal of Biological Chemistry* 281(19):13001–4.

Lu, Wenshu, Maria Schneider, Sascha Neumann, Verena Maren Jaeger, Surayya Taranum, Martina Munck, Sarah Cartwright, Christine Richardson, James Carthew, Kowoon Noh, Martin Goldberg, Angelika a. Noegel, and Iakowos Karakesisoglou. 2012. “Nesprin Interchain Associations Control Nuclear Size.” *Cellular and Molecular Life Sciences*

69(20):3493–3509.

Luke, Y., H. Zaim, I. Karakesisoglou, V. M. Jaeger, L. Sellin, W. Lu, M. Schneider, S. Neumann, A. Beijer, M. Munck, V. C. Padmakumar, J. Gloy, G. Walz, and A. A. Noegel. 2008a. “Nesprin-2 Giant (NUANCE) Maintains Nuclear Envelope Architecture and Composition in Skin.” *Journal of Cell Science* 121(11):1887–98.

Luke, Y., H. Zaim, I. Karakesisoglou, V. M. Jaeger, L. Sellin, W. Lu, M. Schneider, S. Neumann, A. Beijer, M. Munck, V. C. Padmakumar, J. Gloy, G. Walz, and A. A. Noegel. 2008b. “Nesprin-2 Giant (NUANCE) Maintains Nuclear Envelope Architecture and Composition in Skin.” *Journal of Cell Science* 121(11):1887–98.

Luxton, G. W. Gan., Edgar R. Gomes, Eric S. Folker, Erin Vintinner, and Gregg G. Gundersen. 2010. “Linear Arrays of Nuclear Envelope Proteins Harness Retrograde Actin Flow for Nuclear Movement.” *Science* 329(5994):956–59.

Madsen, C. and H. D. Schrøder. 1996. “Stereological Estimation of Nuclear Mean Volume in Invasive Meningiomas.” *APMIS : Acta Pathologica, Microbiologica, et Immunologica Scandinavica* 104(2):103–7.

Maeshima, Kazuhiro, Haruki Iino, Saera Hihara, Tomoko Funakoshi, Ai Watanabe, Masaomi Nishimura, Reiko Nakatomi, Kazuhide Yahata, Fumio Imamoto, Tsutomu Hashikawa, Hideo Yokota, and Naoko Imamoto. 2010. “Nuclear Pore Formation but Not Nuclear Growth Is Governed by Cyclin-Dependent Kinases (Cdks) during Interphase.” *Nature Structural and Molecular Biology* 17(9):1065–71.

Malhotra, Saurabh, Viktoryia Kazlouskaya, Christian Andres, Jiang Gui, and Dirk Elston. 2013. “Diagnostic Cellular Abnormalities in Neoplastic and Non-Neoplastic Lesions of the Epidermis: A Morphological and Statistical Study.” *Journal of Cutaneous Pathology* 40(4):371–78.

Malik, Poonam, Nadia Korfali, Vlastimil Srsen, Vassiliki Lazou, Dzmitry G. Batrakou, Nikolaj Zuleger, Deirdre M. Kavanagh, Gavin S. Wilkie, Martin W. Goldberg, and Eric C. Schirmer. 2010. “Cell-Specific and Lamin-Dependent Targeting of Novel Transmembrane Proteins in the Nuclear Envelope.” *Cellular and Molecular Life Sciences* 67:1353–69.

Malik, Poonam, Nikolaj Zuleger, and Eric C. Schirmer. 2010. “Nuclear Envelope Influences on Genome Organization.” *Biochemical Society Transactions* 38:268–72.

Maniotis, A. J., C. S. Chen, and D. E. Ingber. 1997. “Demonstration of Mechanical Connections between Integrins, Cytoskeletal Filaments, and Nucleoplasm That Stabilize Nuclear Structure.” *Proceedings of the National Academy of Sciences of the United States of America* 94(3):849–54.

Marchais-Oberwinkler, Sandrine, Claudia Henn, Gabriele Möller, Tobias Klein, Matthias Negri, Alexander Oster, Alessandro Spadaro, Ruth Werth, Marie Wetzel, Kuiying Xu, Martin Frotscher, Rolf W. Hartmann, and Jerzy Adamski. 2011. “17β-Hydroxysteroid Dehydrogenases (17β-HSDs) as Therapeutic Targets: Protein Structures, Functions, and Recent Progress in Inhibitor Development.” *Journal of Steroid Biochemistry and Molecular Biology* 125(1–2):66–82.

Markiewicz, Ewa, Katarzyna Tilgner, Nick Barker, Mark Van De Wetering, Hans Clevers, Margareth Dorobek, Irena Hausmanowa-Petrusewicz, Frans C. S. Ramaekers, Jos L. V. Broers, W. Matthijs Blankesteijn, Georgia Salpingidou, Robert G. Wilson, Juliet A. Ellis, and Christopher J. Hutchison. 2006. “The Inner Nuclear Membrane Protein Emerin Regulates β-Catenin Activity by Restricting Its Accumulation in the Nucleus.” *EMBO Journal* 25(14):3275–85.

Mattout-Drubezki, a. and Y. Gruenbaum. 2003. “Dynamic Interactions of Nuclear Lamina Proteins with Chromatin and Transcriptional Machinery.”

Cellular and Molecular Life Sciences 60(10):2053–63.

McGregor, Alexandra Lynn, Chieh-Ren Hsia, and Jan Lammerding. 2016. "Squish and Squeeze — the Nucleus as a Physical Barrier during Migration in Confined Environments." *Current Opinion in Cell Biology* 40:32–40.

Meachem, M. D., H. J. Burgess, J. L. Davies, and B. A. Kidney. 2012. "Utility of Nuclear Morphometry in the Cytologic Evaluation of Canine Cutaneous Soft Tissue Sarcomas." *Journal of Veterinary Diagnostic Investigation* 24(3):525–30.

Meinke, Peter and Eric C. Schirmer. 2015. "LINC'ing Form and Function at the Nuclear Envelope." *FEBS Letters* 589(19):2514–21.

Miao, Qi, Kun Ma, Dong Chen, Xiaoxing Wu, and Sheng Jiang. 2019. "Targeting Tropomyosin Receptor Kinase for Cancer Therapy." *European Journal of Medicinal Chemistry* 175:129–48.

Montgomery, Bruce, Peter S. Nelson, Robert Vessella, Tom Kalhorn, David Hess, and Eva Corey. 2010. "Estradiol Suppresses Tissue Androgens and Prostate Cancer Growth in Castration Resistant Prostate Cancer." *BMC Cancer* 10(1):244.

Morey, Céline, Nelly R. Da Silva, Marie Kmita, Denis Duboule, and Wendy a Bickmore. 2008. "Ectopic Nuclear Reorganisation Driven by a Hoxb1 Transgene Transposed into Hoxd." *Journal of Cell Science* 121(Pt 5):571–77.

Mossbacher, U., S. Knollmayer, M. Binder, A. Steiner, K. Wolff, and H. Pehamberger. 1996. "Increased Nuclear Volume in Metastasizing 'Thick' Melanomas." *The Journal of Investigative Dermatology* 106(3):437–40.

Na, Y. R. R., S. H. H. Seok, D. J. J. Kim, J. H. H. Han, T. H. H. Kim, H. Jung, B. H. H. Lee, and J. H. H. Park. 2009. "Isolation and Characterization of Spheroid Cells from Human Malignant Melanoma Cell Line WM-266-4."

Tumor Biology 30(5–6):300–309.

Nandakumar, Vivek, Laimonas Kelbauskas, Kathryn F. Hernandez, Kelly M. Lintecum, Patti Senechal, Kimberly J. Bussey, Paul C. W. Davies, Roger H. Johnson, and Deirdre R. Meldrum. 2012. “Isotropic 3D Nuclear Morphometry of Normal, Fibrocystic and Malignant Breast Epithelial Cells Reveals New Structural Alterations.” *PLoS ONE* 7(1).

Natarajan, S., S. Mahajan, K. Boaz, and T. George. 2010. “Prediction of Lymph Node Metastases by Preoperative Nuclear Morphometry in Oral Squamous Cell Carcinoma: A Comparative Image Analysis Study.” *Indian Journal of Cancer* 47(4):406–11.

Neumann, Frank R. and Paul Nurse. 2007. “Nuclear Size Control in Fission Yeast.” *Journal of Cell Biology* 179(4):593–600.

Neumann, Sascha, Maria Schneider, Rebecca L. Daugherty, Cara J. Gottardi, Sabine A. Eming, Asa Beijer, Angelika A. Noegel, and Iakowos Karakesisoglou. 2010. “Nesprin-2 Interacts with α-Catenin and Regulates Wnt Signaling at the Nuclear Envelope.” *Journal of Biological Chemistry* 285(45):34932–38.

Newport, John W., Katherine L. Wilson, and William G. Dunphy. 1990. “A Lamin-Independent Pathway for Nuclear Envelope Assembly.” *Journal of Cell Biology* 111(6 PART 1):2247–59.

Osada, S. I. 2003. “XMAN1, an Inner Nuclear Membrane Protein, Antagonizes BMP Signaling by Interacting with Smad1 in Xenopus Embryos.” *Development* 130(9):1783–94.

Pan, Deng, Luis D. Estévez-Salmerón, Shannon L. Stroschein, Xueliang Zhu, Jun He, Sharleen Zhou, and Kunxin Luo. 2005. “The Integral Inner Nuclear Membrane Protein MAN1 Physically Interacts with the R-Smad Proteins to Repress Signaling by the Transforming Growth Factor-β Superfamily of Cytokines.” *Journal of Biological Chemistry*

280(16):15992–1.

Parada, Luis A., Philip G. McQueen, and Tom Misteli. 2004. “Tissue-Specific Spatial Organization of Genomes.” *Genome Biology* 5(7):R44.

Pfisterer, Karin, Asier Jayo, and Maddy Parsons. 2017. “Control of Nuclear Organization by F-Actin Binding Proteins.” *Nucleus* 8(2):126–33.

Prunuske, Amy J. and Katharine S. Ullman. 2006. “The Nuclear Envelope: Form and Reformation.” *Current Opinion in Cell Biology* 18(1):108–16.

Qiu, Wei, Robert L. Campbell, Anne Gangloff, Philippe Dupuis, Roch P. Boivin, Martin R. Tremblay, Donald Poirier, and Sheng Xiang Lin. 2002. “A Concerted, Rational Design of Type 1 17beta-Hydroxysteroid Dehydrogenase Inhibitors: Estradiol-Adenosine Hybrids with High Affinity.” *The FASEB Journal : Official Publication of the Federation of American Societies for Experimental Biology* 16(13):1829–31.

Quinlan, R. A., A. Roobol, C. I. Pogson, and K. Gull. 1981. “A Correlation between in Vivo and in Vitro Effects of the Microtubule Inhibitors Colchicine, Parbendazole and Nocodazole on Myxamoebae of Physarum Polycephalum.” *Journal of General Microbiology* 122(1):1–6.

Raab, M., M. Gentili, H. de Belly, H. R. Thiam, P. Vargas, A. J. Jimenez, F. Lautenschlaeger, R. Voituriez, A. M. Lennon-Dumenil, N. Manel, and M. Piel. 2016. “ESCRT III Repairs Nuclear Envelope Ruptures during Cell Migration to Limit DNA Damage and Cell Death.” *Science* 352(6283):359–62.

Raj, Lakshmi, Takao Ide, Aditi U. Gurkar, Michael Foley, Monica Schenone, Xiaoyu Li, Nicola J. Tolliday, Todd R. Golub, Steven A. Carr, Alykhan F. Shamji, Andrew M. Stern, Anna Mandinova, Stuart L. Schreiber, and Sam W. Lee. 2011. “Selective Killing of Cancer Cells by a Small Molecule Targeting the Stress Response to ROS.” *Nature* 475(7355):231–34.

Raj, Lakshmi, Takao Ide, Aditi U. Gurkar, Michael Foley, Monica Schenone, Xiaoyu Li, Nicola J. Tolliday, Todd R. Golub, Steven A. Carr, Alykhan F. Shamji, Andrew M. Stern, Anna Mandinova, Stuart L. Schreiber, Sam W. Lee, U. Bharadwaj, T. K. Eckols, M. Kolosov, M. M. Kasembeli, A. Adam, D. Torres, X. Zhang, L. E. Dobrolecki, W. Wei, M. T. Lewis, B. Dave, J. C. Chang, M. D. Landis, C. J. Creighton, M. A. Mancini, and D. J. Tweardy. 2015. “Selective Killing of Cancer Cells by a Small Molecule Targeting the Stress Response to ROS.” *Oncogene* 475(7355):231–34.

Rashid, Farhat and Anwar Ul Haque. 2011. “Frequencies of Different Nuclear Morphological Features in Prostate Adenocarcinoma.” *Annals of Diagnostic Pathology* 15(6):414–21.

Riddick, Gregory and Ian G. Macara. 2005. “A Systems Analysis of Importin-{alpha}-{beta} Mediated Nuclear Protein Import.” *The Journal of Cell Biology* 168(7):1027–38.

Rizzotto, Andrea and Eric C. Schirmer. 2017. “Breaking the Scale: How Disrupting the Karyoplasmic Ratio Gives Cancer Cells an Advantage for Metastatic Invasion.” *Biochemical Society Transactions* 45(6):1333–44.

Röber, R. a, K. Weber, and M. Osborn. 1989. “Differential Timing of Nuclear Lamin A/C Expression in the Various Organs of the Mouse Embryo and the Young Animal: A Developmental Study.” *Development (Cambridge, England)* 105(2):365–78.

Robson, Michael I., Jose I. de las Heras, Rafal Czapiewski, Phú Lê Thành, Daniel G. Booth, David A. Kelly, Shaun Webb, Alastair R. W. Kerr, and Eric C. Schirmer. 2016. “Tissue-Specific Gene Repositioning by Muscle Nuclear Membrane Proteins Enhances Repression of Critical Developmental Genes during Myogenesis.” *Molecular Cell* 62(6):834–47.

Robson, Michael I., Jose I. de las Heras, Rafal Czapiewski, Aishwarya Sivakumar, Alastair R. W. Kerr, and Eric Schirmer. 2017. “Constrained

Release of Lamina-Associated Enhancers and Genes from the Nuclear Envelope during T-Cell Activation Facilitates Their Association in Chromosome Compartments." *Genome Research* 44(0):gr.212308.116.

Romanuik, Tammy L., Gang Wang, Olena Morozova, Allen Delaney, Marco a Marra, and Marianne D. Sadar. 2010. "LNCaP Atlas: Gene Expression Associated with in Vivo Progression to Castration-Recurrent Prostate Cancer." *BMC Medical Genomics* 3:43.

Roux, Kyle J., Melissa L. Crisp, Qian Liu, Daein Kim, Serguei Kozlov, Colin L. Stewart, and Brian Burke. 2009. "Nesprin 4 Is an Outer Nuclear Membrane Protein That Can Induce Kinesin-Mediated Cell Polarization." *Proceedings of the National Academy of Sciences* 106(7):2194–99.

Rowat, A. C., J. Lammerding, and J. H. Ipsen. 2006. "Mechanical Properties of the Cell Nucleus and the Effect of Emerin Deficiency." *Biophysical Journal* 91(12):4649–64.

Saad, Reda S., Amal Kanbour-Shakir, Erxiong Lu, Judith Modery, and Anisa Kanbour. 2006. "Cytomorphologic Analysis and Histological Correlation of High-Grade Squamous Intraepithelial Lesions in Postmenopausal Women." *Diagnostic Cytopathology* 34(7):467–71.

Saleem, Shakir, Ruqaiyah Khan, Muhammad Afzal, and Imran Kazmi. 2017. "Oxyphenbutazone Promotes Cytotoxicity in Rats and Hep3B Cellsvia Suppression of PGE2and Deactivation of Wnt/β-Catenin Signaling Pathway." *Molecular and Cellular Biochemistry*, July 4, 1–10.

Samanta, Swapan and Pranab Dey. 2012. "Micronucleus and Its Applications" edited by Z. Baloch. *Diagnostic Cytopathology* 40(1):84–90.

Sanchez, Connie, Elin H. Reines, and Stuart A. Montgomery. 2014. "A Comparative Review of Escitalopram, Paroxetine, and Sertraline: Are They All Alike?" *International Clinical Psychopharmacology* 29(4):185–

96.

Schirmer, Eric C., Laurence Florens, Tinglu Guan, John R. Yates, and Larry Gerace. 2003. “Nuclear Membrane Proteins with Potential Disease Links Found by Subtractive Proteomics.” *Science (New York, N.Y.)* 301(5638):1380–82.

Schirmer, Eric C. and Roland Foisner. 2007. “Proteins That Associate with Lamins: Many Faces, Many Functions.” *Experimental Cell Research* 313(10):2167–79.

Schirmer, Eric C., Tinglu Guan, and Larry Gerace. 2001. “Involvement of the Lamin Rod Domain in Heterotypic Lamin Interactions Important for Nuclear Organization.” *Journal of Cell Biology* 152(3):479–89.

Schmoranzer, Jan, James P. Fawcett, Miriam Segura, Serena Tan, Richard B. Vallee, Tony Pawson, and Gregg G. Gundersen. 2009. “Par3 and Dynein Associate to Regulate Local Microtubule Dynamics and Centrosome Orientation during Migration.” *Current Biology* 19(13):1065–74.

Schneider, Naira Fernanda Zanchett, Lara Persich, Sayonarah C. Rocha, Ana Carolina Pacheco Ramos, Vanessa Faria Cortes, Izabella Thaís Silva, Jennifer Munkert, Rodrigo M. Pádua, Wolfgang Kreis, Alex G. Taranto, Leandro A. Barbosa, Fernão C. Braga, and Cláudia M. O. Simões. 2018. “Cytotoxic and Cytostatic Effects of Digitoxigenin Monodigitoxoside (DGX) in Human Lung Cancer Cells and Its Link to Na,K-ATPase.” *Biomedicine and Pharmacotherapy* 97:684–96.

Seibert, Julia K., Luca Quagliata, Cristina Quintavalle, Thomas G. Hammond, Luigi Terracciano, and Alex Odermatt. 2015. “A Role for the Dehydrogenase DHRS7 (SDR34C1) in Prostate Cancer.” *Cancer Medicine* 7:n/a-n/a.

Shih, Shyang Rong, Yi Cheng Chang, Hung Yuan Li, Jau Yu Liau, Chia Yen

Lee, Chung Ming Chen, and Tien Chun Chang. 2013. “Preoperative Prediction of Papillary Thyroid Carcinoma Prognosis with the Assistance of Computerized Morphometry of Cytology Samples Obtained by Fine-Needle Aspiration: Preliminary Report.” *Head and Neck* 35(1):28–34.

Shimojima, Masaya, Shinsuke Yuasa, Chikaaki Motoda, Gakuto Yozu, Toshihiro Nagai, Shogo Ito, Mark Lachmann, Shin Kashimura, Makoto Takei, Dai Kusumoto, Akira Kunitomi, Nozomi Hayashiji, Tomohisa Seki, Shugo Tohyama, Hisayuki Hashimoto, Masaki Kodaira, Toru Egashira, Kenshi Hayashi, Chiaki Nakanishi, Kenji Sakata, Masakazu Yamagishi, and Keiichi Fukuda. 2017. “Emerin Plays a Crucial Role in Nuclear Invagination and in the Nuclear Calcium Transient.” *Scientific Reports* 7.

Shumaker, Dale K., Kenneth K. Lee, Yvette C. Tanhehco, Robert Craigie, and Katherine L. Wilson. 2001. “LAP2 Binds to BAF·DNA Complexes: Requirement for the LEM Domain and Modulation by Variable Regions.” *EMBO Journal* 20(7):1754–64.

Simon, Dan N. and Michael P. Rout. 2014. “Cancer and the Nuclear Pore Complex.” Pp. 285–307 in *Cancer Biology and the Nuclear Envelope: Recent Advances May Elucidate Past Paradoxes*, edited by E. C. Schirmer and J. I. de las Heras. New York, NY: Springer New York.

Skarka, Adam, Lucie Škarydová, Hana Štambergová, and Vladimír Wsól. 2014. “Purification and Reconstitution of Human Membrane-Bound DHRS7 (SDR34C1) from Sf9 Cells.” *Protein Expression and Purification* 95:44–49.

Slater, D. N., S. Rice, R. Stewart, S. E. Melling, E. M. Hewer, and J. H. F. Smith. 2005. “Proposed Sheffield Quantitative Criteria in Cervical Cytology to Assist the Grading of Squamous Cell Dyskaryosis, as the British Society for Clinical Cytology Definitions Require Amendment.” *Cytopathology* 16(4):179–92.

Solovei, Irina, Audrey S. Wang, Katharina Thanisch, Christine S. Schmidt,

Stefan Krebs, Monika Zwerger, Tatiana V Cohen, Didier Devys, Roland Foisner, Leo Peichl, Harald Herrmann, Helmut Blum, Dieter Engelkamp, Colin L. Stewart, Heinrich Leonhardt, and Boris Joffe. 2013. “LBR and Lamin A/C Sequentially Tether Peripheral Heterochromatin and Inversely Regulate Differentiation.” *Cell* 152(3):584–98.

Srsen, Vlastimil, Nadia Korfali, and Eric C. Schirmer. 2011. “Nuclear Envelope Influences on Cell-Cycle Progression.” *Biochemical Society Transactions* 39(6):1742–46.

Štambergová, Hana, Lucie Zemanová, Tereza Lundová, Beata Malčeková, Adam Skarka, Miroslav Šafr, Vladimír Wsól, Hana ??tambergov??, Lucie Zemanov??, Tereza Lundov??, Beata Mal??ekov??, Adam Skarka, Miroslav ??afr, and Vladim??r Ws??l. 2016. “Human DHRS7, Promising Enzyme in Metabolism of Steroids and Retinoids?” *Journal of Steroid Biochemistry and Molecular Biology* 155:112–19.

Steeg, Patricia S. and Dan Theodorescu. 2008. “Metastasis: A Therapeutic Target for Cancer.” *Nature Clinical Practice. Oncology* 5(4):206–19.

Stick, Reimer and Peter Hausen. 1985. “Changes in the Nuclear Lamina Composition during Early Development of Xenopus Laevis.” *Cell* 41(1):191–200.

Sullivan, Teresa, Diana Escalante-Alcalde, Harshida Bhatt, Miriam Anver, Narayan Bhat, Kunio Nagashima, Colin L. Stewart, and Brian Burke. 1999. “Loss of A-Type Lamin Expression Compromises Nuclear Envelope Integrity Leading to Muscular Dystrophy.” *Journal of Cell Biology* 147(5):913–19.

Suntharalingam, Mythili and Susan R. Wente. 2003. “Peering through the Pore: Nuclear Pore Complex Structure, Assembly, and Function.” *Developmental Cell* 4(6):775–89.

Swift, Joe, Irena L. Ivanovska, Amnon Buxboim, Takamasa Harada, P. C. D.

P. Dingal, Joel Pinter, J. David Pajerowski, Kyle R. Spinler, J. W. Shin, Manorama Tewari, Florian Rehfeldt, David W. Speicher, and Dennis E. Discher. 2013. “Nuclear Lamin-A Scales with Tissue Stiffness and Enhances Matrix-Directed Differentiation.” *Science* 341(6149):1240104–1240104.

Szczerbal, Izabela, Helen A. Foster, and Joanna M. Bridger. 2009. “The Spatial Repositioning of Adipogenesis Genes Is Correlated with Their Expression Status in a Porcine Mesenchymal Stem Cell Adipogenesis Model System.” *Chromosoma* 118(5):647–63.

Taira, Tomoki, Akihiko Kawahara, Tomohiko Yamaguchi, Hideyuki Abe, Yusuke Ishida, Yoshinobu Okabe, Yoshiki Naito, Hirohisa Yano, and Masayoshi Kage. 2012a. “Morphometric Image Analysis of Pancreatic Disease by ThinPrep Liquid-Based Cytology.” *Diagnostic Cytopathology* 40(11):970–75.

Taira, Tomoki, Akihiko Kawahara, Tomohiko Yamaguchi, Hideyuki Abe, Yusuke Ishida, Yoshinobu Okabe, Yoshiki Naito, Hirohisa Yano, and Masayoshi Kage. 2012b. “Morphometric Image Analysis of Pancreatic Disease by ThinPrep Liquid-Based Cytology.” *Diagnostic Cytopathology* 40(11):970–75.

Tan, P. H., B. B. Goh, G. Chiang, and B. H. Bay. 2001. “Correlation of Nuclear Morphometry with Pathologic Parameters in Ductal Carcinoma in Situ of the Breast.” *Modern Pathology : An Official Journal of the United States and Canadian Academy of Pathology, Inc* 14(10):937–41.

Then, Chee-Kin, Kao-Hui Liu, Ming-Hsuan Liao, Kuo-Hsuan Chung, Jia-Yi Wang, and Shing-Chuan Shen. 2017. “Antidepressants, Sertraline and Paroxetine, Increase Calcium Influx and Induce Mitochondrial Damage-Mediated Apoptosis of Astrocytes.” *Oncotarget* 8(70):115490–502.

Thorpe, Stephen D. and Myriam Charpentier. 2017. “Highlight on the Dynamic Organization of the Nucleus.” *Nucleus* 8(1):2–10.

Thorpe, Stephen D. and David A. Lee. 2017. “Dynamic Regulation of Nuclear Architecture and Mechanics—a Rheostatic Role for the Nucleus in Tailoring Cellular Mechanosensitivity.” *Nucleus* 8(3):287–300.

Tsai, Li-Huei and Joseph G. Gleeson. 2005. “Nucleokinesis in Neuronal Migration.” *Neuron* 46(3):383–88.

Tsao, Che-Kai, Matthew D. Galsky, Alexander C. Small, Tiffany Yee, and William K. Oh. 2012. “Targeting the Androgen Receptor Signalling Axis in Castration-Resistant Prostate Cancer (CRPC).” *BJU International* 110(11):1580–88.

van Velthoven, R., M. Petein, W. J. Oosterlinck, C. Zandona, A. Zlotta, A. P. Van der Meijden, J. L. Pasteels, H. Roels, C. Schulman, and R. Kiss. 1995. “Image Cytometry Determination of Ploidy Level, Proliferative Activity, and Nuclear Size in a Series of 314 Transitional Bladder Cell Carcinomas.” *Human Pathology* 26(1):3–11.

Venables, R. S., S. McLean, D. Luny, E. Moteleb, S. Morley, R. a Quinlan, E. B. Lane, and C. J. Hutchison. 2001. “Expression of Individual Lamins in Basal Cell Carcinomas of the Skin.” *British Journal of Cancer* 84(4):512–19.

Veta, Mitko, Robert Kornegoor, André Huisman, Anoek H. J. J. Verschuur-Maes, Max A. Viergever, Josien P. W. W. Pluim, and Paul J. Van Diest. 2012. “Prognostic Value of Automatically Extracted Nuclear Morphometric Features in Whole Slide Images of Male Breast Cancer.” *Modern Pathology* 25(12):1559–65.

Visakorpi, Tapio, Eija Hyytinen, Pasi Koivisto, Minna Tanner, Riitta Keinänen, Christian Palmberg, Aarno Palotie, Teuvo Tammela, Jorma Isola, and Olli P. Kallioniemi. 1995. “In Vivo Amplification of the Androgen Receptor Gene and Progression of Human Prostate Cancer.” *Nature Genetics* 9(4):401–6.

Walther, Tobias C., Annabelle Alves, Helen Pickersgill, Isabelle Loïodice, Martin Hetzer, Vincent Galy, Bastian B. Hülsmann, Thomas Köcher, Matthias Wilm, Terry Allen, Iain W. Mattaj, and Valérie Doye. 2003. “The Conserved Nup107-160 Complex Is Critical for Nuclear Pore Complex Assembly.” *Cell* 113(2):195–206.

Wang, Chun I., Chih Liang Wang, Chih Wei Wang, Chi De Chen, Chih Ching Wu, Ying Liang, Ying Huang Tsai, Yu Sun Chang, Jau Song Yu, and Chia Jung Yu. 2011. “Importin Subunit Alpha-2 Is Identified as a Potential Biomarker for Non-Small Cell Lung Cancer by Integration of the Cancer Cell Secretome and Tissue Transcriptome.” *International Journal of Cancer* 128(10):2364–72.

Wilhelmsen, Kevin, Sandy H. M. Litjens, Ingrid Kuikman, Ntambua Tshimbalanga, Hans Janssen, Iman Den Van Bout, Karine Raymond, and Arnoud Sonnenberg. 2005. “Nesprin-3, a Novel Outer Nuclear Membrane Protein, Associates with the Cytoskeletal Linker Protein Plectin.” *Journal of Cell Biology* 171(5):799–810.

Wilkie, G. S., N. Korfali, S. K. Swanson, P. Malik, V. Srsen, D. G. Batrakou, J. de las Heras, N. Zuleger, a. R. W. Kerr, L. Florens, and E. C. Schirmer. 2011. “Several Novel Nuclear Envelope Transmembrane Proteins Identified in Skeletal Muscle Have Cytoskeletal Associations.” *Molecular & Cellular Proteomics* 10(1):M110.003129.

Willis, Naomi D., Thomas R. Cox, Syed F. Rahman-Casañs, Kim Smits, Stefan A. Przyborski, Piet van den Brandt, Manon van Engeland, Matty Weijenberg, Robert G. Wilson, Adriaan de Bruïne, and Christopher J. Hutchison. 2008. “Lamin A/C Is a Risk Biomarker in Colorectal Cancer.” *PLoS ONE* 3(8).

Wistuba, I. I., A. F. Gazdar, and J. D. Minna. 2001. “Molecular Genetics of Small Cell Lung Carcinoma.” *Seminars in Oncology* 28(2 Suppl 4):3–13.

Xu, Xiaoqiang, Xiuhong Gao, Linhong Jin, Pinaki S. Bhadury, Kai Yuan,

Deyu Hu, Baoan Song, and Song Yang. 2011. “Antiproliferation and Cell Apoptosis Inducing Bioactivities of Constituents from Dysosma Versipellis in PC3 and Bcap-37 Cell Lines.” *Cell Division* 6:14.

Yan, Jun, Shuangmu Zhuo, Gang Chen, Xiufeng Wu, Dong Zhou, Shusen Xie, Jiahao Jiang, Mingang Ying, Fan Jia, Jianxin Chen, and Jian Zhou. 2012. “Preclinical Study of Using Multiphoton Microscopy to Diagnose Liver Cancer and Differentiate Benign and Malignant Liver Lesions.” *Journal of Biomedical Optics* 17(2):026004.

Zeimet, Alain G., Heidi Fiegl, Georg Goebel, Francis Kopp, Claude Allasia, Daniel Reimer, Ilona Steppan, Elisabeth Mueller-Holzner, Melanie Ehrlich, and Christian Marth. 2011. “DNA Ploidy, Nuclear Size, Proliferation Index and DNA-Hypomethylation in Ovarian Cancer.” *Gynecologic Oncology* 121(1):24–31.

Zhang, Qiuping, Cornelia Bethmann, Nathalie F. Worth, John D. Davies, Christina Wasner, Anja Feuer, Cassandra D. Ragnauth, Qijian Yi, Jason A. Mellad, Derek T. Warren, Matthew A. Wheeler, Juliet A. Ellis, Jeremy N. Skepper, Matthias Vorgerd, Beate Schlotter-Weigel, Peter L. Weissberg, Roland G. Roberts, Manfred Wehnert, and Catherine M. Shanahan. 2007. “Nesprin-1 and -2 Are Involved in the Pathogenesis of Emery - Dreifuss Muscular Dystrophy and Are Critical for Nuclear Envelope Integrity.” *Human Molecular Genetics* 16(23):2816–33.

Zink, Daniele, Andrew H. Fischer, and Jeffrey a Nickerson. 2004. “Nuclear Structure in Cancer Cells.” *Nature Reviews. Cancer* 4(9):677–87.

Zuleger, Nikolaj, Shelagh Boyle, David A. Kelly, Jose I. de las Heras, Vassiliki Lazou, Nadia Korfali, Dzmitry G. Batrakou, K. Natalie Randles, Glenn E. Morris, David J. Harrison, Wendy A. Bickmore, and Eric C. Schirmer. 2013. “Specific Nuclear Envelope Transmembrane Proteins Can Promote the Location of Chromosomes to and from the Nuclear Periphery.” *Genome Biology* 14(2):R14.

Appendix

Compounds screen Script

```
// Adapted from NucleiCounting and extended to do single cell statistics.

// Input parameters

input(IN_ImageField, 0, "Image Field", "i", "Number of the image field to
analyze. If set to 0 all image fields of the well are processed.")
input(nuc_Channel, 1, "Channel number for the nucleus stain")
input(cyto_Channel, 2, "Channel number for cytoplasm detection")
input(filename_output,"c:/temp/testdata.txt","Filename for Results","s")

// Get images

Singlewell(compact=yes)
if(!defined("SourceData.Channel"))
                set(NumberOfChannels=1) // needs to be adapted when
analysing non-flex images
end()
OperaTemplates::ControlImages()

// Check inputs

if( nuc_Channel>NumberOfChannels or nuc_Channel<0 )  error( "Illegal
Nuclear Channel selection" )  end()
```

```
// Prepare empty nuclei that will accumulate nuclei from all image fields

Create("objectlist)
rename(all_nuclei=objectlist)
Create("objectlist")
rename(all_cytoplasm=objectlist)
set(ProcessedImageFields = 0)
set(totalCellNumber = 1)

// LOOP OVER ALL FIELDS (or just the selected one)

FOREACH(StartField .. EndField, "_FieldCounter")

	// Get images of the current image field and select the nucleus image (channels are named IM_CH1, IM_CH2, etc.)

	OperaTemplates::AssignPlane()
	set(IM_nuc = _["IM_CH" & nuc_Channel])
	set( IM_cyto=_["IM_CH" & cyto_Channel] )

	// Don't try to analyse invalid fields
	if(IM_nuc.max==0)
		Continue()
	end()

	// Do the actual image analysis

	Nuclei_Detection_Select(IM_nuc,ShowIllustrations=no

	// do NUC stuff
```

```
    rename(objects=nuclei)
    RemoveBorderObjects()
    rename(nuclei=objects)

      // get cytoplasm information

    Cytoplasm_Detection_a(IM_cyto,ShowIllustrations=no) // detects cells by channel 1 image (cytoplasm is not stained on many channel 2 images)
    CytoplasmRegion(Stencil="Body",ShowIllustrations=yes, WholeCells=wholecells)
    CalcIntensity(Cytoplasm, image=IM_cyto, objects=wholecells | wholecells=objects)
    CalcIntensity(Centers, image=IM_cyto, objects=wholecells | wholecells=objects)
    CalcArea(CytoplasmRegion, objects=wholecells | wholecells=objects)
    RingRegion(ShowIllustrations=no, WholeCells = wholecells)
    CalcIntensity(RingRegion, image=IM_cyto, objects=wholecells | wholecells=objects)
    //imageview(Wholecells.RingRegion, "Ring Region", image=IM_cyto, gamma=3)
    NucleusRegion(VisualImage=IM_cyto, WholeCells = wholecells)
    CalcIntensity(NucleusRegion,image=IM_cyto, objects=wholecells | wholecells=objects)

          // Add nuclei to the all_nuclei list

          AddObjects(nuclei, objects=all_nuclei, CheckOverlap=no, DeleteGeometry=yes)

          rename(all_nuclei=objects)

    // Add cytoplasm  to the all_cytoplasm list
```

```
        AddObjects(WholeCells, objects=all_cytoplasm, CheckOverlap=no,
DeleteGeometry=yes)
   rename(all_cytoplasm=objects)
                set(_Wellindex_row = floor(wellindex / 1000000))

                set(_Wellindex_column = floor ( (wellindex -
1000000*_wellindex_row)/1000))

                push ( _Wellindex_tochar," ","A","B","C","D","E","F",
"G","H","I","J","K","L","M","N","O","P")
                                        if ((_Wellindex_column > 24) or
(_Wellindex_row>16))
        set(Out_Wellidx="R"&_Wellindex_row&" C"&_Wellindex_column)
                                        else()
        set(Out_Wellidx=_Wellindex_tochar[_Wellindex_row]&_Wellindex_col
umn)
                                        end()
printfopen(filename_output &"_"&
Sourcedata.barcode[0]&".txt",append=TRUE)
if (ProcessedImageFields == 0)
        printf("Plate\tWell\tField\tCellnr\tarea\tInt\tcytoArea\tcytoInt\tcytoNucInt
\tfieldCellindex\n")
end()
set(FieldIdx = ProcessedImageFields +1)
//printfloop("%s\t%s\t%1.f\t%k\t%1.f\t%1.f\t%1.f\t%1.f\t%1.f\n",Sourcedata.ba
rcode[0],Out_Wellidx,FieldIdx,Nuclei.area,Nuclei.intensity,WholeCells.area,
WholeCells.MembraneRegion_intensity,totalCellNumber )
printfloop("%s\t%s\t%1.f\t%k\t%1.f\t%8.3f\t%1.f\t%8.3f\t%8.3f\t%1.f\n",Sourc
edata.barcode[0],Out_Wellidx,FieldIdx,Nuclei.area,Nuclei.intensity,WholeCell
s.CytoplasmRegion_area,WholeCells.RingRegion_intensity,WholeCells.Nucl
eusRegion_intensity,totalCellNumber )
   set(totalCellNumber = totalCellNumber  + Nuclei.index.max)
```

```
        // Count successfully analysed fields
        set( ProcessedImageFields=ProcessedImageFields+1 )
END()
// Numerical outputs
output( ProcessedImageFields, "Processed Image fields" )
output( all_nuclei.count, "Total number of nuclei" )
output( nuclei.area.mean, "area nuclei" )
output( nuclei.intensity.mean, "intensity nuclei" )
output( WholeCells.CytoplasmRegion_area.mean, "area cytoplasm" )
output( WholeCells.RingRegion_intensity.mean, "intensity cytoplasm" )
output( WholeCells.Cytoplasm_intensity.mean, "intensity of cyto signal in
nuclei" )
```

NETs screen Script

```
// Adapted from NucleiCounting and extended to do single cell statistics.

// Input parameters

input(IN_ImageField, 0, "Image Field", "i", "Number of the image field to
analyze. If set to 0 all image fields of the well are processed.")
input(nuc_Channel, 1, "Channel number for the nucleus stain")
input(cyto_Channel, 2, "Channel number for cytoplasm detection")
input(filename_output,"c:/temp/testdata.txt","Filename for Results","s")

// Get images

Singlewell(compact=yes)
if(!defined("SourceData.Channel"))
                set(NumberOfChannels=1) // needs to be adapted when
analysing non-flex images
end()
```

```
OperaTemplates::ControlImages()

// Check inputs

if( nuc_Channel>NumberOfChannels or nuc_Channel<0 )  error( "Illegal
Nuclear Channel selection" )  end()

// Prepare empty nuclei that will accumulate nuclei from all image fields

Create("objectlist")
rename(all_nuclei=objectlist)
Create("objectlist")
rename(all_cytoplasm=objectlist)
set(ProcessedImageFields = 0)
set(totalCellNumber = 1)

// LOOP OVER ALL FIELDS (or just the selected one)

FOREACH(StartField .. EndField, "_FieldCounter")

        // Get images of the current image field and select the nucleus image
(channels are named IM_CH1, IM_CH2, etc.)

        OperaTemplates::AssignPlane()
        set(IM_nuc = _["IM_CH" & nuc_Channel])
        set( IM_cyto=_["IM_CH" & cyto_Channel] )



        // Don't try to analyse invalid fields

        if(IM_nuc.max==0)
```

```
            Continue()

        end()

        ////////////////////////////////////////////   COLOR OVERLAY IMAGE
//////////////////////////////////////////

    // Create and display a color overlay image of the three channels

    gamma(2.5, image=IM_cyto | Red=image)
    gamma(2.5, image=IM_nuc | Green=image)
    gamma(2.5, image=IM_nuc | Blue=image)
    RgbJoin(Red, Green, Blue, method="fillrangeall" | JoinedImage=image)
// Acapella 2.0
    delete(Red, Green, Blue)

    // Do the actual image analysis
        Nuclei_Detection_Select(IM_nuc)

        // do NUC stuff

    rename(objects=nuclei)
    RemoveBorderObjects()
        CalcArea(Border)
        CalcAttr(Roundness, 3.54491*sqrt(area-
border_area/2.0)/border_area-0.1)        // corrected roundness replacing
CalcAttr( "Roundness" ), see Online Help
        CalcWidthLength()
        DefineAttr( WidthToLength, "2*half_width / full_length" )
    rename(nuclei=objects)

    // get cytoplasm information
```

```
   Cytoplasm_Detection_a(IM_cyto) // detects cells by channel 1 image
(cytoplasm is not stained on many channel 2 images)
   CytoplasmRegion(Stencil="Body",ShowIllustrations=no,
WholeCells=wholecells)
   CalcIntensity(Cytoplasm, image=IM_cyto, objects=wholecells |
wholecells=objects)
   CalcIntensity(Centers, image=IM_cyto, objects=wholecells |
wholecells=objects)
   CalcArea(CytoplasmRegion, objects=wholecells | wholecells=objects)
   RingRegion(ShowIllustrations=no, WholeCells = wholecells)
   CalcIntensity(RingRegion, image=IM_cyto, objects=wholecells |
wholecells=objects)

   //imageview(Wholecells.RingRegion, "Ring Region", image=IM_cyto,
gamma=3)
   NucleusRegion(VisualImage=IM_cyto, WholeCells = wholecells)
   CalcIntensity(NucleusRegion,image=IM_cyto, objects=wholecells |
wholecells=objects)
   CalcAttr("NetExpressed", "RingRegion_intensity -
NucleusRegion_intensity", objects=wholecells | wholecells=objects)

         // Add nuclei to the all_nuclei list

         AddObjects(nuclei, objects=all_nuclei, CheckOverlap=no,
DeleteGeometry=yes)
         rename(all_nuclei=objects)



  // Add cytoplasm  to the all_cytoplasm list
```

```
        AddObjects(WholeCells, objects=all_cytoplasm, CheckOverlap=no,
DeleteGeometry=yes)
   rename(all_cytoplasm=objects)
                set(_Wellindex_row = floor(wellindex / 1000000))
                set(_Wellindex_column = floor ( (wellindex -
1000000*_wellindex_row)/1000))
                push ( _Wellindex_tochar," ","A","B","C","D","E","F",
"G","H","I","J","K","L","M","N","O","P")
                                        if ((_Wellindex_column > 24) or
(_Wellindex_row>16))
        set(Out_Wellidx="R"&_Wellindex_row&" C"&_Wellindex_column)
                                        else()
        set(Out_Wellidx=_Wellindex_tochar[_Wellindex_row]&_Wellindex_col
umn)
                                        end()


printfopen(filename_output &"_"&
Sourcedata.barcode[0]&".txt",append=TRUE)
if (ProcessedImageFields == 0)
        printf("Plate\tWell\tField\tCellnr\tarea\tInt\tcytoArea\tringNucInt\tnetNuc
int\tfieldcellindex\n")
end()

set(FieldIdx = ProcessedImageFields +1)
printfloop("%s\t%s\t%1.f\t%k\t%1.f\t%8.3f\t%8.3f\t%8.3f\t%8.3f\t%1.f\n",Sour
cedata.barcode[0],Out_Wellidx,FieldIdx,Nuclei.area,Nuclei.intensity,WholeCe
lls.CytoplasmRegion_area,WholeCells.RingRegion_intensity,WholeCells.Nuc
leusRegion_intensity,totalCellNumber )
   set(totalCellNumber = totalCellNumber  + Nuclei.index.max)

        // Count successfully analysed fields
```

```
        set( ProcessedImageFields=ProcessedImageFields+1 )
END()

// Numerical outputs

output( ProcessedImageFields, "Processed Image fields" )
output( all_nuclei.count, "Total number of nuclei" )
output( nuclei.area.mean, "area nuclei" )
output( nuclei.intensity.mean, "intensity nuclei" )
output( WholeCells.CytoplasmRegion_area.mean, "area cytoplasm" )
output( WholeCells.RingRegion_intensity.mean, "intensity of net in
cytoplasm" )
output( WholeCells.NucleusRegion_intensity.mean, "intensity of net in nuclei"
)
```

List of plasmids used in this study

#Addgene	Addgene name	Log #	Name	Alias
		447	NET26 pmRFP-N2	
61980	NET59 pmRFP-N2	450	NET37 pmRFP-N2	
61981	NET39 Short pmRFP-N2	451	NET39 Short pmRFP-N2	
		485	mNET20 mRFP	
		489	NET50 pmRFP-N2	
61984	NET31 pEGFP-N2	490	NET31 pmRFP-N2	
		588	Emerin pEGFP-N2	
		593	NET47 pEGFPNN2	
61987	NET51 pEGFP-N2	594	NET51 pEGFP-N2	
61988	NET23 pEGFP-N2	596	NET23 pEGFP-N2	
		597	NET33 pEGFP-N2	
		607	NET37 GFP	

		609	NET43 GFP	
		610	NET55 GFP	
		637	Emerin GFP-C1	
		641	NET97 pmRFP-N2	
61995	LBR pmRFP-N2	643	LBR pmRFP-N2	
		645	NET37 GFP	
		646	LBR pEGFP-N2	
		663	STT3A pmRFP	NET99
		700	NET45 pmRFP-N2	
		719	NKP9 pmRFP-N2	
		721	TAPBPL pmRFP-N2	
		787	NKP90 RFP	
62002	NKP37 RFP	788	NKP37 RFP	
		790	NKP68 RFP	
62004	NKP83 RFP	791	NKP83 RFP	
62005	NKP16 RFP	793	NKP16 RFP	
		794	NKP40 RFP	
		800	Tmem38A mRFP-N2	mNET1
		802	Sec61 GFP-C1	
62009	NKP63 RFP	805	NKP63 RFP	
62010	SUN2 GFP	812	SUN2 GFP	
		815	NET30 pEGFP-N2	
62012	NET59 pEGFP-N2	816	NET59 pEGFP-N2	
62013	NET92 RFP	822	NET92 RFP	
62014	NET94 RFP	823	NET94 RFP	
62015	NET100 RFP	824	NET100 RFP	
62016	NET84 RFP	825	NET84 RFP	
		890	METTL7A GFP	
62018	WFS1 pmGFP-N2	891	WFS1 pmGFP-N2	
62019	CKAP4 pmRFP	894	CKAP4 pmRFP	mNETY
		1007	NKP64 GFP	

		1009	NKP38 GFP	
		1032	NKP33 GFP	
		1034	NKP91 GFP	
		1045	NET39 GFP-C1	
		1051	STT3A pEGFP-N2	NET99
		1072	Tmem214 pEGFP-N2	
		1074	Tmem194 pEGFP-N2	
		1078	RHBDD1 pEGFP-N2	NET82
62029	POPDC2 pmRFP-N2	1085	POPDC2 pmRFP-N2	mNET3
		1087	POPDC2 pEGFP-N2	mNET3
62031	KLHL31 pgkRFP	1088	KLHL31 pgkRFP	mNET8
62032	KHLH31 pEGFP-N2	1089	KHLH31 pEGFP-N2	mNET8
62033	Tmem70 pEGFP-N2	1092	Tmem70 pEGFP-N2	
62034	NET5s pEGFP-N2	1154	NET5s pEGFP-N2	SAMP1, Imo1
62035	NET5L pEGFP-N2	1155	NET5L pEGFP-N2	SAMP1, Imo2
		1159	Emerin Active GFP	
		1159	Emerin Resting GFP	
62036	NET77 GFP	1173	NET77 GFP	
62037	NKP22 GFP	1174	NKP22 GFP	
62038	NKP40 GFP	1175	NKP40 GFP	
		1176	NKP66 GFP	
		1181	NET29A.Hs pEGFP-N2	
		1201	NET4 pEGFP-N2	
		1219	NET39 RFP-C1	
		1285	NET39 GFP-C1	
		1299	NLS pEGFP-N3	
62044		1317	LAP2 Full I pAcGFP-N1	
		1326	NET29A.Mm pEGFP-N2	Tmem120a
		1327	NET29b.Mm pEGFP-N2	

		1348	Tmem214 pmRFP-N2	
		1389	Tmem194 pmRFP-N2	
		1390	RHBDD1 pmRFP-N2	NET82
		1401	Tmem38A pEGFP-N2	mNET1
		1472	WFS1 pEGFP-N2	
62054		1761	SQSTM1.Mm pEGFP-C2	NET77
		1764	NET51 pEGFP-C3	
		1765	TAPBPL pEGFP-C3	
62056		1766	LBR GFP-C3	
		1768	NET34 GFP	
		1769	NET51 pEGFP-N2	
		1771	NET99 GFP	
		1772	NKP9 GFP	
		1774	LAP2b GFP	